ANALYSIS OF A THREE-SPECIES FOODWEB MODEL

ANALYSIS OF A MATHEMATICAL MODEL OF A THREE-SPECIES FOODWEB

By

WENJIANG FU, B.Sc.(Peking University) M.Sc.(Tsinghua University)

A Thesis
Submitted to the School of Graduate Studies
in Partial Fulfilment of the Requirements
for the Degree
Master of Science

McMaster University

MASTER OF SCIENCE (1991) MCMASTER UNIVERSITY
(Mathematics) Hamilton, Ontario

TITLE: Analysis of a Mathematical Model of a Three-Species Foodweb

AUTHOR: Wenjiang Fu
B.Sc.(Peking University) M.Sc.(Tsinghua University)

SUPERVISOR: G.S.K. Wolkowicz

NUMBER OF PAGES: vii, 86

Abstract

A model of two predators competing for the same prey also involving predation interaction between the two predators is considered. Coexistence in forms of equilibria and periodic orbits is obtained by using bifurcation and dynamical systems theory. Global dynamics is obtained by studying the survival functions and persistence is obtained by using a theorem of Freedman and Waltman. Finally, numerical results for a specific example demonstrate the above. A Hopf bifurcation at the interior equilibrium and its unstable periodic orbit are observed.

Acknowledgements

I would like to extend my sincere thanks to my supervisor Dr. Wolkowicz, for introducing me to such an interesting field and encouraging me to study this model. I appreciate her energy, time and critical comments on this thesis, which made this thesis done so quickly.

I would also like to give my thanks to my defence committee members, Professors A. Nicas, A. Peirce and G. Wolkowicz, who gave me a wonderful time.

I would like to thank my family, especially my parents for their love. I'm also owing to my friend Q. Ding for the encouragements.

Contents

List of Figures

Chapter 1

Introduction

1.1 The background

During the last several decades, much work in mathematical biology and ecology has been focused on studying the dynamics of predator-prey systems using population models, for example, see [6, 16, 18, 31, 35]. The classical predation population model goes back to the Kolmogorov model in the general case, see [7, 10, 11] and Chapter 5 of [8].

In the Kolmogorov predation model as shown below, it is assumed that the growth rate of a species is proportional to the number of the species present.

$$\begin{cases} x' &= xf(x,y) \\ y' &= yg(x,y). \end{cases}$$

Some conditions must be put on f and g to make x a prey and y a predator, see Chapter 5 of [8].

Some population models deal exclusively with predation interaction among the species and ignore other types of interactions. However, natural ecosystems may not be so simple. Instead, there are usually many species and the interactions among them may be very complicated. Besides the main predation interaction, some ecosystems are usually affected by certain seasonal or environmental factors. Imagine how complex and complicated a natural ecosystem is. For example, consider barracudas

eating the other fish. Besides being predators, they have cleaner fish that swim with them and clean their teeth. A model trying to take all possible factors into consideration would be mathematically intractable. Therefore restricting the model to a chemostat, where interaction and outside influences are easy to control, simplifies it reasonably and is very useful, as pointed out by Waltman et al. in [35].

A chemostat is an experimental apparatus that is used to culture microorganisms in the laboratory. *It is of ecological interest for being a laboratory model of a very simple lake where mathematics is tractable, the parameters are measurable and the experiments are reasonable*, [34]. Therefore it is of great importance both analytically and experimentally. The importance was well demonstrated in [2, 5, 6, 34, 35] and some other articles.

The apparatus consists of three connected vessels. The first contains all of the nutrients needed for growth of a microorganism. The nutrient is pumped at some rate into the second vessel, the culture vessel. The culture vessel is charged with a variety of microorganisms, so it contains a mixture of nutrient and organisms. Its output is collected in the third vessel which represents the "production" of the chemostat.

The culture vessel is well stirred and all other significant parameters affect- ing growth, for example, temperature, are measured and therefore controlled. Since the output is continuous, the chemostat is often referred to as "continuous culture" to contrast it with the more common "batch culture" of microorganisms. A schematic is shown in Figure A.1. Some specific applications were studied in [35].

For the chemostat, a model based on the population densities can be derived and described by a system of ordinary differential equations (O.D.E.), see [34].

Because population densities must be non-negative, we restrict ourselves to the positive cone of the phase space. Understanding under what conditions distinct populations can coexist and avoid extinction is of importance to the ecologists. Corresponding to coexistence are attractors in the interior of the positive cone such as equilibria and periodic orbits of an O.D.E. system.

Mathematically, an equilibrium of an O.D.E. system is a point in the phase space at which the vector field of the system vanishes. Hence an equilibrium represents the zero speed or stationary state of the system. A system once going into such a state

will stay there forever provided that there is absolutely no disturbance. A periodic orbit is a closed loop in the phase space that the system goes along. It returns to the same state after a constant period of time. Thus the system repeats the state again and again. These two kinds of phenomena display some sort of balance among the species. Therefore if stable and situated in the positive cone, they represent coexistence of species.

One important aspect related to coexistence is the stability of the equilibria and the periodic orbits. In a natural ecosystem, a lot of factors contribute to the system, some of them impose disturbance. For example, a system may be disturbed by some environmental events such as infective diseases or disasters like floods or typhoons, which suddenly change the system considerably. These kinds of disturbances may force the population densities to fluctuate drastically, and hence may pull the system from an unstable state to a totally different one. Therefore if an equilibrium or a periodic orbit is unstable, a small perturbation by the disturbance caused by the external events will make the system lose the balance and may result in the extinction of some species. Therefore stability plays an important role in ecosystems.

Using bifurcation and dynamical systems theory, one can analyze the local and global dynamics by studying the eigenvalues at the equilibria and the Floquet exponents at the periodic orbits. When the invariant sets of the O.D.E. systems are too complicated to describe, persistence is a useful concept for answering questions related to species survival: Do some of the species considered become extinct or do all of them coexist. However, the specific type of the coexistence, when it occurs, is usually not specified, see [4, 13].

Now let's go back to the model. Among various predation population models, the foodchain and foodweb models are of interest. The former consists of links of a chain with one species on each link, where one species feeds on the one next to it, that in turn feeds on another next to it. The latter consists of one or more species feeding on one or more other species. Both are clearly described in Figure A.2.

Pioneer's work goes back to Volterra, Lotka and Verhulst. The single species

logistic growth model is attributed to Verhulst, see [32, 8, 35]. The functional model

$$\begin{cases} x' &= x(\alpha - \beta y) \\ y' &= y(-\gamma + \delta x), \end{cases}$$

where y is the predator, x the prey and $\alpha, \beta, \gamma, \delta > 0$, is well known as the Lotka-Volterra predator-prey model, see [8, 25, 33]. Another model frequently studied involves the Holling type or Michaelis-Menten type response function,

$$\begin{cases} x' &= x(\alpha - \frac{my}{a+x}) \\ y' &= y(-\gamma + \frac{mx}{a+x}), \end{cases}$$

where again y is the predator, x the prey and $\alpha, \gamma, m, a > 0$. Models using these types of response functions have been intensively studied, see [1, 2, 11, 12, 14, 15, 16, 19, 20, 21, 22, 29, 30, 34, 36]. The Michaelis-Menten type of functional response is assumed to be a good model for most microorganisms and small invertebrates. *In microorganisms, resource uptake occurs at the level of enzyme-mediated transport of specific nutrients across the cell wall, and uptake rates are generally characterized by the Michaelis-Menten equations for enzyme-catalyzed reactions*, see [35].

The model considered here consists of two predators x_1 and x_2 competing for the same prey s, while one of the predators, x_2, eats the other x_1 as well. Therefore predator x_1 is also a prey. The prey s is self-renewable and assumed to have a logistic growth rate. Thus it has an upper limit K, called the carrying capacity of the environment. This is the concentration that would appear if both predators are absent. It is assumed that the amount of the consumption of the predator x_2 feeding on x_1 is proportional to a parameter ϵ, which is the main bifurcation parameter for the model. Due to the energy, time or even taste, this interaction between the two predators affects the predation of x_2 on s, usually reducing it by an amount proportional to an increasing function $g(\epsilon)$. Finally the Michaelis-Menten type response functions are assumed. The model interactions are shown in Figure A.3.

One can see clearly from the figure that this model has two extreme cases. First, $\epsilon = 0$. Thus $g(\epsilon) = 0$. It becomes a model of two predators competing for the same prey without any interaction between the two predators. It was well studied in [3, 17, 21, 29, 35]. An interior periodic orbit was obtained in [3]. The stability

of this periodic orbit was obtained in [29]. However, in this case there is no interior equilibrium in general. Secondly, $g(\epsilon) = 1$ for large ϵ. It becomes the simple foodchain model, which is similar to that studied by Freedman and Waltman in [9]. They used the Lotka-Volterra type instead of the Michaelis-Menten type response function for the upper trophic consumption of x_2 on x_1. There exist at most two interior equilibria for this case. Under different conditions, there could be one or two or none. But the bifurcation was disregarded in [9] because the parameter ϵ can be incorporated in the response function and did not appear explicitly in their model. Thus our model here unifies the two cases while including each as a limiting case. At intermediate value of ϵ, as expected, the model inherits some properties of both extreme cases while it displays some quite different characters as well, for example, the stable interior periodic orbit inherited from the case $\epsilon = 0$, the interior equilibrium, the interior Hopf bifurcation and its unstable periodic orbit.

1.2 Thesis outline

This thesis is organized as follows. The model and its explanation are given in Section 2.1. Some preliminary results are given in Section 2.2. In Chapter 3, we analyze the equilibria and their local dynamics. Furthermore, the existence and the uniqueness of the interior equilibrium are obtained by using fundamental analysis and the Implicit Function Theorem. Section 4.2 shows that the steady-state bifurcation at the equilibrium $\bar{P}_i$ in the $s - x_i$ plane generates the interior equilibrium P_0 when ϵ varies. Section 4.3 shows that the steady-state bifurcation at the limit cycle $\bar{\Gamma}_1$ in the $s - x_1$ plane generates a stable interior periodic orbit Γ when either ϵ increases or D_2 decreases or both. This interior periodic orbit collapses to the limit cycle $\bar{\Gamma}_2$ in the $s - x_2$ plane when either ϵ increases or D_1 increases or both. In Section 4.4, the other extreme case, i.e. the simple foodchain is considered. There exist at most two interior equilibria. Under different conditions, there may exist one interior equilibrium or two or none. The bifurcations of these interior equilibria are also considered. It is followed by the global dynamics and the persistence using a theorem of Freedman and Waltman in Section 5.2 and Section 5.1, respectively. Finally numerical results for a

specific case with a fixed set of parameters are given in Chapter 6. These demonstrate all the results in Chapter 3, Sections 4.2 and 4.3, which give the interior equilibrium and the stable interior periodic orbit. Moreover, a Hopf bifurcation at the interior equilibrium and its unstable periodic orbit are observed. Thus at least two interior periodic orbits exist, one stable and the other unstable.

Chapter 2

The model and the preliminaries

2.1 The model

The system considered here is a three species model with two predators feeding on the same prey, while one predator also eats the other predator. Thus one of the predators is also a prey. The Michaelis-Menten type response functions are used to model the consumption. The model is given by the following system of ordinary differential equations.

$$\begin{cases} s' &= \gamma s(1-\frac{s}{K}) - \frac{m_1 s x_1}{y_1(a_1+s)} - \frac{m_2 s x_2}{y_2(a_2+s)}(1-g(\epsilon)) \\ x_1' &= \frac{m_1 s x_1}{a_1+s} - D_1 x_1 - \frac{m_3 x_1 x_2 \epsilon}{y_3(a_3+x_1)} \\ x_2' &= \frac{m_2 s x_2}{a_2+s}(1-g(\epsilon)) - D_2 x_2 + \frac{m_3 x_1 x_2 \epsilon}{a_3+x_1}, \end{cases} \tag{2.1.1}$$

with

$$s(0) \geq 0, x_i(0) \geq 0, i = 1, 2,$$

where s is the density of the prey at time t, and x_1, x_2 are the densities of the two predators at time t. m_i is the maximum growth rate of x_i feeding on s (m_3 of x_2 on x_1), D_i the death rate of x_i. y_i is the yield factor for x_i feeding on s (y_3 for x_2 on x_1) under the basic assumption that the conversion to biomass is proportional to consumption. a_i is the half-saturation constant for x_i on s (a_3 for x_2 on x_1), which is the prey density at which the functional response of the predation is half maximal. The parameters γ and K are the intrinsic rate of increase and the carrying

capacity for the prey population, respectively. ϵ is the rate for x_2 feeding on x_1 and the function $g(\epsilon)$ is the reduction rate for x_2 feeding on s due to the consumption of x_2 on x_1 , thus satisfying the following conditions. $g(0) = 0, 0 \leq g(\epsilon) \leq B \leq 1$ and $0 \leq g'(\epsilon) \leq B_1$ for $0 \leq \epsilon < +\infty$, where B and B_1 are positive constants. Hence all parameters stated above are positive. No time delay from the consumption on the preys to the yield of the predators is assumed.

When $\epsilon = 0$, the system reduces to the system studied in [17] and [3]. When $g(\epsilon) = 1$, it reduces to a simple three species foodchain model, which is similar to that studied in [9]. To simplify system (2.1.1), one can use the following scaling.

$$\frac{x_i}{y_i} \to x_i, \ \frac{m_i}{\gamma} \to m_i, \ \frac{t}{\gamma} \to t, \ \frac{D_i}{\gamma} \to D_i, \ \text{ for } i = 1, 2,$$

and

$$\frac{a_3}{y_1} \to a_3, \ \frac{m_3}{\gamma} \to m_3, \ \frac{y_1 y_3}{y_2} \to y_3.$$

Then (2.1.1) becomes

$$\begin{cases} s' &= s(1 - \frac{s}{K}) - \frac{m_1 s x_1}{a_1 + s} - \frac{m_2 s x_2}{a_2 + s}(1 - g(\epsilon)) \\ x_1' &= \frac{m_1 s x_1}{a_1 + s} - D_1 x_1 - \frac{m_3 x_1 x_2 \epsilon}{y_3(a_3 + x_1)} \\ x_2' &= \frac{m_2 s x_2}{a_2 + s}(1 - g(\epsilon)) - D_2 x_2 + \frac{m_3 x_1 x_2 \epsilon}{a_3 + x_1}, \end{cases} \tag{2.1.2}$$

with

$$s(0) \geq 0, x_i(0) \geq 0, i = 1, 2.$$

Thus we study system (2.1.2) instead of (2.1.1).

2.2 Some preliminary results

We consider the solutions in the positive octant and have the following results.

Lemma 1 *The positive octant is invariant under the flow of system* (2.1.2).

Proof Notice that system (2.1.2) has three invariant sets $s = 0, x_1 = 0$ and $x_2 = 0$, which are the boundaries of the positive octant. By the uniqueness of the solutions

of system (2.1.2), any solution with initial value in the interior of the positive octant does not intersect any of the three boundary planes, and thus stays in the interior forever. This shows that the interior is also invariant under the flow of system (2.1.2). This completes the proof.

∎

We use the eventual uniform boundedness to describe the solutions of system (2.1.2).

Definition 1 *The solutions of a differential equation $x' = F(x,t)$ with $x \in \mathbf{R^n}$ are said to be eventually uniformly bounded if there exists a compact region $\mathcal{D} \subset \mathbf{R^n}$, independent of the solutions, such that for any initial value $x_0 \in \mathbf{R^n}$, there exists a time $t_0(x_0)$, such that the solution $x(t,x_0)$ with initial value x_0 satisfies $x(t,x_0) \in \mathcal{D}$ for all $t \geq t_0(x_0)$.*

Lemma 2 *The solutions of system* (2.1.2) *with initial conditions in the positive octant are eventually uniformly bounded.*

Proof Suppose $(s(t), x_1(t), x_2(t))$ is a solution of (2.1.2) with $s(0) \geq 0$ and $x_i(0) \geq 0$, $i = 1, 2$. By Lemma 1, one has $s(t) \geq 0$ and $x_i(t) \geq 0, i = 1, 2$ for any $t \geq 0$.

Step 1. $s(t)$ is eventually uniformly bounded by $K + \sigma_1$ for any $\sigma_1 > 0$.
From the first equation of (2.1.2), one has $s' \leq s(1 - s/K)$. Then $s' < 0$ and $s(t)$ is decreasing for any $s > K$. There exists $t_1 > 0$, such that $s(t_1) < K + \sigma_1$. If not, $s(t) \geq K + \sigma_1$ for any t. Then $\lim_{t\to\infty} s(t)$ exists by the monotonicity. Denote $s^0 = \lim_{t\to\infty} s(t)$. $s(t) \geq s^0 \geq K + \sigma_1$. $s'(t) \leq s(1 - s/K) \leq s^0(1 - s^0/K) < 0$ for any t since $s(t) \geq s^0$ and $s(1 - s/K)$ is decreasing for $s > K$. By Mean Value Theorem

$$s(t) - s(0) = s'(\xi)t \leq s^0(1 - s^0/K)t \to -\infty \text{ as } t \to +\infty.$$

where $\xi \in [0, t]$. This contradicts $\lim_{t\to\infty} s(t) = s^0$. Thus t_1 exists. Furthermore one has that $s(t) < K + \sigma_1$ for any $t \geq t_1$. If not, there exists $t_1^* > t_1$ such that

$s(t_1^*) = K + \sigma_1$ and $s(t) < K + \sigma_1$ for $t_1 \le t < t_1^*$. This obviously implies that $s'(t_1^*) \ge 0$. But

$$s'(t_1^*) \le (K + \sigma_1)(1 - \frac{K + \sigma_1}{K}) = -\frac{\sigma_1}{K}(K + \sigma_1) < 0.$$

This contradiction shows that $s(t) \le K + \sigma_1$ for any $t \ge t_1$.

Step 2. $x_1(t)$ is eventually uniformly bounded by some constant C_1.

It is obvious that $s(1 - s/K) \le K/4$. From the first equation of (2.1.2), one has $s' \le K/4 - m_1 s x_1/(a_1 + s)$ together with $x_1' \le m_1 s x_1/(a_1 + s) - D_1 x_1$ from the second equation. Combining these two gives $(x_1 + s)' \le -D_1 x_1 + K/4$. Thus $(x_1 + s)' \le -D_1(x_1 + s - \bar{C}_1)$ for $t \ge t_1$, where $\bar{C}_1 = K/(4D_1) + K + \sigma_1$. Then $(x_1 + s - \bar{C}_1)' \le -D_1(x_1 + s - \bar{C}_1)$. It is equivalent to $((x_1 + s - \bar{C}_1)e^{D_1 t})' \le 0$. Taking the integral on both sides from t_1 to t, one obtains

$$x_1(t) + s(t) - \bar{C}_1 \le (x_1(t_1) + s(t_1) - \bar{C}_1)e^{D_1(t_1 - t)} \to 0 \text{ as } t \to +\infty.$$

Thus for any fixed $\sigma_2 > 0$, there exists $t_2 > t_1$, such that $x_1 \le \bar{C}_1 + \sigma_2$ for all $t \ge t_2$. Take $C_1 = \bar{C}_1 + \sigma_2$. Then $x_1(t) \le C_1$ for all $t \ge t_2$.

Step 3. $x_2(t)$ is eventually uniformly bounded by some constant C_2.

Suppose $m_1 > D_1$. One has

$$\begin{aligned} x_1' &\le (m_1 - D_1)x_1 - \frac{m_3 x_1 x_2 \epsilon}{y_3(a_3 + x_1)} \\ &\le (m_1 - D_1)C_1 - \frac{m_3 x_1 x_2 \epsilon}{y_3(a_3 + x_1)} \end{aligned}$$

from the second equation of (2.1.2) and

$$s' \le K/4 - \frac{m_2 s x_2}{a_2 + s}(1 - g(\epsilon))$$

from the first one. Combining these two inequalities with the third equation of (2.1.2) gives

$$\begin{aligned} (x_2 + y_3 x_1 + s)' &\le -D_2 x_2 + K/4 + C_1 y_3(m_1 - D_1) \\ &\le -D_2(x_2 + y_3 x_1 + s - \bar{C}_2), \end{aligned}$$

where $\bar{C}_2 = C_1 y_3(m_1 - D_1)/D_2 + K/(4D_2) + K + \sigma_1 + y_3 C_1$. In the same way as in step 2, one has

$$x_2(t) + y_3 x_1(t) + s(t) - \bar{C}_2 \leq$$
$$(x_2(t_2) + y_3 x_1(t_2) + s(t_2) - \bar{C}_2) e^{D_2(t_2 - t)} \to 0 \text{ as } t \to +\infty.$$

Thus for any fixed $\sigma_3 > 0$, there exists a sufficiently large t_3, $t_3 > t_2$ such that $x_2 + y_3 x_1 + s \leq \bar{C}_2 + \sigma_3$ for any $t \geq t_3$. Take $C_2 = \bar{C}_2 + \sigma_3$. $x_2 \leq C_2$ for all $t \geq t_3$.

Then take $\mathcal{D} = [0, K + \sigma_1] \times [0, C_1] \times [0, C_2]$, the solution $(s(t), x_1(t), x_2(t)) \in \mathcal{D}$ for $t \geq t_3$. Thus it is eventually uniformly bounded by $\mathcal{D}$.

∎

In order to organize the domain of the parameters, it is necessary to give some results on the survival function $f_i(s)$. This function plays an important role in the analysis of the competition between the predators.

Definition 2 *The function* $f_i(s) = \frac{m_i s}{a_i + s} - D_i$, *for* $s > -a_i$ *is called the survival function of the species* x_i.

Lemma 3

(i). $f_i(s)$ *is monotonically increasing with the upper bound* $m_i - D_i$.

(ii). $f_i(s)$ *vanishes at* $\lambda_i = a_i/(b_i - 1) > 0$ *if* $b_i > 1$, *where* $b_i = m_i/D_i$.

(iii). $f_1(s)$ *and* $f_2(s)$ *intersect at a unique point for the branch* $s > -a_i$ *if* $m_1 - D_1 > m_2 - D_2$ *and* $a_2 > a_1$.

Proof (i). $f_i'(s) = \frac{m_i a_i}{(a_i + s)^2} > 0$. Thus $f_i(s)$ is increasing. $\lim_{s \to +\infty} f_i(s) = m_i - D_i$, which is the upper bound. (ii). It is easy to see that $f_i(\lambda_i) = 0$ if $b_i > 1$. $f_i(s)$ is shown in Figure A.4. (iii). Set $f_1(s) = f_2(s)$. Then $\frac{m_1 s}{a_1 + s} - D_1 = \frac{m_2 s}{a_2 + s} - D_2$. This reduces to $(m_1 - D_1) - (m_2 - D_2) - \frac{m_1 a_1}{a_1 + s} = -\frac{m_2 a_2}{a_2 + s}$. Denote $M = (m_1 - D_1) - (m_2 - D_2)$ and take the translation $u = a_1 + s$. Then $M - \frac{m_1 a_1}{u} = -\frac{m_2 a_2}{(a_2 - a_1) + u}$. We obtain a quadratic equation $Mu^2 + Nu - m_1 a_1 (a_2 - a_1) = 0$, where N is the coefficient of the first order term. Since $M > 0$ and $a_2 > a_1$, it is easy to see that this quadratic function of u has two distinct roots, one is positive, the other negative, as shown in

Figure A.5. Thus there exists a unique intersection of $f_1(s)$ and $f_2(s)$ for the branch $s > -a_1$ corresponding to the positive root of u. The negative root corresponds to the intersection on the branch $s < -a_1$, which has no interest for our system. The intersection is shown in Figure A.6.

∎

The extreme case of (2.1.2), where $\epsilon = 0$, has been well studied, for example see [3, 17]. Some of the results are given in the following lemmas. The other extreme case, where $g(\epsilon) = 1$, will be discussed in section 4.4.

Lemma 4 *Suppose* $\epsilon = 0$.

(i). *Necessary conditions for each* x_i, $i = 1, 2$, *to survive are* $b_i > 1$ *and* $0 < \lambda_i < K$. *In such case, there exists a unique equilibrium* P_i *in the interior of the* $s - x_i$ *plane with the components* $P_1(\lambda_1, x_1^*, 0)$ *and* $P_2(\lambda_2, 0, x_2^*)$ *where* $x_i^* = (1 - \lambda_i/K)(a_i + \lambda_i)/m_i$.

(ii). *There is no periodic orbit in the interior of the* $s - x_i$ *plane if* $0 < \lambda_i < K < a_i + 2\lambda_i$. P_i *is asymptotically stable in this case.*

(iii). P_i *comes from the bifurcation at* $(K, 0, 0)$ *when* K *increases through* λ_i. *For* $K < \lambda_i$, *there is no equilibrium in the interior of the* $s - x_i$ *plane.*

(iv). *A Hopf bifurcation occurs at* P_i *when* $K = a_i + 2\lambda_i$. *This gives a unique periodic orbit around* P_i *in the* $s - x_i$ *plane for* $K > a_i + 2\lambda_i$.

Proof The proof of (i) and (ii) is in [17]. The proof of (iv) is in [24, 23, 29]. Smith showed the Hopf bifurcation when $K = a_i + 2\lambda_i$ and the uniqueness for small $K - (a_i + 2\lambda_i) > 0$ in [29]. Liou and Cheng [24] and Kuang and Freedman [23] showed the uniqueness for any $K - (a_i + 2\lambda_i) > 0$.

Now we prove (iii). It is easy to see that there is no equilibrium in the interior of the $s - x_i$ plane for $K < \lambda_i$. To prove the bifurcation at $(K, 0, 0)$, we consider the reduced 2-dimensional system

$$\begin{cases} s' &= s(1 - \frac{s}{K}) - \frac{m_i s x_i}{a_i + s} \\ x_i' &= \frac{m_i s x_i}{a_i + s} - D_i x_i. \end{cases}$$

The linearization at $(K, 0)$ is

$$\begin{cases} s' &= K - s - \frac{m_i K}{a_i + K} x_i \\ x_i' &= f_i(K) x_i. \end{cases}$$

The two eigenvalues at $(K,0)$ are -1 and $f_i(K)$.

$$\lim_{K\to\lambda_i} f_i(K) = 0, \ \lim_{K\to\lambda_i} \frac{\partial f_i(K)}{\partial K} = \frac{m_i a_i}{(a_i+\lambda_i)^2} > 0.$$

By Theorem 5 in Chapter 4, a bifurcation at $(K,0)$ gives birth to a pair of equilibria in the interior of the $s-x_i$ plane. One is in the positive cone, the other not. Furthermore, $\lim_{\lambda_i\to K} x_i^* = 0$. Thus $\lim_{\lambda_i\to K} P_i = (K,0,0)$. This completes the proof. ∎

While the case with one predator absent is discussed in Lemma 4, the one with two competing predators will be discussed in the following lemmas.

Lemma 5 *Suppose* $\epsilon = 0$ *and* $0 < \lambda_1 < \lambda_2 < K$.
(i). $\lim_{t\to\infty} x_2 = 0$ *if* $b_1 \geq b_2$. *Thus the inequality* $b_1 < b_2$ *must hold if* x_2 *survives.*
(ii). *If* $a_1 < a_2$ *and* $K < a_2 + 2\lambda_2$, *then* $\limsup_{t\to\infty} x_1(t) > 0$. *Thus* x_1 *survives.*

The proof is in [17].

Lemma 6 *Suppose* $\epsilon = 0$ *and* $0 < \lambda_1 < \lambda_2 < K$.
(i). *If there exists a compact invariant set of the flow of* (2.1.2) *in the interior of the positive octant,* $f_1(s)$ *and* $f_2(s)$ *intersect in* $(0,K)$.
(ii). *If* $a_1 < a_2$ *and* $m_1 - D_1 > m_2 - D_2$, (i) *implies* $1 < b_1 < b_2$ *and* $D_1 > D_2$.

Proof With the cylindrical coordinate substitution $s = s$, $x_1 = \rho\cos\theta$, $x_2 = \rho\sin\theta$, system (2.1.2) with $\epsilon = 0$ becomes

$$\begin{cases} s' &= s(1-\frac{s}{K}) - \frac{m_1 s\rho\cos\theta}{a_1+s} - \frac{m_2 s\rho\sin\theta}{a_2+s} \\ \rho' &= \rho[f_1(s)\cos^2\theta + f_2(s)\sin^2\theta] \\ \theta' &= \frac{1}{2}[f_2(s) - f_1(s)]\sin 2\theta. \end{cases} \tag{2.2.1}$$

(i). If $f_1(s)$ and $f_2(s)$ do not intersect in $(0,K)$, $f_2(s)-f_1(s)$ does not vanish in $(0,K)$. Thus θ' does not vanish in $(0,K)\times(0,\pi/2)$. Since $\lambda_1 < \lambda_2$, $f_1(\lambda_2) > f_1(\lambda_1) =$

$0 = f_2(\lambda_2)$. Thus $f_1(s) > f_2(s)$ for $s \in (0, K)$. Hence $\theta' < 0$ for $0 \leq t < +\infty$. If there exists a compact invariant set, $\theta(t)$ attains a maximum and minimum on the set. Denote $\theta^0 = \theta(t_0) = \max_{0 \leq t \leq \infty} \theta(t)$. Then $0 < \theta^0 < \pi/2$ and $\theta'(t_0) = 0$. This contradicts $\theta' < 0$ for $\theta \in (0, \pi/2)$.

(ii). The survival of x_1 and x_2 implies $1 < b_1 < b_2$ by Lemmas 4 and 5. Since $m_1 - D_1 > m_2 - D_2$ and $a_1 < a_2$, $f_1(s)$ and $f_2(s)$ intersect at a unique point by Lemma 3. If $D_1 \leq D_2$, they intersect at some $-a_1 < s < 0$. This contradicts (i). ∎

From the above lemmas, it is reasonable to consider the coexistence of system (2.1.2) in the parameter region $0 < \lambda_1 < \lambda_2 < K$, $1 < b_1 < b_2$, $a_1 < a_2$ and $D_1 > D_2$. For $\epsilon = 0$, conditions for coexistence are given in [3]. In the following sections, all parameters are assumed to be in this region with $\epsilon > 0$ unless stated otherwise.

Chapter 3

Equilibria and their local dynamics

It is easy to see that there are two equilibria of system (2.1.2) on the s-axis, $E_0(0,0,0)$ and $E_1(K,0,0)$. They have very simple local dynamics. The linearizations are

$$\begin{cases} s' &= s \\ x_1' &= -D_1 x_1 \\ x_2' &= -D_2 x_2 \end{cases}$$

at E_0, and

$$\begin{cases} s' &= (K-s) - \frac{m_1 K}{a_1+K} x_1 - \frac{m_2 K}{a_2+K} x_2 (1-g(\epsilon)) \\ x_1' &= f_1(K) x_1 \\ x_2' &= \bar{f}_2(K) x_2 \end{cases}$$

at E_1, where $\bar{f}_2(s) = \frac{m_2 s}{a_2+s}(1-g(\epsilon)) - D_2$. The dynamics at E_0 and E_1 are shown in Figures A.7 and A.8.

Lemma 7 (i). *There exists a unique equilibrium $\bar{P}_1(\bar{\lambda}_1, \bar{x}_1, 0)$ in the $s - x_1$ plane for any $\epsilon > 0$, where $\bar{\lambda}_1 = \lambda_1$, $\bar{x}_1 = x_1^*$. Thus $\bar{P}_1 = P_1$ independent of ϵ.*
(ii). *If $B < 1 - (a_2 + K)/(b_2 K)$, there exists a unique equilibrium $\bar{P}_2(\bar{\lambda}_2, 0, \bar{x}_2)$ in the $s - x_2$ plane for any $\epsilon > 0$, where $\bar{\lambda}_2 = a_2/[b_2(1-g(\epsilon)) - 1]$ and $\bar{x}_2 = a_2(1 - \frac{\bar{\lambda}_2}{K})/[m_2(1-g(\epsilon)) - D_2]$. Thus $\bar{P}_2$ depends on ϵ and $\bar{\lambda}_2$ is increasing in ϵ.*
(iii). *If $g(\epsilon_0) = 1 - \frac{a_2+K}{b_2 K}$ for some $\epsilon_0 > 0$ while $g(\epsilon) < 1 - \frac{a_2+K}{b_2 K}$ for $\epsilon < \epsilon_0$, then $\bar{P}_2$*

collapses to $E_1(K,0,0)$ *when* ϵ *increases to* ϵ_0.
(iv). *For* $\epsilon \geq \epsilon_0$, *there is no equilibrium in the interior of the* $s - x_2$ *plane.*

Proof (i) and (ii) can be easily shown by simple direct calculation. For the monotonicity, one notices that $g(\epsilon)$ is increasing in ϵ. Thus $\bar{\lambda}_2$ is increasing in ϵ. One notices that for $\bar{m}_2 = m_2(1-g(\epsilon))$, (iii) and (iv) are analogous to (iii) of Lemma 4. The only difference is that ϵ is chosen as the bifurcation parameter. One has $\lim_{\epsilon\to\epsilon_0} \bar{\lambda}_2(\epsilon) = K$ and $\lim_{\epsilon\to\epsilon_0} \bar{x}_2(\epsilon) = 0$. Thus $\lim_{\epsilon\to\epsilon_0} \bar{P}_2 = E_1$.

∎

Theorem 1 *For* $\bar{\lambda}_i < K < a_i + 2\bar{\lambda}_i$, *the unique equilibrium* $\bar{P}_i$ *is asymptotically stable in the* $s - x_i$ *plane. A Hopf bifurcation occurs at* $\bar{P}_i$ *when* $a_i + 2\bar{\lambda}_i = K$, *while* $\bar{P}_i$ *loses its stability. The bifurcation generates a unique stable periodic orbit* $\bar{\Gamma}_i$ *around* $\bar{P}_i$ *in the* $s - x_i$ *plane for* $a_i + 2\bar{\lambda}_i < K$, *while* $\bar{P}_i$ *becomes unstable. The orbit* $\bar{\Gamma}_1$ *and its period* T_1 *are independent of* ϵ *while* $\bar{\Gamma}_2$ *and* T_2 *are dependent on* $g(\epsilon)$.

Proof With the absence of one predator, system (2.1.2) reduces to a 2-dimensional one, either

$$\begin{cases} s' &= s(1-\frac{s}{K}) - \frac{m_1 s x_1}{a_1+s} \\ x_1' &= f_1(s)x_1, \end{cases}$$

or

$$\begin{cases} s' &= s(1-\frac{s}{K}) - \frac{m_2 s x_2}{a_2+s}(1-g(\epsilon)) \\ x_2' &= \bar{f}_2(s)x_2. \end{cases}$$

Clearly, the former one does not involve ϵ while the latter one does. With $\bar{m}_2 = m_2(1-g(\epsilon))$, the latter one is analogous to the former one, which is exactly the same as considered in Lemma 4. Thus the proof is similar. Since the former one does not involve ϵ while the latter does, $\bar{\Gamma}_1$ and T_1 are independent of ϵ while $\bar{\Gamma}_2$ and T_2 are dependent on $g(\epsilon)$.

∎

Next consider the interior equilibrium. Notice that $\bar{f}_2$ has similar properties to f_2. Let the right hand side functions of system (2.1.2) equal zero. One has

$$\begin{cases} 1-\frac{s}{K}-\frac{m_1x_1}{a_1+s}-\frac{m_2x_2}{a_2+s}(1-g(\epsilon))=0 \\ f_1(s)=\frac{m_3x_2\epsilon}{y_3(a_3+x_1)} \\ \bar{f}_2(s)=-\frac{m_3x_1\epsilon}{a_3+x_1}. \end{cases} \tag{3.0.1}$$

Obviously $f_1(s)>0$ and $\bar{f}_2(s)<0$ at the equilibrium in the interior of the positive octant. Since $\bar{f}_2(s)$ vanishes at $\bar{\lambda}_2 \geq \lambda_2 > \lambda_1$, then $\lambda_1 < s < \bar{\lambda}_2$. From the third equation of (3.0.1), one has $x_1 = \frac{-a_3\bar{f}_2(s)}{\epsilon m_3+\bar{f}_2(s)}$. Substituting into the second equation, one has $x_2 = \frac{y_3a_3f_1(s)}{\epsilon m_3+\bar{f}_2(s)}$. Substituting both into the first equation, one has

$$(1-\frac{s}{K})-\left(\frac{m_1}{a_1+s}\right)\left(\frac{-a_3\bar{f}_2(s)}{\epsilon m_3+\bar{f}_2(s)}\right)-\left(\frac{m_2(1-g(\epsilon))}{a_2+s}\right)\left(\frac{y_3a_3f_1(s)}{\epsilon m_3+\bar{f}_2(s)}\right)=0.$$

Then

$$[\epsilon m_3+\bar{f}_2(s)](1-\frac{s}{K})+\frac{a_3m_1}{a_1+s}\bar{f}_2(s)-\frac{m_2y_3a_3(1-g(\epsilon))}{a_2+s}f_1(s)=0. \tag{3.0.2}$$

Let $L(s)=m_3(1-s/K), R_1(s)=\frac{m_2y_3a_3f_1(s)}{a_2+s}, \bar{R}_2(s)=-(1-\frac{s}{K}+\frac{a_3m_1}{a_1+s})\bar{f}_2(s)$. Then (3.0.2) becomes

$$\epsilon L(s)+R_1(s)g(\epsilon)=R_1(s)+\bar{R}_2(s). \tag{3.0.3}$$

The right hand side function $R_1(s)+\bar{R}_2(s)$ is positive for $\lambda_1 < s < \bar{\lambda}_2 < K$. It is also uniformly bounded with respect to ϵ since $\bar{f}_2(s)$, the only term involving ϵ, is uniformly bounded and all the other terms are bounded for $\lambda_1 < s < \bar{\lambda}_2$.

Denote the left hand side function of (3.0.3) by $R(s,\epsilon)$. For $\epsilon > 0$ and $s \in (\lambda_1, \bar{\lambda}_2)$, $R(s,0)=0, R(s,\epsilon)>0$, $\lim_{\epsilon\to+\infty} R(s,\epsilon)=+\infty$ uniformly for $B < 1-\frac{a_2+K}{b_2K}$ and

$$\frac{\partial R}{\partial \epsilon}(s,\epsilon)=L(s)+R_1(s)g'(\epsilon)>0.$$

Summarizing the above, one has

Theorem 2 *Suppose* $B < 1 - \frac{a_2+K}{b_2K}$. *For any fixed* $s \in (\lambda_1, \bar{\lambda}_2)$, *there exists* $\epsilon_s > 0$, *such that* (3.0.3) *is satisfied and hence there exists an interior equilibrium. For sufficiently small* ϵ *and large* ϵ, *there is no such equilibrium. Under certain assumptions on the parameters, the uniqueness of the interior equilibrium holds.*

Proof By the above discussion, one knows that for any fixed $s \in (\lambda_1, \bar{\lambda}_2)$, $R(s, \epsilon)$ will intersect the right hand side function for some $\epsilon_s > 0$, thus giving the interior equilibrium $P_0(s_0, x_{10}, x_{20})$ with $\lambda_1 < s_0 < \bar{\lambda}_2$ and $\epsilon_s m_3 + \bar{f}_2(s_0) > 0$. Since the right hand side function attains a positive maximum and minimum, there is no intersection of the functions on each side of equation (3.0.3) for sufficiently small ϵ or large ϵ.

For the conditions of the existence and the uniqueness of the interior equilibrium, more detailed arguments are required. Rewriting (3.0.3), one has

$$\epsilon L(s) - R_1(s)(1 - g(\epsilon)) = \bar{R}_2(s). \tag{3.0.4}$$

Adding $R_3(s) = (m_1 - D_1)(1 - g(\epsilon))m_2 y_3 a_3/(a_2 + s)$ to both sides of (3.0.4), one has

$$\epsilon L(s) - \bar{R}_1(s)(1 - g(\epsilon)) = \bar{R}_2(s) + R_3(s), \tag{3.0.5}$$

where

$$\bar{R}_1(s) = \frac{m_2 y_3 a_3}{a_2 + s}[f_1(s) - (m_1 - D_1)].$$

Before completing the proof, we need several lemmas.

Lemma 8 *Given two positive functions* f *and* h: $\mathbf{R} \to \mathbf{R}^+$. *If both* f *and* h *are decreasing and convex, and if* f'' *and* h'' *exist, then* $f \cdot h$ *is decreasing and convex.*

Proof Since f and g are decreasing and convex, $f', h' \leq 0$, and $f'', h'' \geq 0$. Then $(f \cdot h)' = f' \cdot h + f \cdot h' \leq 0$ and $(f \cdot h)'' = f'' \cdot h + 2f' \cdot h' + f \cdot h'' \geq 0$. Thus $f \cdot h$ is decreasing and convex.

∎

Lemma 9 *Both the left hand side function and the right hand side function of equation* (3.0.5) *are decreasing and convex in* s.

Proof First, $L(s)$ is decreasing and linear, therefore is convex. Secondly, since both $m_2y_3a_3/(a_2+s)$ and $m_1-D_1-f_1(s)$ are positive, decreasing and convex, $-\bar{R}_1(s)=[m_1-D_1-f_1(s)]m_2y_3a_3/(a_2+s)$ is decreasing and convex by Lemma 8. Thirdly, both $-\bar{f}_2(s)$ and $1-s/K+a_3m_1/(a_1+s)$ are positive, decreasing and convex. Thus $\bar{R}_2(s)=-\bar{f}_2(s)(1-s/K+a_3m_1/(a_1+s))$ is decreasing and convex by Lemma 8. Last, $R_3(s)$ is decreasing and convex. Obviously, the sum of decreasing and convex functions is decreasing and convex. This completes the proof. ∎

Lemma 9 describes how the two functions of both sides of equation (3.0.5) can intersect in a simple way. By the construction of (3.0.5) from (3.0.4), the functions of both sides of (3.0.4) intersect in a similar way to the one of (3.0.5). By the arguments of Lemma 9, $L(s)$ and $\bar{R}_2(s)$ are decreasing and convex. There can be two ways in which the functions of both sides of (3.0.4) intersect (see Figures A.9 and A.10),

$$\begin{cases} \epsilon L(\lambda_1) < \bar{R}_2(\lambda_1) \\ \epsilon L(\bar{\lambda}_2) - R_1(\bar{\lambda}_2)(1-g(\epsilon)) > 0 \end{cases} \tag{3.0.6}$$

and

$$\begin{cases} \epsilon L(\lambda_1) > \bar{R}_2(\lambda_1) \\ \epsilon L(\bar{\lambda}_2) - R_1(\bar{\lambda}_2)(1-g(\epsilon)) < 0. \end{cases} \tag{3.0.7}$$

Lemma 10 *If*

$$y_3 < \frac{-f_2(\lambda_1)(a_2+\lambda_2)L(\lambda_2)}{m_2a_3f_1(\lambda_2)}(1+\frac{a_3m_1}{(a_1+\lambda_1)L(\lambda_1)}),$$

B can be chosen small enough such that

$$\frac{R_1(\bar{\lambda}_2(B))}{L(\bar{\lambda}_2(B))} < \frac{R_2(\lambda_1)}{L(\lambda_1)}.$$

Then the interior equilibrium exists for

$$\epsilon \in (\frac{R_1(\bar{\lambda}_2(B))}{L(\bar{\lambda}_2(B))}, \frac{R_2(\lambda_1)}{L(\lambda_1)}),$$

and we have case (3.0.6).

Proof (3.0.6) is equivalent to

$$\frac{R_1(\bar{\lambda}_2)}{L(\bar{\lambda}_2)}(1-g(\epsilon)) < \epsilon < \frac{\bar{R}_2(\lambda_1)}{L(\lambda_1)}.$$

Since $\bar{R}_2(s) > R_2(s)$, where $R_2(s) = -[1 - s/K + a_3 m_1/(a_1+s)]f_2(s)$, it suffices that

$$\frac{R_1(\bar{\lambda}_2)}{L(\bar{\lambda}_2)} < \epsilon < \frac{R_2(\lambda_1)}{L(\lambda_1)}.$$

Notice that $\bar{\lambda}_2$ depends on ϵ. Since $R_1(s)$ is increasing and $L(s)$ is decreasing, $\frac{R_1(s)}{L(s)}$ is increasing. Thus $\frac{R_1(\bar{\lambda}_2)}{L(\bar{\lambda}_2)}$ is increasing in ϵ by (ii) of Lemma 7. To set B, let

$$\frac{R_1(\bar{\lambda}_2(B))}{L(\bar{\lambda}_2(B))} < \frac{R_2(\lambda_1)}{L(\lambda_1)}. \tag{3.0.8}$$

Logically, it is necessary that $\frac{R_1(\lambda_2)}{L(\lambda_2)} < \frac{R_2(\lambda_1)}{L(\lambda_1)}$ when $B = 0$. By the definitions of $R_1(s)$ and $R_2(s)$, one has

$$\frac{m_2 y_3 a_3 f_1(\lambda_2)}{(a_2+\lambda_2)L(\lambda_2)} < \frac{-(L(\lambda_1) + a_3 m_1/(a_1+\lambda_1))f_2(\lambda_1)}{L(\lambda_1)}.$$

Thus

$$y_3 < \frac{-f_2(\lambda_1)(a_2+\lambda_2)L(\lambda_2)}{m_2 a_3 f_1(\lambda_2)}(1 + \frac{a_3 m_1}{(a_1+\lambda_1)L(\lambda_1)}). \tag{3.0.9}$$

Hence one can choose $\epsilon \in (\frac{R_1(\bar{\lambda}_2(B))}{L(\bar{\lambda}_2(B))}, \frac{R_2(\lambda_1)}{L(\lambda_1)})$ to meet (3.0.6) by choosing B small enough such that (3.0.8) holds.

∎

The uniqueness can be obtained by putting further restrictions on the parameters.

Lemma 11 *If* $y_3 \le \frac{a_2(1-B)(a_1+\lambda_1)}{a_1(a_2+\lambda_1)}$ *and* $m_3 \le \frac{1}{\epsilon}[D_2 - m_2 + \frac{(K+a_2)(m_2(1-B)-D_2)^2}{m_2 a_2(1-B)}]$, *then the interior equilibrium is unique.*

Proof Consider the derivatives of the functions of (3.0.5). Let $\epsilon L'(s) - \bar{R}_1'(s)(1 - g(\epsilon)) > \bar{R}_2'(s) + R_3'(s)$ for $s \in (\lambda_1, \bar{\lambda}_2)$ in case (3.0.6). Then the two functions intersect at most once. This gives the uniqueness. This inequality is equivalent to

$$\epsilon L'(s) - R_1'(s)(1-g(\epsilon)) > \bar{R}_2'(s). \tag{3.0.10}$$

In order to show this, it suffices to show that $\epsilon L'(s) - R_1'(s) > \bar{R}_2'(s)$ since $-R_1'(s) < 0$. Direct calculation gives $L'(s) = -m_3/K$, $R_1'(s) = m_2 y_3 a_3[\frac{-f_1(s)}{(a_2+s)^2} + \frac{m_1 a_1}{(a_2+s)(a_1+s)^2}]$ and

$$\bar{R}_2'(s) = -(1 - \frac{s}{K} + \frac{a_3 m_1}{a_1 + s})(1 - g(\epsilon))\frac{m_2 a_2}{(a_2+s)^2} + \bar{f}_2(s)(\frac{1}{K} + \frac{m_1 a_3}{(a_1+s)^2}).$$

Then one has

$$\begin{aligned} &-\epsilon m_3/K - m_2 y_3 a_3[\frac{m_1 a_1}{(a_2+s)(a_1+s)^2} - \frac{f_1(s)}{(a_2+s)^2}] \\ &\quad > -(1 - \frac{s}{K} + \frac{a_3 m_1}{a_1+s})\frac{m_2 a_2(1-g(\epsilon))}{(a_2+s)^2} + \bar{f}_2(s)(\frac{1}{K} + \frac{m_1 a_3}{(a_1+s)^2}). \end{aligned}$$

To show this, it suffices to show that

$$\begin{cases} m_2 y_3 a_3 f_1(s)/(a_2+s)^2 > m_1 a_3 \bar{f}_2(s)/(a_1+s)^2 \\ -\frac{m_2 y_3 a_3 m_1 a_1}{(a_2+s)(a_1+s)^2} \geq -\frac{a_3 m_1 m_2 a_2 (1-g(\epsilon))}{(a_1+s)(a_2+s)^2} \\ -\epsilon m_3/K \geq -(1 - s/K) m_2 a_2 (1 - g(\epsilon))/(a_2+s)^2 + \bar{f}_2(s)/K. \end{cases}$$

The first inequality is obviously true since $\bar{f}_2(s) < 0$. The latter two are equivalent to the system

$$\begin{cases} y_3 \leq \frac{a_2(1-g(\epsilon))(a_1+s)}{a_1(a_2+s)} \\ \epsilon m_3 \leq m_2 a_2 (1 - g(\epsilon))(K - s)/(a_2+s)^2 - \bar{f}_2(s). \end{cases}$$

For the first inequality to hold, it suffices to show that $y_3 \leq \frac{a_2(1-B)(a_1+\lambda_1)}{a_1(a_2+\lambda_1)}$. The second one is equivalent to

$$\begin{aligned} \epsilon m_3 &\leq \frac{m_2(1-g(\epsilon))}{(a_2+s)^2}[a_2(K-s) - s(a_2+s)] + D_2 \\ &= \frac{m_2(1-g(\epsilon))}{(a_2+s)^2}[-(s+a_2)^2 + a_2 K + a_2^2] + D_2 \\ &= D_2 - m_2(1-g(\epsilon)) + \frac{m_2 a_2 (K+a_2)(1-g(\epsilon))}{(a_2+s)^2}. \end{aligned}$$

To show this, it suffices to show that $\epsilon m_3 \leq D_2 - m_2 + \frac{m_2 a_2 (K+a_2)(1-B)}{(a_2+\tilde{\lambda}_2)^2}$, where $\tilde{\lambda}_2 = a_2/[b_2(1-B)-1]$. This is equivalent to

$$\epsilon m_3 \leq D_2 - m_2 + \frac{(K+a_2)(m_2(1-B)-D_2)^2}{m_2 a_2 (1-B)}.$$

Hence if

$$\begin{cases} y_3 & \leq & \frac{a_2(1-B)(a_1+\lambda_1)}{a_1(a_2+\lambda_1)} \\ m_3 & \leq & \frac{1}{\epsilon}[D_2 - m_2 + \frac{(K+a_2)(m_2(1-B)-D_2)^2}{m_2 a_2(1-B)}], \end{cases} \tag{3.0.11}$$

the uniqueness holds. ∎

Lemmas 8 and 10 complete the proof of Theorem 2 in case (3.0.6). Similar results in case (3.0.7) can be obtained in the same way. ∎

Remarks

1. If (3.0.8), (3.0.9) and (3.0.11) hold, there exists a unique equilibrium in the interior of the positive octant.
2. The first inequality of (3.0.11) can be further reduced to $y_3 \leq 1 - B$, since

$$\frac{a_2(a_1+\lambda_1)}{a_1(a_2+\lambda_1)} > 1.$$

This is easier to test in specific cases.

For the unique interior equilibrium P_0, the relation between ϵ and s_0, the s-component of P_0, can be derived by the following theorem.

Theorem 3 *In case of* (3.0.6) *or* (3.0.7), *there exists a function* $\epsilon(s)$ *on the* s-*component of* P_0 *determined by* (3.0.4) *for small* B_1. $\epsilon(s)$ *is decreasing in case* (3.0.6) *and increasing in case* (3.0.7).

Proof Let $F(\epsilon, s) = \epsilon L(s) - R_1(s)(1-g(\epsilon)) - \bar{R}_2(s)$.

$$\begin{aligned} \frac{\partial F}{\partial \epsilon} &= L(s) + R_1(s)g'(\epsilon) - (1 - \frac{s}{K} + \frac{a_3 m_1}{a_1+s})\frac{m_2 s}{a_2+s}g'(\epsilon) \\ &= L(s) + g'(\epsilon)[R_1(s) - (1 - \frac{s}{K} + \frac{a_3 m_1}{a_1+s})\frac{m_2 s}{a_2+s}]. \end{aligned}$$

$R_1(s) - (1 - s/K + a_3m_1/(a_1 + s))m_2s/(a_2 + s)$ is bounded for $\lambda_1 < s < \bar{\lambda}_2$. Since $L(s) > 0$ and $g'(\epsilon) < B_1$, $\frac{\partial F}{\partial \epsilon} > 0$ for small B_1.

By the Implicit Function Theorem (see page 196 of [32] or Appendix B of [8]), there exists a unique function $\epsilon(s)$ satisfying $F(\epsilon(s), s) \equiv 0$. Thus (3.0.4) determines the function $\epsilon(s)$.

Regarding ϵ as a function of s and taking the derivative with respect to s on both sides of (3.0.4), we obtain

$$\epsilon'(s)L(s) + \epsilon(s)L'(s) - R_1'(s)(1 - g(\epsilon)) + R_1(s)g'(\epsilon)\epsilon'(s)$$

$$= \bar{R}_2'(s) + g'(\epsilon)\epsilon'(s)(1 - \frac{s}{K} + \frac{a_3m_1}{a_1 + s})\frac{m_2s}{a_2 + s}.$$

Then

$$\epsilon'(s)[L(s) + R_1(s)g'(\epsilon) - g'(\epsilon)\frac{m_2s}{a_2 + s}(1 - \frac{s}{K} + \frac{a_3m_1}{a_1 + s})]$$

$$= -[\epsilon(s)L'(s) - R_1'(s)(1 - g(\epsilon))] + \bar{R}_2'(s). \qquad (3.0.12)$$

Notice

$$L(s) + g'(\epsilon)[R_1(s) - \frac{m_2s}{a_2 + s}(1 - \frac{s}{K} + \frac{a_3m_1}{a_1 + s})] > 0.$$

as shown above. The right hand side of (3.0.12) is negative in case (3.0.6) by (3.0.10). Thus $\epsilon'(s) < 0$. $\epsilon(s)$ is decreasing. In case (3.0.7), (3.0.10) is reversed. Thus the right hand side of (3.0.12) is positive. Then $\epsilon'(s) > 0$. $\epsilon(s)$ is increasing.

∎

Remark

In Theorem 3, $\epsilon(s)$ should be written as $\epsilon(s_0)$, a function of the s-component s_0 of P_0. However, it may cause misunderstanding. So we omit the subindex for simplicity.

Now consider the local dynamics at $\bar{P}_1$ and $\bar{P}_2$. Notice that Theorem 1 states that Hopf bifurcation in the coordinate plane occurs at $\bar{P}_i$ when $\bar{P}_i$ loses its stability and generates a unique stable periodic orbit $\bar{\Gamma}_i$.

In the direction orthogonal to the plane, the stability depends on ϵ. One can see it clearly with the following theorem.

Notation

By saying the stability in the orthogonal direction, we mean the stability in the direction orthogonal to the coordinate plane.

Theorem 4 *Assume* $\epsilon = 0$.

(i). *For* $\lambda_1 < \lambda_2$, P_2 *is repelling and* P_1 *is attracting in the orthogonal direction.*

(ii). *There is no periodic orbit in any plane* $\theta = \theta_0 \in (0, \pi/2)$, *where* θ_0 *is a constant.*

(iii). (i) *also holds for sufficiently small* $\epsilon > 0$.

Proof (i) Take the same cylindrical substitution as in (2.2.1). Consider θ' at P_i,

$$\theta'(P_1) = \frac{1}{2}[f_2(\lambda_1) - f_1(\lambda_1)]\sin(2 \cdot 0) = 0.$$

$$\theta'(P_2) = \frac{1}{2}[f_2(\lambda_2) - f_1(\lambda_2)]\sin(2 \cdot \frac{\pi}{2}) = 0.$$

$$\frac{\partial \theta'}{\partial \theta}(P_1) = [f_2(\lambda_1) - f_1(\lambda_1)]\cos(2 \cdot 0) = f_2(\lambda_1) < 0.$$

$$\frac{\partial \theta'}{\partial \theta}(P_2) = [f_2(\lambda_2) - f_1(\lambda_2)]\cos(2 \cdot \frac{\pi}{2}) = f_1(\lambda_2) > 0.$$

Thus P_1 is attracting while P_2 is repelling.

(ii) If there is a periodic orbit $(s(t), x_1(t), x_2(t))$ in $\theta = \theta_0 \in (0, \pi/2)$, $\theta(t) \equiv \theta_0$. Thus $\theta'(t) \equiv 0$. Then $f_2(s) - f_1(s) \equiv 0$. By Lemma 3, $s(t) \equiv \bar{s}$, a constant. Then $s'(t) \equiv 0$. From system (2.2.1) $\rho' = \rho f_2(\bar{s})$. For $\lambda_1 < \lambda_2$, $f_2(\bar{s}) \neq 0$. If $f_2(\bar{s}) > 0$, $\rho' > 0$. Thus ρ is unbounded. Hence so are x_1 and x_2, contradicting boundedness. If $f_2(\bar{s}) < 0$, ρ converges to 0. Then both x_1 and x_2 become extinct while s remains constant. This also contradicts the basic assumption. Therefore there is no such periodic orbit.

(iii) The proof will be given in Corollary 1 in Section 5.2.

∎

The local dynamics at $\bar{P}_1$ and $\bar{P}_2$ for small $\epsilon > 0$ are shown in Figure A.11.

Chapter 4

The bifurcations

4.1 A bifurcation theorem

To prove the bifurcations of system (2.1.2), we need a bifurcation theorem for the O.D.E. systems.

Theorem 5 *Consider the O.D.E. system*

$$X' = Z(X, \eta) \tag{4.1.1}$$
$$X \in \mathbf{R^n}, \eta \in \mathbf{R}, \quad Z : \mathbf{R^n} \times \mathbf{R} \to \mathbf{R^n},$$

where η is a parameter. $Z(0, \eta) = 0$ for any $\eta \in \mathbf{R}$. Let $\pi_1(\eta), \cdots, \pi_n(\eta)$ be the n eigenvalues of (4.1.1) at $(0, \eta)$, $Re(\pi_i(\eta))$ the real part of $\pi_i(\eta)$. Suppose $\pi_1(\eta)$ is real and simple, $\pi_1(0) = 0$, and Z is $\mathbf{C^n}$.
(i). *If $\pi_1'(0) > 0, Re(\pi_i(\eta)) < 0, i = 2, \cdots, n$, there exists a unique $\mathbf{C^{n-1}}$ curve ℓ_s of stable equilibria in a small neighborhood of $(0,0)$ in $\mathbf{R^n} \times \mathbf{R^+}$.*
(ii). *If $\pi_1'(0) < 0, Re(\pi_i(\eta)) > 0, i = 2, \cdots, n$, there exists a unique $\mathbf{C^{n-1}}$ curve ℓ_u of unstable equilibria in a small neighborhood of $(0,0)$ in $\mathbf{R^n} \times \mathbf{R^+}$.*
(iii). *If $\pi_1'(0) > 0, Re(\pi_i(\eta)) > 0, i = 2, \cdots, n$, there exists a unique $\mathbf{C^{n-1}}$ curve ℓ_u of unstable equilibria in a small neighborhood of $(0,0)$ in $\mathbf{R^n} \times \mathbf{R^-}$.*
These unique $\mathbf{C^{n-1}}$ curves are tangent to $\mathbf{R^n}$ and the eigenvector of $\pi_1(0) = 0$ at $(0,0)$.

These points and the points of $(0,\eta)$ *are the only equilibria in a small neighborhood of* $(0,0)$.

Proof Consider the flow ϕ^α of (4.1.1) for any fixed $\alpha > 0$.

$$\phi^\alpha : \ \mathbf{R^n} \times \mathbf{R} \to \mathbf{R^n} \quad X(t,\eta) \mapsto X(t+\alpha,\eta).$$

ϕ^α_η has fixed point $(0,\eta)$, at which the n eigenvalues are $\omega_i(\eta) = e^{\pi_i(\eta)}, i = 1,\cdots,n$. $\omega_1(\eta) = e^{\pi_1(\eta)}$ is real and simple, $\omega_1(0) = 1$. ϕ^α_η is $\mathbf{C}^n$ since Z is $\mathbf{C}^n$.

(i). If $\pi_1'(0) > 0$ and $Re(\pi_i(\eta)) < 0, i = 2,\cdots,n$, $\omega_1'(0) = \pi_1'(0)e^{\pi_1(0)} > 0$, the norm $\|\omega_i(\eta)\| = e^{Re(\pi_i(\eta))} < 1, i = 2,\cdots,n$. By the theorem on page 24 in Marsden and McCracken [26] and Ruelle and Takens [28], there exists a unique $\mathbf{C}^{n-1}$ curve ℓ_s of attracting fixed points of ϕ^α in a small neighborhood of $(0,0)$ in $\mathbf{R^n} \times \mathbf{R^+}$. ℓ_s is tangent to $\mathbf{R^n}$ and also tangent to the eigenvector of $\pi_1(0)$ at $(0,0)$. These points of ℓ_s and the points of $(0,\eta)$ are the only fixed points of ϕ^α. Thus the points on ℓ_s are stable equilibria of (4.1.1). These points and the points of $(0,\eta)$ are the only equilibria in a small neighborhood of $(0,0)$.

(ii). Consider the reverse time equation. Taking the substitution $\tau = -t$, one has

$$\frac{dX}{d\tau} = -\frac{dX}{dt} = -Z(X,\eta). \tag{4.1.2}$$

At $(0,\eta)$, (4.1.2) has the eigenvalues $\bar{\pi}_i(\eta) = -\pi_i(\eta), i = 1,\cdots,n$. $\bar{\pi}_1(0) = 0$, $\bar{\pi}_1'(0) > 0$, $Re(\bar{\pi}_i(\eta)) < 0, i = 2,\cdots,n$. By (i), there exists a $\mathbf{C}^{n-1}$ curve ℓ_u of stable equilibria of (4.1.2) in a small neighborhood of $(0,0)$ in $\mathbf{R^n} \times \mathbf{R^+}$. ℓ_u is tangent to $\mathbf{R^n}$ and the eigenvector of $\bar{\pi}_1(0)$ at $(0,0)$. Thus ℓ_u is the $\mathbf{C}^{n-1}$ curve of unstable equilibria of (4.1.1).

(iii). Take the substitution $\tau = -t$, $\zeta = -\eta$, (4.1.1) becomes

$$\frac{dX}{d\tau} = \bar{Z}(X,\zeta), \tag{4.1.3}$$

where $\bar{Z}(X,\zeta) = -Z(X,-\zeta)$ since

$$\frac{dX}{d\tau} = -\frac{dX}{dt} = -Z(X,\eta) = -Z(X,-\zeta).$$

The n eigenvalues at $(0,\zeta)$ are $\beta_i(\zeta) = -\pi_i(-\zeta), i = 1,\cdots,n$. $\beta_1(0) = 0, \beta_1'(0) > 0$. $Re(\beta_i(\zeta)) = -Re(\pi_i(-\zeta)) < 0, i = 2,\cdots,n$. By (i), there exists a unique $\mathbf{C}^{n-1}$ curve ℓ_u of stable equilibria of (4.1.3) in a small neighborhood of $(0,0)$ in $\mathbf{R^n} \times \mathbf{R^+}$. Thus ℓ_u is of unstable equilibria of (4.1.1) in $\mathbf{R^n} \times \mathbf{R^-}$.

∎

4.2 The bifurcation at $\bar{P}_1$ or $\bar{P}_2$ generating an interior equilibrium.

By Theorem 1, Hopf bifurcations occur in the coordinate planes at $\bar{P}_1$ and $\bar{P}_2$. We will show that there is another bifurcation at $\bar{P}_1$ or $\bar{P}_2$ in the direction orthogonal to the plane, that gives birth to the interior equilibrium.

Theorem 6 *The interior equilibrium comes from the bifurcation at $\bar{P}_1$ and collapses to $\bar{P}_2$ for $K < a_i + 2\lambda_i, i = 1,2$,or comes from the bifurcation at $\bar{P}_2$ and collapses to $\bar{P}_1$ for $K > a_i + 2\lambda_i, i = 1,2$ when ϵ increases.*

Proof We consider the limit of the interior equilibrium $P_0(s_0, x_{10}, x_{20})$. Notice P_0 satisfies (3.0.1) and s_0 satisfies (3.0.4). Regard ϵ as a function of s_0 determined by (3.0.4), and take the limit of (3.0.4) as s_0 approximates to λ_1. Then

$$\epsilon_1 L(\lambda_1) = \bar{R}_2(\lambda_1),$$

since $\lim_{s_0\to\lambda_1} R_1(s_0) = 0$, where $\epsilon_1 = \lim_{s_0\to\lambda_1} \epsilon(s_0)$. Plugging into $x_{10} = \frac{-a_3\bar{f}_2(s_0)}{\epsilon m_3 + \bar{f}_2(s_0)}$, one has

$$\lim_{s_0\to\lambda_1} x_{10} = \frac{-a_3\bar{f}_2(\lambda_1)}{\bar{f}_2(\lambda_1) + m_3\bar{R}_2(\lambda_1)/L(\lambda_1)} = \bar{x}_1,$$

while

$$\lim_{s_0\to\lambda_1} x_{20} = \lim_{s_0\to\lambda_1} \frac{y_3 a_3 f_1(s_0)}{\epsilon m_3 + \bar{f}_2(s_0)} = 0.$$

Thus $\lim_{s_0 \to \lambda_1} P_0 = \bar{P}_1$.

Take the linearization of (2.1.2) at $\bar{P}_1$ for any $\epsilon > 0$.

$$\begin{pmatrix} s' \\ x_1' \\ x_2' \end{pmatrix} = V \begin{pmatrix} s \\ x_1 \\ x_2 \end{pmatrix},$$

where

$$V = \begin{pmatrix} 1 - \frac{2\lambda_1}{K} - \frac{m_1 a_1 \bar{x}_1}{(a_1+\lambda_1)^2} & -\frac{m_1\lambda_1}{a_1+\lambda_1} & -\frac{m_2\lambda_1}{a_2+\lambda_1}(1-g(\epsilon)) \\ \frac{m_1 a_1 \bar{x}_1}{(a_1+\lambda_1)^2} & 0 & -\frac{m_3 \bar{x}_1 \epsilon}{y_3(a_3+\bar{x}_1)} \\ 0 & 0 & \bar{f}_2(\lambda_1) + \frac{m_3 \bar{x}_1 \epsilon}{a_3+\bar{x}_1} \end{pmatrix}.$$

It is easy to see that one eigenvalue is

$$\pi_1(\epsilon) = \bar{f}_2(\lambda_1) + \frac{m_3 \bar{x}_1 \epsilon}{a_3 + \bar{x}_1},$$

and its eigenvector crosses the $s - x_1$ plane transversally. The other two eigenvalues satisfy a quadratic equation

$$k^2 - (1 - \frac{2\lambda_1}{K} - \frac{m_1 a_1 \bar{x}_1}{(a_1+\lambda_1)^2})k + \frac{m_1^2 a_1 \lambda_1 \bar{x}_1}{(a_1+\lambda_1)^3} = 0.$$

By the Routh-Hurwitz criterion, the real parts of the eigenvalues have the same sign as

$$\Delta_1 = \frac{1}{2}(1 - \frac{2\lambda_1}{K} - \frac{m_1 a_1 \bar{x}_1}{(a_1+\lambda_1)^2}).$$

$$\Delta_1 \begin{cases} < 0 & \text{if} \quad K < a_1 + 2\lambda_1 \\ = 0 & \text{if} \quad K = a_1 + 2\lambda_1 \\ > 0 & \text{if} \quad K > a_1 + 2\lambda_1. \end{cases}$$

At $\epsilon = \epsilon_1, \pi_1(\epsilon_1) = 0$,

$$\pi_1'(\epsilon_1) = \frac{m_3 \bar{x}_1}{a_3 + \bar{x}_1} - \frac{m_2 \lambda_1}{a_1 + \lambda_1} g'(\epsilon_1) > 0$$

if B_1 is sufficiently small. By Theorem 5, if $K < a_1 + 2\lambda_1$, a stable interior equilibrium is generated from the bifurcation at $\bar{P}_1$ when ϵ increases through ϵ_1; If $K > a_1 + 2\lambda_1$, an unstable interior equilibrium collapses to $\bar{P}_1$ when ϵ increases through ϵ_1. By

Theorem 5, there exists another equilibrium in either case, but it is not in the positive octant. Thus we are not interested in it.

The same discussion can be made for $\bar{P}_2$. Taking the limit of (3.0.4) when s_0 approaches $\bar{\lambda}_2$, one has

$$\epsilon_2 L(\bar{\lambda}_2) - R_1(\bar{\lambda}_2)(1 - g(\epsilon_2)) = 0,$$

where $\epsilon_2 = \lim_{s_0 \to \bar{\lambda}_2} \epsilon(s_0)$. Substituting into $x_{20} = \frac{y_3 a_3 f_1(s_0)}{\epsilon m_3 + f_2(s_0)}$, one has

$$\lim_{s_0 \to \bar{\lambda}_2} x_{20} = \frac{y_3 a_3 f_1(\bar{\lambda}_2)}{\epsilon_2 m_3} = \bar{x}_2,$$

while

$$\lim_{s_0 \to \bar{\lambda}_2} x_{10} = \lim_{s_0 \to \bar{\lambda}_2} \frac{-a_3 \bar{f}_2(s_0)}{\epsilon m_3 + \bar{f}_2(s_0)} = 0.$$

Thus $\lim_{s_0 \to \bar{\lambda}_2} P_0 = \bar{P}_2$.

Take the linearization at $\bar{P}_2$ for any ϵ. Then

$$\begin{pmatrix} s' \\ x_1' \\ x_2' \end{pmatrix} = U \begin{pmatrix} s \\ x_1 \\ x_2 \end{pmatrix},$$

where

$$U = \begin{pmatrix} 1 - \frac{2\bar{\lambda}_2}{K} - \frac{m_2 a_2 \bar{x}_2}{(a_2 + \bar{\lambda}_2)^2}(1 - g(\epsilon)) & -\frac{m_1 \bar{\lambda}_2}{a_1 + \bar{\lambda}_2} & -\frac{m_2 \bar{\lambda}_2}{a_2 + \bar{\lambda}_2}(1 - g(\epsilon)) \\ 0 & f_1(\bar{\lambda}_2) - \frac{m_3 \bar{x}_2 \epsilon}{y_3 a_3} & 0 \\ \frac{m_2 a_2 \bar{x}_2}{(a_2 + \bar{\lambda}_2)^2}(1 - g(\epsilon)) & \frac{m_3 \bar{x}_2 \epsilon}{a_3} & 0 \end{pmatrix}.$$

One eigenvalue is $\pi_1(\epsilon) = f_1(\bar{\lambda}_2) - \frac{m_3 \bar{x}_2 \epsilon}{y_3 a_3}$. Its eigenvector crosses the $s - x_2$ plane transversally. The other two eigenvalues satisfy

$$k^2 - \left[1 - \frac{2\bar{\lambda}_2}{K} - \frac{m_2 a_2 \bar{x}_2}{(a_2 + \bar{\lambda}_2)^2}(1 - g(\epsilon))\right] k + \frac{m_2^2 a_2 \bar{\lambda}_2 \bar{x}_2}{(a_2 + \bar{\lambda}_2)^3}(1 - g(\epsilon))^2 = 0.$$

In the same way as above, by the Routh-Hurwitz criterion, the real parts of the eigenvalues have the same sign as

$$\Delta_2 = \frac{1}{2}[1 - \frac{2\bar{\lambda}_2}{K} - \frac{m_2 a_2 \bar{x}_2}{(a_2 + \bar{\lambda}_2)^2}(1 - g(\epsilon))].$$

$$\Delta_2 \begin{cases} < 0 & \text{if} \quad K < a_2 + 2\bar{\lambda}_2 \\ = 0 & \text{if} \quad K = a_2 + 2\bar{\lambda}_2 \\ > 0 & \text{if} \quad K > a_2 + 2\bar{\lambda}_2. \end{cases}$$

At $\epsilon = \epsilon_2, \pi_1(\epsilon_2) = 0$, and

$$\begin{aligned} \pi_1'(\epsilon_2) &= -\frac{m_3\bar{x}_2}{y_3 a_3} + \frac{m_1 a_1}{(a_1+\bar{\lambda}_2)^2}\bar{\lambda}_2'(\epsilon_2) \\ &= -\frac{m_3\bar{x}_2}{y_3 a_3} + \left(\frac{m_1 a_1}{(a_1+\bar{\lambda}_2)^2}\right)\left(\frac{a_2 b_2 g'(\epsilon_2)}{(b(1-g(\epsilon_2))-1)^2}\right) < 0 \end{aligned}$$

if B_1 is sufficiently small. By Theorem 5, if $K < a_2 + 2\bar{\lambda}_2$, a stable interior equilibrium collapses to $\bar{P}_2$ when ϵ increases through ϵ_2; If $K > a_2 + 2\lambda_2$, an unstable interior equilibrium is generated from $\bar{P}_2$ when ϵ increases through ϵ_2. Similarly, there is another equilibrium by Theorem 5, which has a negative coordinate. So we are not interested in it.

In case (3.0.6), $\epsilon(s_0)$ is decreasing by Theorem 3. So is $s_0(\epsilon)$. Thus $\epsilon_2 < \epsilon_1$. For $K > a_i + 2\lambda_2, i = 1, 2$, when ϵ increases from 0, the bifurcation occurs first at $\bar{P}_2$ with $s_0 = \bar{\lambda}_2$ when $\epsilon = \epsilon_2$. This bifurcation makes $\bar{P}_2$ obtain stability in the orthogonal direction and generates an unstable interior equilibrium P_0. Then when ϵ increases through ϵ_1, a bifurcation occurs at $\bar{P}_1$ with $s_0 = \lambda_1$. This bifurcation makes $\bar{P}_1$ lose its stability and makes P_0 collapse to $\bar{P}_1$. In case (3.0.7), $\epsilon(s_0)$ is increasing by Theorem 3. So is $s_0(\epsilon)$. Thus $\epsilon_1 < \epsilon_2$. For $K < a_i + 2\bar{\lambda}_i, i = 1, 2$, when ϵ increases from 0, a bifurcation occurs first at $\bar{P}_1$ with $s_0 = \bar{\lambda}_1$ when $\epsilon = \epsilon_1$. This bifurcation makes $\bar{P}_1$ lose its stability in the orthogonal direction and generates a stable interior equilibrium P_0. Then when ϵ increases through ϵ_2, a bifurcation occurs at $\bar{P}_2$ with $s_0 = \lambda_2$. This bifurcation makes $\bar{P}_2$ obtain its stability in the orthogonal direction and makes P_0 collapse to $\bar{P}_2$.

∎

4.3 The bifurcations at the limit cycles $\bar{\Gamma}_1$ and $\bar{\Gamma}_2$

In [3], Butler and Waltman showed the existence of the interior periodic orbit coming from the bifurcation at Γ_1 for $\epsilon = 0$. For $\epsilon > 0$, similar results hold when ϵ varies as one of the bifurcation parameters.

We consider the Poincaré map at the limit cycles to show the bifurcation.

Lemma 12 *The spectrum of the linearization of the Poincaré map union* $\{1\}$ *is equal to the spectrum of the linearization of the solution map.*

The proof is on page 60 in Marsden and McCracken [26].

Lemma 13 *One of the Floquet exponents of system* (2.1.2) *at* $\bar{\Gamma}_i, i = 1, 2$, *is negative, another is* 0.

Proof See Butler and Waltman [3].

Theorem 7 *Suppose* $K > a_1 + 2\bar{\lambda}_1$. *When* D_2 *decreases or* ϵ *increases, a bifurcation at* $\bar{\Gamma}_1$ *occurs and generates a stable interior periodic orbit* Γ *while* $\bar{\Gamma}_1$ *loses its stability in the orthogonal direction.*

Proof Consider the Poincaré map Φ at some point of $\bar{\Gamma}_1$. The linearization of (2.1.2) at $\bar{\Gamma}_1$ is

$$\begin{pmatrix} s' \\ x_1' \\ x_2' \end{pmatrix} = A(t) \begin{pmatrix} s \\ x_1 \\ x_2 \end{pmatrix},$$

where

$$A(t) = \begin{pmatrix} 1 - \frac{2s}{K} - \frac{m_1 a_1 x_1}{(a_1+s)^2} & -\frac{m_1 s}{a_1+s} & -\frac{m_2 s}{a_2+s}(1-g(\epsilon)) \\ \frac{m_1 a_1 x_1}{(a_1+s)^2} & f_1(s) & -\frac{m_3 x_1 \epsilon}{y_3(a_3+x_1)} \\ 0 & 0 & \bar{f}_2(s) + \frac{m_3 x_1 \epsilon}{a_3+x_1} \end{pmatrix}.$$

By Lemma 4.2 in Butler and Waltman [3], the third Floquet exponent of Φ at $\bar{\Gamma}_1$ is

$$\begin{aligned} \Lambda_1 &= \frac{1}{T_1}\int_0^{T_1} \bar{f}_2(s) + \frac{m_3 x_1 \epsilon}{a_3 + x_1}\, dt \\ &= -D_2 + \frac{m_2}{T_1}(1 - g(\epsilon)) \int_0^{T_1} \frac{s\, dt}{a_2 + s} + \frac{m_3 \epsilon}{T_1} \int_0^{T_1} \frac{x_1\, dt}{a_3 + x_1}, \end{aligned} \tag{4.3.1}$$

where T_1 is the period of $\bar{\Gamma}_1$. The associated eigenvector crosses the $s - x_1$ plane transversally. Since $\bar{\Gamma}_1$ and T_1 are independent of ϵ by Theorem 1, $\frac{\partial \Lambda_1}{\partial D_2} = -1 < 0$, and

$$\frac{\partial \Lambda_1}{\partial \epsilon} = \frac{m_3}{T_1}\int_0^{T_1} \frac{x_1\,dt}{a_3 + x_1} - \frac{m_2}{T_1} g'(\epsilon)\int_0^{T_1} \frac{s\,dt}{a_2 + s} > 0,$$

if B_1, the bound of $g'(\epsilon)$, is sufficiently small. By Lemmas 12 and 13, Φ has two eigenvalues, one inside the unit circle and the other crossing the unit circle transversally when D_2 decreases or ϵ increases through the value which makes $\Lambda_1 = 0$. By the theorem on page 24 in Marsden and McCracken [26] and Ruelle and Takens [28], a bifurcation occurs at $\bar{\Gamma}_1$ and a unique stable periodic orbit is generated in the interior, while $\bar{\Gamma}_1$ loses its stability in the orthogonal direction. The parameter region is shown in Figure A.12.

When $\epsilon = 0$, $\Lambda_1 = 0$ at $D_2 = D_2^* = \frac{m_2}{T_1}\int_0^{T_1} \frac{s\,dt}{a_2+s}$. It goes back to the case in [3].

A similar result holds for $\bar{\Gamma}_2$.

Theorem 8 *Suppose $K > a_2 + 2\bar{\lambda}_2$. When D_1 or ϵ decreases, a bifurcation at $\bar{\Gamma}_2$ occurs and generates a unique stable interior periodic orbit while $\bar{\Gamma}_2$ loses its stability in the orthogonal direction.*

Proof The proof is similar to that for Theorem 7 except that the third Floquet exponent is

$$\begin{aligned}\Lambda_2 &= \frac{1}{T_2}\int_0^{T_2} f_1(s) - \frac{m_3 x_2 \epsilon}{a_3 y_3} dt \\ &= \frac{m_1}{T_2}\int_0^{T_2} \frac{s\,dt}{a_1 + s} - D_1 - \frac{m_3\epsilon}{a_3 y_3 T_2}\int_0^{T_2} x_2\,dt, \end{aligned} \tag{4.3.2}$$

where T_2 is the period of $\bar{\Gamma}_2$. Both T_2 and $\bar{\Gamma}_2$ are dependent on $g(\epsilon)$ by Theorem 1. Hence $\frac{\partial \Lambda_2}{\partial D_1} = -1 < 0$. The partial derivative of Λ_2 with respect to ϵ can be very

complicated. However, it is very simple if $B = 0$. Then for $B = 0$,

$$\frac{\partial \Lambda_2}{\partial \epsilon} = -\frac{m_3}{a_3 y_3 T_2} \int_0^{T_2} x_2 \, dt < 0.$$

Thus for sufficiently small B and B_1, $\frac{\partial \Lambda_2}{\partial \epsilon} < 0$ by continuity and the differentiability of the solutions on the parameters. Therefore when D_1 or ϵ or both decrease and make Λ_2 change signs, by the same theorems in [26] and [28], a bifurcation occurs at $\bar{\Gamma}_2$, which generates a unique stable periodic orbit, while $\bar{\Gamma}_2$ loses its stability in the orthogonal direction for sufficiently small B and B_1. The parameter region for $B = 0$ is shown in Figure A.13.

Remarks

1. For $\Lambda_1 = 0$, we have ϵ_1^* satisfying $\Lambda_1(\epsilon_1^*, D_2) = 0$, while for $\Lambda_2 = 0$, we have ϵ_2^* satisfying $\Lambda_2(\epsilon_2^*, D_1) = 0$. For certain D_1 and D_2, if $\epsilon_1^* < \epsilon_2^*$, then we know that as ϵ increases from 0 , a bifurcation first occurs at $\bar{\Gamma}_1$ when ϵ increases through ϵ_1^*, which generates a stable interior periodic orbit while making $\bar{\Gamma}_1$ lose its stability. Then, when ϵ increases through ϵ_2^*, a bifurcation occurs at $\bar{\Gamma}_2$ which makes the stable interior periodic orbit collapse to $\bar{\Gamma}_2$ and $\bar{\Gamma}_2$ becomes stable.

2. The interesting thing is that for increasing ϵ, while the interior equilibrium may either come from $\bar{P}_1$ and collapse to $\bar{P}_2$ for $K < a_i + 2\lambda_i, i = 1, 2$, or come from $\bar{P}_2$ and collapse to $\bar{P}_1$ for $K > a_i + 2\lambda_i, i = 1, 2$, the interior periodic orbit only comes from $\bar{\Gamma}_1$ and collapses to $\bar{\Gamma}_2$. The reverse process can never happen for the periodic orbit.

4.4 The simple food chain

Now we consider another extreme case, the food chain model, when $g(\epsilon) = 1$ for $\epsilon \geq \bar{\epsilon} > 0$. Thus (2.1.2) becomes

$$\begin{cases} s' &= s(1 - \frac{s}{K}) - \frac{m_1 s x_1}{a_1 + s} \\ x_1' &= \frac{m_1 s x_1}{a_1 + s} - D_1 x_1 - \frac{m_3 x_1 x_2 \epsilon}{y_3 (a_3 + x_1)} \\ x_2' &= \frac{m_3 x_1 x_2 \epsilon}{a_3 + x_1} - D_2 x_2. \end{cases} \tag{4.4.1}$$

It is easy to see that the system has the equilibria $E_0(0,0,0)$, $E_1(K,0,0)$ and $\bar{P}_1(\bar{\lambda}_1, \bar{x}_1, 0)$. However, $\bar{P}_2$ no longer exists. The periodic orbit $\bar{\Gamma}_1$ also exists for large K, but $\bar{\Gamma}_2$ does not.

In a similar way, we still can consider the steady-state bifurcation at $\bar{\Gamma}_1$.

Theorem 9 *The steady-state bifurcation at $\bar{\Gamma}_1$ generates the stable interior periodic orbit Γ when ϵ increases or D_2 decreases.*

Proof The proof is similar to that of Theorem 7 except that

$$\Lambda_1 = \frac{1}{T_1}\int_0^{T_1} \frac{m_3 x_1 \epsilon}{a_3 + x_1} - D_2\, dt = -D_2 + \frac{\epsilon m_3}{T_1}\int_0^{T_1} \frac{x_1 dt}{a_3 + x_1}.$$

∎

Remark

Since $\bar{\Gamma}_2$ does not exist, this stable interior periodic orbit can not collapse to the $s - x_2$ plane in the same way as before. Instead, it grows large and may collapse in some other ways.

Another difference is that there may exist two interior equilibria in this case.

We consider the system satisfied by the equilibria.

$$\begin{cases} 1 - \frac{s}{K} = \frac{m_1 x_1}{a_1 + s} \\ f_1(s) = \frac{m_3 x_2 \epsilon}{y_3(a_3 + x_1)} \\ \frac{m_3 x_1 \epsilon}{a_3 + x_1} = D_2. \end{cases} \tag{4.4.2}$$

Let (s_0, x_{10}, x_{20}) denote the coordinates of any possible interior equilibrium. From the third equation, one has $x_{10} = \frac{a_3 D_2}{\epsilon m_3 - D_2}$. Plugging into the second equation implies $x_{20} = \frac{y_3 a_3 f_1(s_0)}{\epsilon m_3 - D_2}$. From the first equation, one has

$$(1 - \frac{s_0}{K})(a_1 + s_0) = m_1 x_{10}. \tag{4.4.3}$$

$x_{10} > 0$ implies $\epsilon > D_2/m_3$, which can be guaranteed by $\bar{\epsilon} > D_2/m_3$. $x_{20} > 0$ implies $f_1(s_0) > 0$. Thus $s_0 > \lambda_1$. Denote $H(s) = (1 - \frac{s}{K})(a_1 + s)$, which determines the interior equilibria. It's easy to see that

$$H(s) = -\frac{1}{K}(s - \frac{K - a_1}{2})^2 + \frac{(K + a_1)^2}{4K}.$$

The graph is shown in Figures A.14 and A.15.

Theorem 10 *Suppose* $\bar{\epsilon} > \frac{D_2}{m_3}$.
(i). *There is no interior equilibrium if* $\epsilon < \frac{D_2}{m_3} + \frac{4Km_1a_3D_2}{m_3(K+a_1)^2}$.
(ii). *There exists a unique interior equilibrium if* $\epsilon = \frac{D_2}{m_3} + \frac{4Km_1a_3D_2}{m_3(K+a_1)^2}$ *and* $K > a_1 + 2\lambda_1$.
(iii). *Suppose* $\epsilon > \frac{D_2}{m_3} + \frac{4Km_1a_3D_2}{m_3(K+a_1)^2}$ *and* $K > a_1 + 2\lambda_1$. *If* $\epsilon < \frac{D_2}{m_3} + \frac{m_1a_3D_2}{m_3H(\lambda_1)}$, *there exist two interior equilibria. One of them collapses to* $E_1(K, 0, 0)$, *the other to* $\bar{P}_1$ *when* ϵ *increases. If* $\epsilon \geq \frac{D_2}{m_3} + \frac{m_1a_3D_2}{m_3H(\lambda_1)}$, *there exists a unique interior equilibrium. It collapses to* $E_1(K, 0, 0)$ *when* ϵ *increases.*
(iv). *Suppose* $\epsilon > \frac{D_2}{m_3} + \frac{4Km_1a_3D_2}{m_3(K+a_1)^2}$ *and* $K \leq a_1 + 2\lambda_1$. *If* $\epsilon \leq \frac{D_2}{m_3} + \frac{m_1a_3D_2}{m_3H(\lambda_1)}$, *there exists no interior equilibrium. If* $\epsilon > \frac{D_2}{m_3} + \frac{m_1a_3D_2}{m_3H(\lambda_1)}$, *there exists a unique interior equilibrium. It collapses to* $E_1(K, 0, 0)$ *when* ϵ *increases.*
(v). *There exist at most two interior equilibria for this simple food chain.*

Proof We prove the existence by considering the quadratic function $H(s)$.

(i). If $\epsilon < \frac{D_2}{m_3} + \frac{4Km_1a_3D_2}{m_3(K+a_1)^2}$, then $m_1x_{10} > \frac{(K+a_1)^2}{4K}$, (4.4.3) has no real root. Thus system (4.4.2) has no solution. Therefore there is no interior equilibrium.

(ii). If $\epsilon = \frac{D_2}{m_3} + \frac{4Km_1a_3D_2}{m_3(K+a_1)^2}$, then $m_1x_{10} = \frac{(K+a_1)^2}{4K}$, (4.4.3) has a unique real root $s_0 = (K - a_1)/2$. Thus system (4.4.2) has a unique solution. However, it is in the interior if and only if $s_0 > \lambda_1$. It is equivalent to $\lambda_1 < (K - a_1)/2$.

(iii). Since $\epsilon > \frac{D_2}{m_3} + \frac{4Km_1a_3D_2}{m_3(K+a_1)^2}$, $m_1x_{10} < \frac{(K+a_1)^2}{4K}$. (4.4.3) has two real roots with one on each side of $(K - a_1)/2$. $K > a_1 + 2\lambda_1$ implies $\lambda_1 < (K - a_1)/2$. Thus $H(s)$ is increasing at λ_1. If $\epsilon < \frac{D_2}{m_3} + \frac{m_1a_3D_2}{m_3H(\lambda_1)}$, $H(\lambda_1) < m_1x_{10}$. Then the smaller root of (4.4.3) is greater than λ_1. Thus system 4.4.1 has two interior equilibria with the s-components on both sides of $(K - a_1)/2$. If $\epsilon \geq \frac{D_2}{m_3} + \frac{m_1a_3D_2}{m_3H(\lambda_1)}$, $H(\lambda_1) \geq m_1x_{10}$.

Then the smaller root is not greater than λ_1. Only the greater root of (4.4.3) gives the interior equilibrium. Thus it is unique.

(iv). As in (iii), (4.4.3) has two roots with one on each side of $(K-a_1)/2$. $K \leq a_1+2\lambda_1$ implies $\lambda_1 \geq (K-a_1)/2$. Thus $H(s)$ is decreasing at λ_1. If $\epsilon > \frac{D_2}{m_3} + \frac{m_1 a_3 D_2}{m_3 H(\lambda_1)}$, $H(\lambda_1) > m_1 x_{10}$. Then only the greater root is greater than λ_1, which gives the interior equilibrium of (4.4.1). Thus it is unique. If $\epsilon \leq \frac{D_2}{m_3} + \frac{m_1 a_3 D_2}{m_3 H(\lambda_1)}$, $H(\lambda_1) \leq m_1 x_{10}$. Then no root of (4.4.3) is greater than λ_1. Thus there is no interior equilibrium.

(v). From the above discussion, it's easy to see that there exist at most two interior equilibria.

To consider the bifurcation, one can take the limit of the equilibria as the bifurcation parameter ϵ varies.

First, x_{10} is decreasing in ϵ and converges to 0 when $\epsilon \to \infty$. Secondly, if there exists a unique interior equilibrium, the s-component $s_0 > (K-a_1)/2$ by the above arguments, and $H(s)$ is decreasing at s_0. Since $\lim_{\epsilon\to\infty} x_{10} = 0$, $\lim_{\epsilon\to\infty} H(s_0) = 0$ by (4.4.3). Thus $\lim_{\epsilon\to\infty} s_0 = K$ by (4.4.3) and $\lim_{\epsilon\to\infty} x_{20} = 0$. Hence the interior equilibrium converges to $E_1(K,0,0)$.

If there exist two equilibria, the s-components of the two are on each side of $\frac{K-a_1}{2}$, and $H(s)$ is increasing at the left one and decreasing at the right one. Since $x_{10}(\epsilon)$ is decreasing and $x_{10}(\epsilon) > 0$ for any $\epsilon > \bar{\epsilon}$, $s_0(\epsilon)$ is decreasing for the left one and increasing for the right one by (4.4.3). Therefore as before, for the right one $\lim_{\epsilon\to\infty} x_{10} = 0$, $\lim_{\epsilon\to\infty} x_{20} = 0$, $\lim_{\epsilon\to\infty} s_0 = K$ since $f_1(s)$ is bounded above and $H(s)$ is decreasing. At the left one, $H(s)$ is increasing. Before $\lim_{\epsilon\to\infty} x_{10} = 0$, $\lim_{\epsilon\to\epsilon_0} s_0 = \lambda_1$ for some $\epsilon_0 < \infty$. Thus $\lim_{\epsilon\to\epsilon_0} x_{20} = 0$ and $\lim_{\epsilon\to\epsilon_0} x_{10} = \bar{x}_1$. Therefore the equilibrium converges to $\bar{P}_1(\lambda_1, \bar{x}_1, 0)$. Using Theorem 5, one can analyze the bifurcations in the same way as before. Thus we omit the details.

∎

Chapter 5

The global dynamics

5.1 Persistence

We use the concept of Freedman-Waltman's persistence to describe the global dynamics. See [10].

Definition 3 *A population $\rho(t)$ is said to persist, if $\rho(t) > 0$ for all $t \geq 0$ and $\liminf_{t\to+\infty} \rho(t) > 0$. A system is said to persist if each component population persists.*

We introduce the Freedman-Waltman theorem.

Lemma 14 *[Freedman-Waltman Theorem] The system*

$$\begin{cases} u' &= uf(u,v,w) \\ v' &= vg(u,v,w) \\ w' &= wh(u,v,w), \end{cases} \tag{5.1.1}$$

where $u(0) = u_0 \geq 0$, $v(0) = v_0 \geq 0$, $w(0) = w_0 \geq 0$, persists if the following hypotheses hold.
(H0). *f, g, h are $\mathbf{C}^1$ in (u,v,w).*
(H1). *All solutions of system* (5.1.1) *with non-negative initial conditions are bounded in forward time.*

(H2). *The origin E_0 is unstable in the u-direction and asymptotically stable in the w-direction. There exists a unique equilibrium E_1 on the positive u-axis at $(K_1, 0, 0)$ with no equilibria of the form $(0, K_2, 0)$ or $(0, 0, K_3)$.*
(H3). *E_1 is a hyperbolic saddle point.*
(H4). *Interior to each positive coordinate plane, there is at most one equilibrium, which, if it exists, is unstable in the positive direction orthogonal to that plane, and around which there is no periodic orbit in the plane.*

The proof is in [10].

Theorem 11 *If $K < a_i + 2\lambda_i, i = 1, 2$, system (2.1.2) persists for $\epsilon \in (\epsilon_1', \epsilon_2')$ in case (3.0.7), where ϵ_i' is the bifurcation value at $\bar{P}_i$ in case (3.0.7).*

Proof We check the hypotheses (H0)–(H4) for system (2.1.2). It is easy to see that (H0)–(H3) are satisfied by system (2.1.2). For (H4) we know that system (2.1.2) has $\bar{P}_1$ and $\bar{P}_2$ without $\bar{\Gamma}_1$ and $\bar{\Gamma}_2$. When ϵ increases through the bifurcation value ϵ_1', the equilibrium $\bar{P}_1$ loses its stability in the orthogonal direction. And before ϵ increases to ϵ_2', the bifurcation at $\bar{P}_2$ does not occur. Thus (H4) is satisfied. By Lemma 14, system (2.1.2) persists.

∎

5.2 The global dynamics

Now we consider the global behavior of system (2.1.2) by using the cylindrical coordinate substitution and give some more results on the relation between the dynamics and the survival functions.

By the same cylindrical coordinate substitution as in Lemma 6, system (2.1.2) becomes

$$\begin{cases} s' &= s(1-\frac{s}{K}) - \frac{m_1 s\rho\cos\theta}{a_1+s} - \frac{m_2 s\rho\sin\theta}{a_2+s}(1-g(\theta)) \\ \rho' &= \rho[f_1(s)\cos^2\theta + \bar{f}_2(s)\sin^2\theta + \frac{m_3\rho^2\epsilon\sin 2\theta}{2(a_3+\rho\cos\theta)}(\sin\theta - \frac{\cos\theta}{y_3})] \\ \theta' &= \frac{1}{2}[\bar{f}_2(s) - f_1(s)]\sin 2\theta + \frac{\epsilon m_3\rho(\cos\theta+\sin\theta/y_3)}{2(a_3+\rho\cos\theta)}\sin 2\theta. \end{cases} \tag{5.2.1}$$

From system (5.2.1), one can see clearly that both the two terms involving the consumption of x_2 on x_1 in system (2.1.2) are positive in θ', favouring the growth of x_2. Hence we have the following result that is similar to Lemma 6.

Theorem 12 *Assume $\lambda_1 < \lambda_2$. If $f_1(s)$ and $f_2(s)$ do not intersect in $[0, K]$, x_2 must become extinct for sufficiently small $\epsilon > 0$.*

Proof Since $f_1(s)$ and $f_2(s)$ do not intersect in $[0, K]$ and $\lambda_1 < \lambda_2$, there exists a $\delta > 0$ such that $f_1(s) - f_2(s) > \delta$ for any $s \in [0, K]$. From (5.2.1) we have $\theta' = 1/2[f_2(s) - f_1(s) + G(\epsilon)] \sin 2\theta$, where

$$G(\epsilon) = \frac{-m_2 s g(\epsilon)}{a_2 + s} + \frac{\epsilon m_3 \rho(\cos\theta + \sin\theta/y_3)}{a_3 + \rho\cos\theta}.$$

By Lemma 2, any solutions are eventually uniformly bounded, thus $G(\epsilon) \leq \epsilon m_3[1 + \frac{x_2}{a_3 y_3}] \leq \epsilon C_4$, where C_4 is a positive constant independent of ϵ. Therefore $\theta' < 1/2[-\delta + \epsilon C_4] \sin 2\theta < 0$ for sufficiently small ϵ. Hence θ decreases on $(0, \pi/2)$. Then $\lim_{t\to\infty} \theta(t)$ exists. Denote $\theta^0 = \lim_{t\to\infty} \theta(t)$. If $\theta^0 = 0$, x_2 becomes extinct. If $\theta^0 > 0$, consider the ω-limit set of the flow. There exists a compact invariant set in the ω-limit set in $\theta = \theta^0$. Similarly to Lemma 6, we have $\theta'(t_0) = 0$ for some $t_0 > 0$ satisfying $\theta(t_0) = \theta^0$. This contradicts $\theta'(t) < 0$ for $0 < \theta < \pi/2$.

∎

Corollary 1 *For sufficiently small $\epsilon > 0$ and $\lambda_1 < \lambda_2$, $\bar{P}_1$ is attracting and $\bar{P}_2$ is repelling in the orthogonal direction.*

Proof

$$\theta'(\bar{P}_1) = 1/2[\bar{f}_2(\lambda_1) - f_1(\lambda_1) + G(\epsilon)] \sin 0 = 0.$$

$$\theta'(\bar{P}_2) = 1/2[\bar{f}_2(\bar{\lambda}_2) - f_1(\bar{\lambda}_2) + G(\epsilon)] \sin(2 \cdot \frac{\pi}{2}) = 0.$$

By the argument of Theorem 12, $G(\epsilon) < \min(f_1(\lambda_2), -f_2(\lambda_1))$ for sufficiently small ϵ. Thus

$$\frac{\partial\theta'}{\partial\theta}(\bar{P}_1) = [\bar{f}_2(\lambda_1) - f_1(\lambda_1) + G(\epsilon)] \cos 0 = \bar{f}_2(\lambda_1) + G(\epsilon) < f_2(\lambda_1) + G(\epsilon) < 0.$$

$$\frac{\partial\theta'}{\partial\theta}(\bar{P}_2) = [\bar{f}_2(\bar{\lambda}_2) - f_1(\bar{\lambda}_2) + G(\epsilon)] \cos\pi = f_1(\bar{\lambda}_2) - G(\epsilon) > f_1(\lambda_2) - G(\epsilon) > 0.$$

Therefore $\bar{P}_1$ is attracting while $\bar{P}_2$ is repelling.

∎

Chapter 6

Numerical results for a specific example

We consider a specific example of system (2.1.1) with the following parameters fixed. The numerical results agree with the analytical results we obtained in the previous sections. We draw the graph of the functions or the trajectories of system (2.1.1), instead of giving the analytical expression and the tedious calculation. A Hopf bifurcation is observed and demonstrated numerically. All of the numerical simulations were done using the computer package MatLab, copyrighted by the Math Works Incorporated. The differential equations were solved using the built-in m-file ODE23, which uses the Runge-Kutta's method of order 2–3.

Set $m_1 = 1$, $m_2 = 0.6$, $a_1 = 0.5$, $a_2 = 1$, $D_1 = 0.5$, $K = 2.5$, $r = 3.3$, $y_1 = 0.3$, $y_2 = y_3 = 0.5$, $B = 0$. Then $B_1 = 0$, while D_2 is undetermined and ϵ is the bifurcation parameter. The derived parameters are given by $b_1 = \frac{m_1}{D_1} = 2$, $\lambda_1 = \frac{a_1}{b_1 - 1} = 0.5$, $a_1 + 2\lambda_1 = 1.5 < K$.

On one hand for $b_2 > b_1$, $D_2 < \frac{m_2}{b_1} = 0.3$. On the other hand for $a_2 + 2\lambda_2 < K$, $b_2 > 1 + \frac{2a_2}{K - a_2} = 7/3$, then $D_2 < \frac{m_2}{7/3} = 1.8/7 \approx 0.25714$. Furthermore for $\lambda_1 < \lambda_2$, $b_2 < 1 + \frac{a_2}{\lambda_1} = 3$. Thus $D_2 > \frac{m_2}{3} = 0.2$. Hence the interval of D_2 is $[0.2, 0.25714]$. Therefore we assume $D_2 = 0.2555$. Notice that Γ_1 and Γ_2 are independent of ϵ since $B = 0$.

Clearly this example corresponds to case (3.0.6) by Figures B.1 and B.2. The

function $s_0(\epsilon)$ is decreasing and the intersection of the two functions on both sides of (3.0.4) is unique with the s-component between λ_1 and λ_2.

Taking the linearization of (2.1.1) at the interior equilibrium $P_0(s_0, x_{10}, x_{20})$, one has

$$\begin{pmatrix} s' \\ x_1' \\ x_2' \end{pmatrix} = A_1 \begin{pmatrix} s \\ x_1 \\ x_2 \end{pmatrix},$$

where

$$A_1 = \begin{pmatrix} -\frac{\gamma s_0}{K} + \frac{m_1 s_0 x_{10}}{y_1(a_1+s_0)^2} + \frac{m_2 x_{20} s_0}{y_2(a_2+s_0)^2} & -\frac{m_1 s_0}{y_1(a_1+s_0)} & -\frac{m_2 s_0}{y_2(a_2+s_0)} \\ \frac{m_1 a_1 x_{10}}{(a_1+s_0)^2} & \frac{\epsilon m_3 x_{10} x_{20}}{y_3(a_3+x_{10})^2} & -\frac{\epsilon m_3 x_{10}}{y_3(a_3+x_{10})} \\ \frac{m_2 a_2 x_{20}}{(a_2+s_0)^2} & \frac{\epsilon m_3 a_3 x_{20}}{(a_3+x_{10})^2} & 0 \end{pmatrix}.$$

Here A_1 has been reduced by the system satisfied by $P_0(s_0, x_{10}, x_{20})$, which is similar to (3.0.1). Secondly, the extreme case $\epsilon = 0$ is considered. Figures B.3– B.6 show the stable interior periodic orbit for $D_2 = 0.235$, and x_2 becomes extinct for $D_2 = 0.2555$.

In the following, $D_2 = 0.2555$ is assumed.

Thirdly, the interior stable periodic orbit given by the bifurcation at $\bar{P}_1$ for $\epsilon = 0.06$ is shown in Figures B.7 and B.8, while the cases without such an orbit before the bifurcation for $\epsilon = 0.05$ and after it collapses to $\bar{\Gamma}_2$ for $\epsilon = 0.07$ are shown in Figures B.9–B.12.

Fourthly, Figures C.1 and C.2 show the unstable periodic orbit from the Hopf bifurcation at the interior equilibrium P_0 for $\epsilon = 0.08$ while Figures C.3 –C.6 show the reverse time trajectory near the unstable periodic orbit either diverging to infinity or converging to the equilibrium P_0 . The conditions for the Hopf bifurcation at the interior equilibrium are shown in Figures C.7–C.10.

Finally, Figures C.11–C.14 show the threshold at the Hopf bifurcation for $\epsilon = 0.08$. These also show the instability of the periodic orbit of the Hopf bifurcation.

Remark

Usually, it is not possible to obtain the unstable periodic orbit numerically. Fortunately in this case, the positive real eigenvalue at P_0 is small as shown in Figure C.10.

Thus the equilibrium P_0 is unstable with a little tendency to diverge in this one-dimension. Hence for ϵ near the bifurcation value, the periodic orbit is also unstable in this dimension. One can still obtain the trajectory near the periodic orbit for a period of time before it diverges. Furthermore, one can expect that the periodic orbit is stable in the other 2 dimensions by the Hopf theorem since Figure C.9 shows that for $\epsilon = 0.08$, the real part of the complex eigenvalue is positive. Thus the Hopf bifurcation at the interior equilibrium is numerically demonstrated. This unstable periodic orbit repels the trajectories near it, thus displays a threshold in the interior of the positive octant. No trajectories can go through it.

Chapter 7

Discussion

In this paper, the dynamics of a three species foodweb model for the Michaelis-Menten type response function is considered. The difference of this model from previous ones is that it involves the predator-prey interaction between the two predators x_1 and x_2. This interaction is represented by the terms involving ϵ in the system, where ϵ is the bifurcation parameter. For different amounts of the interaction represented by different values of ϵ, the dynamics are different.

Two extreme cases are observed here, a simple foodchain model with $g(\epsilon) = 1$ for large ϵ and the pure competition foodweb model with $\epsilon = 0$, and $g(\epsilon) = 0$. These two extreme cases have considerably different dynamics. For example, consider the interior equilibria. There is none for $\epsilon = 0$ in general, and there may be one or two or none for $g(\epsilon) = 1$. Thus our model unifies the two extreme cases and includes each as a limiting case. The dynamics, as expected, inherits some properties of the extreme ones.

First, the bifurcation at the equilibrium $\bar{P}_i$ in the $s - x_i$ plane with increasing ϵ gives birth to the interior equilibrium P_0, which does not exist in the pure competition case $\epsilon = 0$ in general, except $\lambda_1 = \lambda_2$. The existence and the uniqueness are given by fundamental analysis and the Implicit Function Theorem.

Secondly, the bifurcation at the periodic orbit $\bar{\Gamma}_1$ generates the stable interior periodic orbit Γ with either increasing ϵ or decreasing D_2 or both. This stable periodic orbit Γ collapses to $\bar{\Gamma}_2$ with increasing ϵ or increasing D_1 or both. This work is similar

to Butler and Waltman [3], but with different parameters . The bifurcation regions are also given.

The interesting thing is that for increasing ϵ, while the interior periodic orbit Γ can only bifurcate from $\bar{\Gamma}_1$ and collapse to $\bar{\Gamma}_2$, the equilibrium P_0 may either bifurcate from $\bar{P}_1$ and collapse to $\bar{P}_2$ or from $\bar{P}_2$ to $\bar{P}_1$, which is determined by either (3.0.6) and $K > a_i + 2\bar{\lambda}_i$ or (3.0.7) and $K < a_i + 2\bar{\lambda}_i, i = 1, 2$.

Thirdly, some global results are given by studying the survival functions and using the cylindrical coordinate substitution. Although the survival functions have already been defined by Hale and Somolinos in [15], they were not further studied. From Theorem 12, one can see that for sufficiently small ϵ these functions play a dominant role. They determine the victor in the competition. Thus one can conclude that if the intrinsic character is weaker, such as $f_2(s) < f_1(s)$, the predator x_2 will die out even though it may consume a small amount of its rival, the predator x_1. Lemma 6 gives the relation between the coexistence and the survival functions: coexistence implies the intersection of the two survival functions. Theorem 4 states that coexistence occurs in such a way that the ratio of the densities of the two predators can not be kept constant. Thus any attempt to keep it constant violates the natural rule. Such a property may be used in any similar case either in ecology or in environmental or social sciences. Furthermore, persistence is considered by using a theorem of Freedman and Waltman.

Finally, numerical results for a specific set of parameters with $B = 0$ show the existence of the interior equilibrium. It is demonstrated that the bifurcation at $\bar{\Gamma}_1$ gives birth to the stable interior periodic orbit , which collapses to $\bar{\Gamma}_2$ with increasing ϵ. It is also observed that a Hopf bifurcation occurs at the interior equilibrium and generates an unstable interior periodic orbit. Usually one cannot numerically obtain the unstable periodic orbit due to the instability. However the positive eigenvalue at the equilibrium, thus the Floquet exponent at the periodic orbit, is fortunately so small that the trajectory stays close to the periodic orbit for a long period of time before it diverges. We are thus fortunate enough to obtain this unstable periodic orbit numerically. This unstable periodic orbit displays a threshold near the equilibrium, which is also numerically shown. Thus when the initial value is relatively close to the

$s-x_i$ plane, the trajectory is repelled away from the equilibrium and the periodic orbit due to the instability, and goes towards to the $s-x_i$ plane. It places a barrier against the rival of x_i to win. This shows that the competition is in favor of the predator x_i if the initial value of x_i is relatively large enough, and may result in the extinction of the other. But in the specific case considered in Chapter 6, the trajectory can not collapse to the periodic orbit $\bar{\Gamma}_1$ since $\bar{\Gamma}_1$ is repelling in the orthogonal direction after the bifurcation. Thus the trajectory either goes to $\bar{P}_1$ along a one-dimensional manifold in the extreme case or goes around for a long period of time and then converges to an attractor, such as $\bar{\Gamma}_2$. Due to the Hopf bifurcation, there is an interval of the parameter ϵ such that there exists two interior periodic orbits simultaneously, one stable from $\bar{\Gamma}_1$, and the other unstable from the Hopf bifurcation at the interior equilibrium. In the specific case in Chapter 6, the numerical results in Figures C.7–C.10 show that the Hopf bifurcation occurs before the steady-state bifurcation at $\bar{\Gamma}_1$. Even after the stable periodic orbit collapses to $\bar{\Gamma}_2$, the unstable periodic orbit still exists in the interior. This periodic orbit for $\epsilon = 0.08$ can be numerically proved not to be the stable one because the stable one collapses to $\bar{\Gamma}_2$ before $\epsilon = 0.07$. And numerically its instability is shown both in forward time and backward time in Figures C.11–C.14 and C.3–C.6.

From the above, one can have a clear view. First, there is no interior equilibrium for small ϵ. Then bifurcation gives birth to the interior equilibrium when ϵ increases. From this equilibrium, a Hopf bifurcation may present an unstable periodic orbit. For large ϵ such that $g(\epsilon) = 1$, there may exist even two equilibria in the interior. Finally when ϵ increases large enough, the bifurcation shows that the interior equilibria will collapse to some equilibria on the boundary. Thus for different amounts of the predation interaction between the two predators, the dynamics are considerably different.

Appendix A

The figures

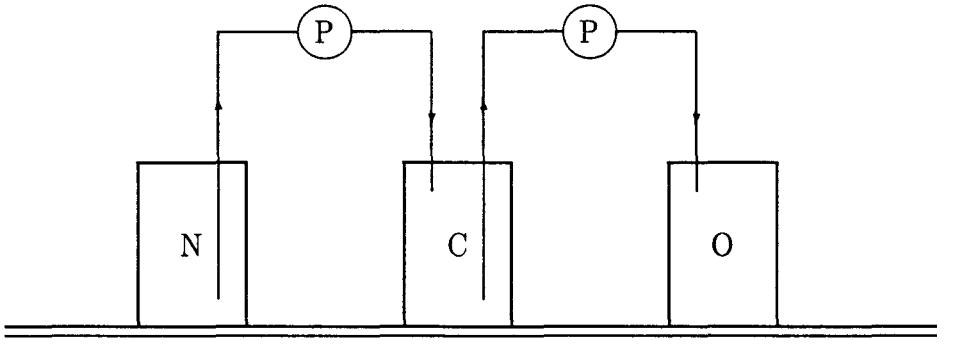

Figure A.1: A schematic diagram of the chemostat.

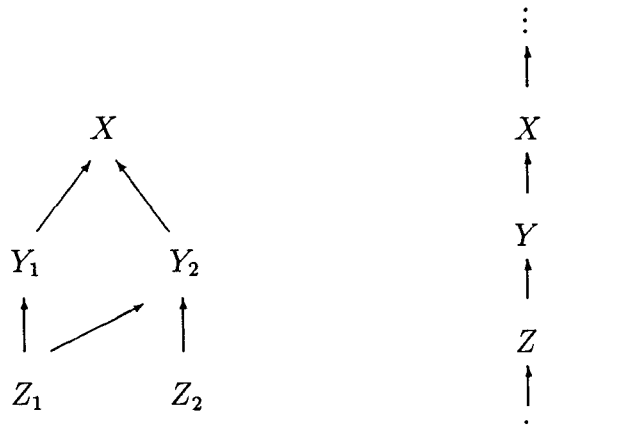

A foodweb A foodchain

Figure A.2: The foodweb and foodchain.
The arrows represent the consumption of the bottom species feeding on the top ones.

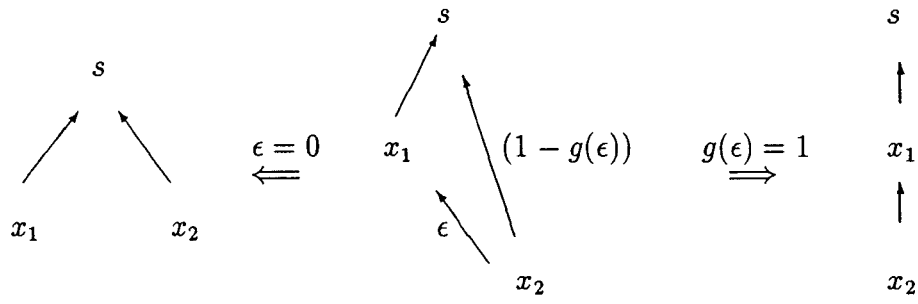

Figure A.3: The model interaction.

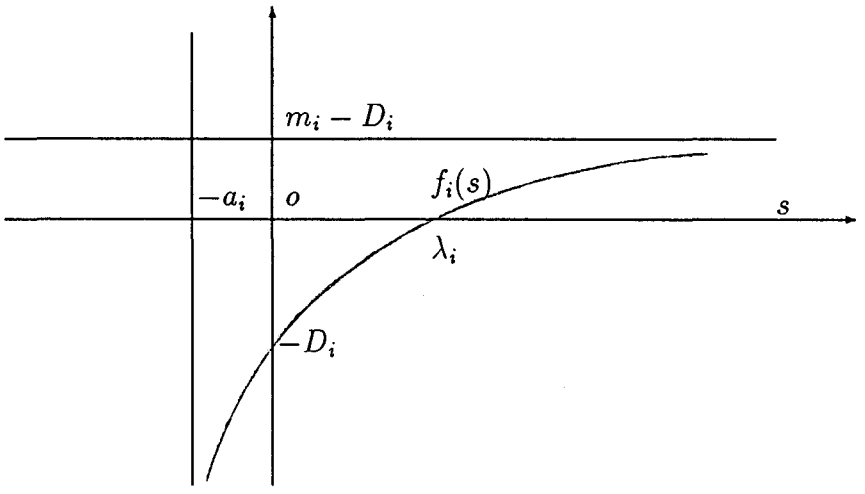

Figure A.4: The graph of the survival function $f_i(s)$.

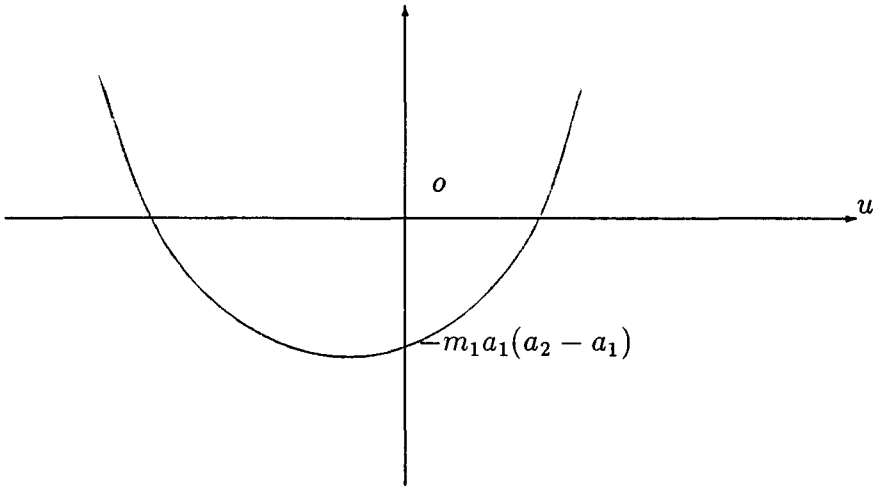

Figure A.5: The graph of the quadratic function $Mu^2 + Nu - m_1a_1(a_2 - a_1)$.

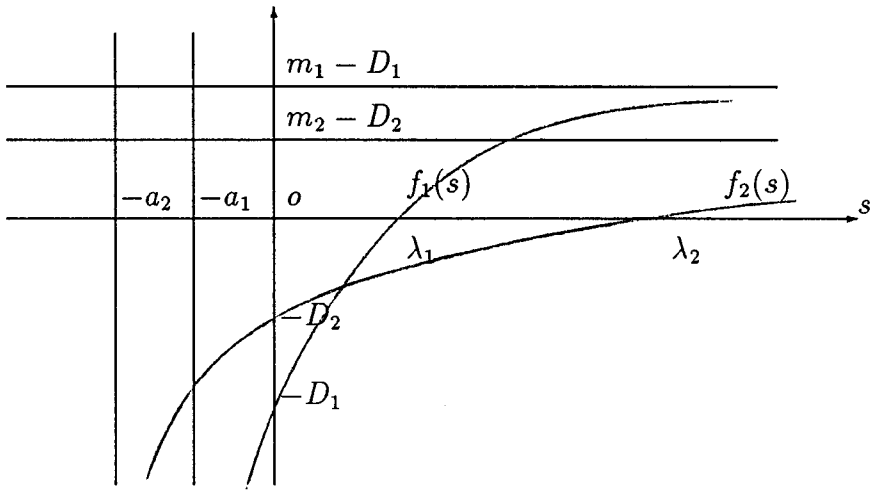

Figure A.6: The intersection of $f_1(s)$ and $f_2(s)$.

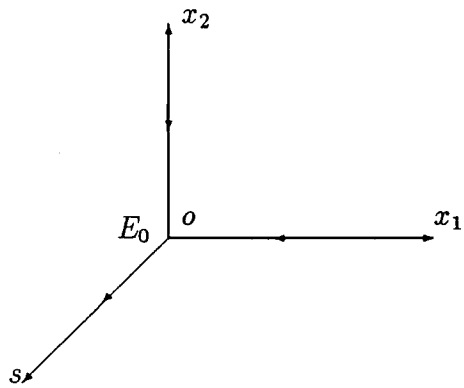

Figure A.7: The dynamics at E_0.

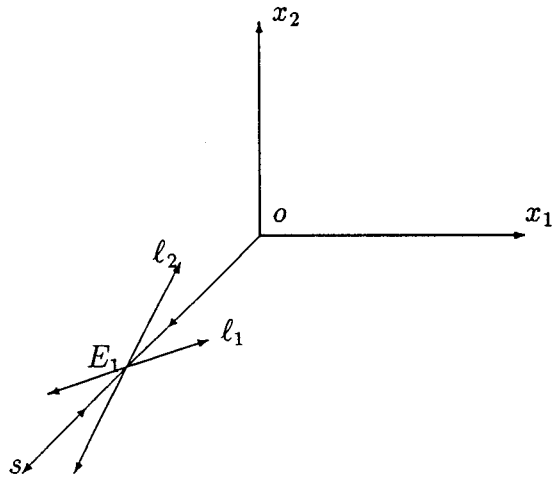

Figure A.8: The dynamics at E_1. ℓ_i is in $s - x_i$ plane, $i = 1, 2$.

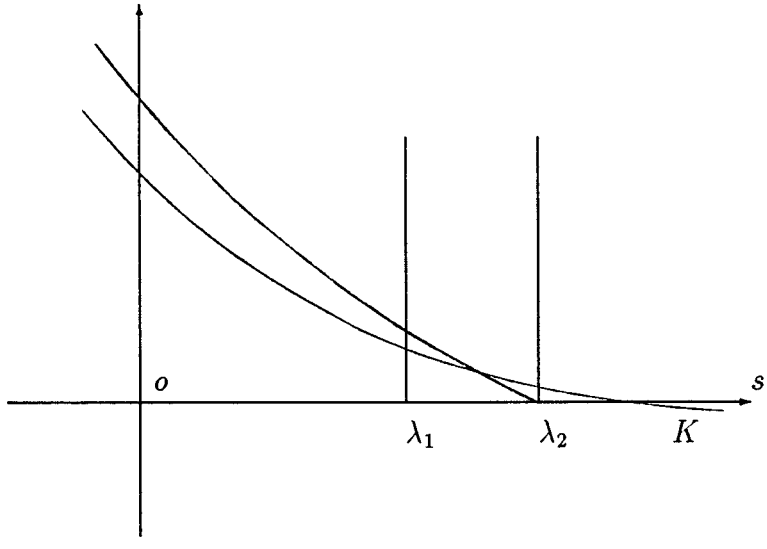

Figure A.9: The intersection of the functions in equation (3.0.4) in the case (3.0.6).

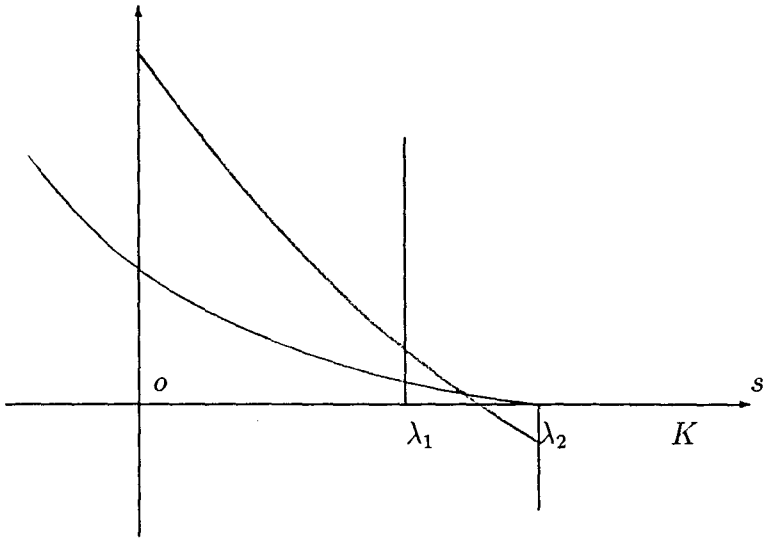

Figure A.10: The intersection of the functions in equation (3.0.4) in the case (3.0.7).

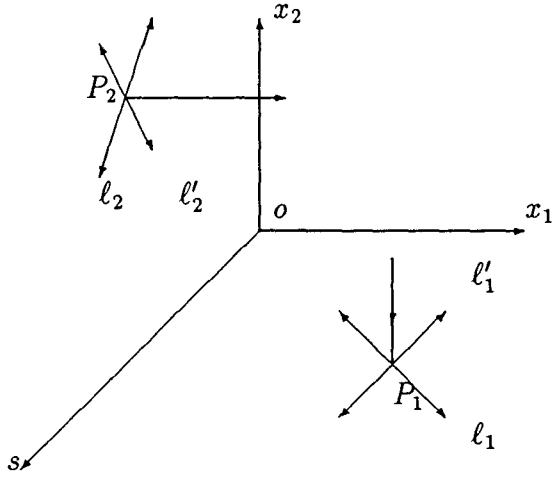

Figure A.11: The local dynamics at $\bar{P}_1$ and $\bar{P}_2$ for small $\epsilon > 0$ and $K > a_i + 2\bar{\lambda}_i$. ℓ_i, ℓ_i' are in $s - x_i$ plane, $i = 1, 2$.

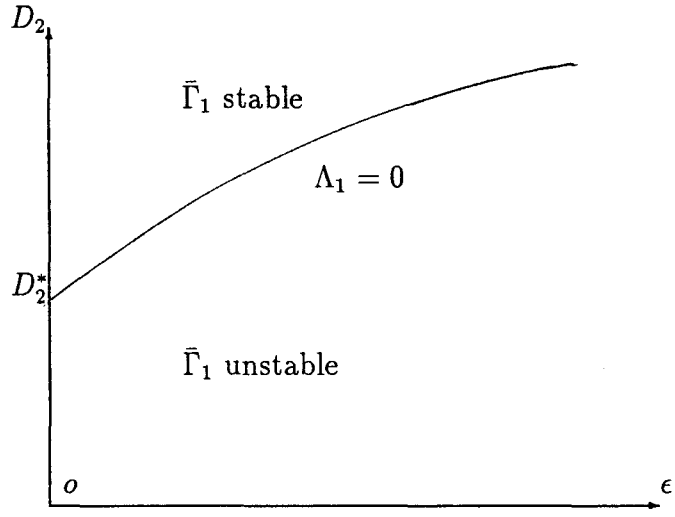

Figure A.12: The parameter region of the bifurcation at $\bar{\Gamma}_1$.

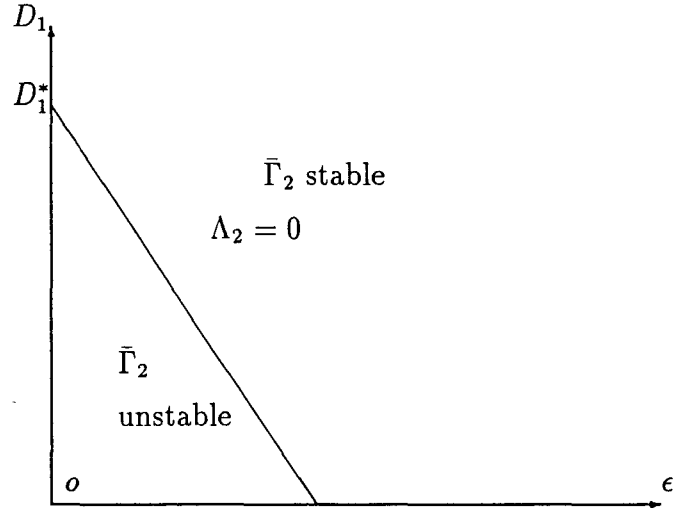

Figure A.13: The parameter region of the bifurcation at $\bar{\Gamma}_2$ for $B = 0$.

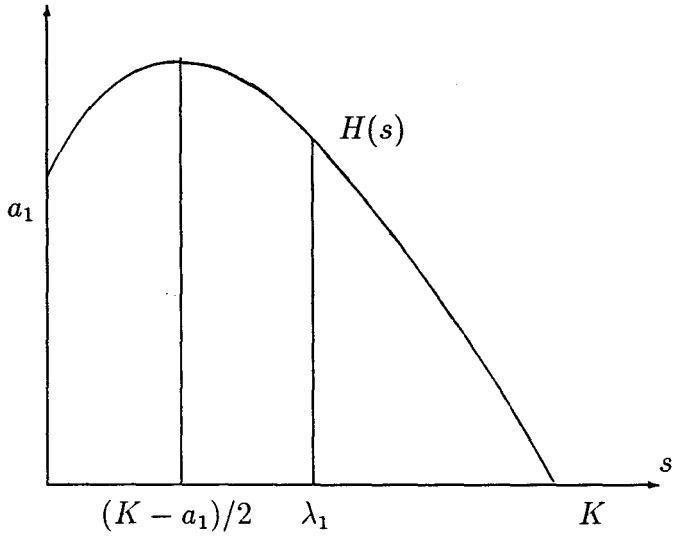

Figure A.14: The quadratic function $H(s)$ with $K < a_1 + 2\lambda_1$.

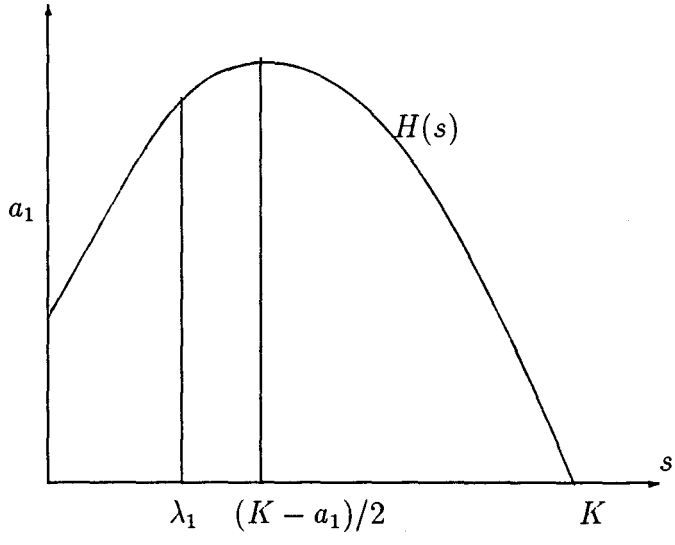

Figure A.15: The quadratic function $H(s)$ with $K > a_1 + 2\lambda_1$.

Appendix B

The graphs of the equilibrium and the stable periodic orbit in the interior of the positive octant

Illustration

In the $t - s, x_1, x_2$ graphs,

——— represents the $t - s$ curves;

$- - -$ represents the $t - x_1$ curves;

$\cdots\cdots$ represents the $t - x_2$ curves.

In the $s - x_1, x_2$ graphs,

$- - -$ represents the $s - x_1$ curves;

$\cdots\cdots$ represents the $s - x_2$ curves.

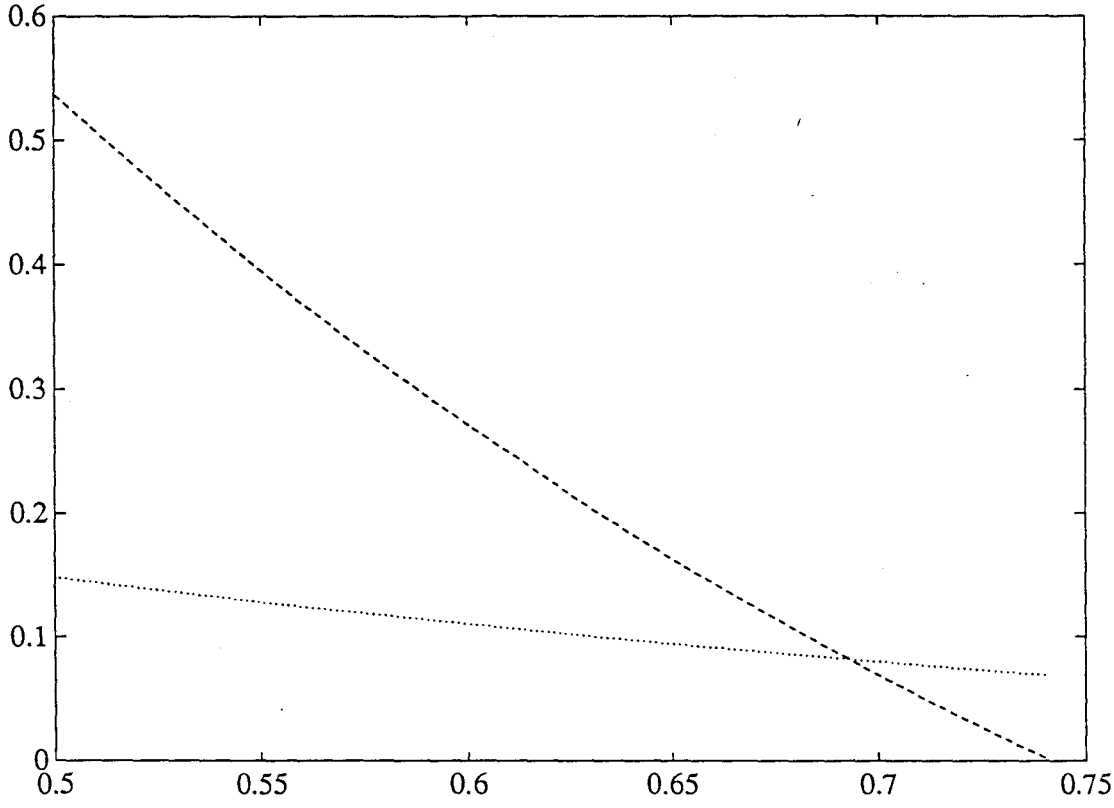

Figure B.1: The unique interior equilibrium given by the unique intersection of the functions of (3.0.4) with $\epsilon = 0.06, D_2 = 0.2555$ and $K = 2.5$.

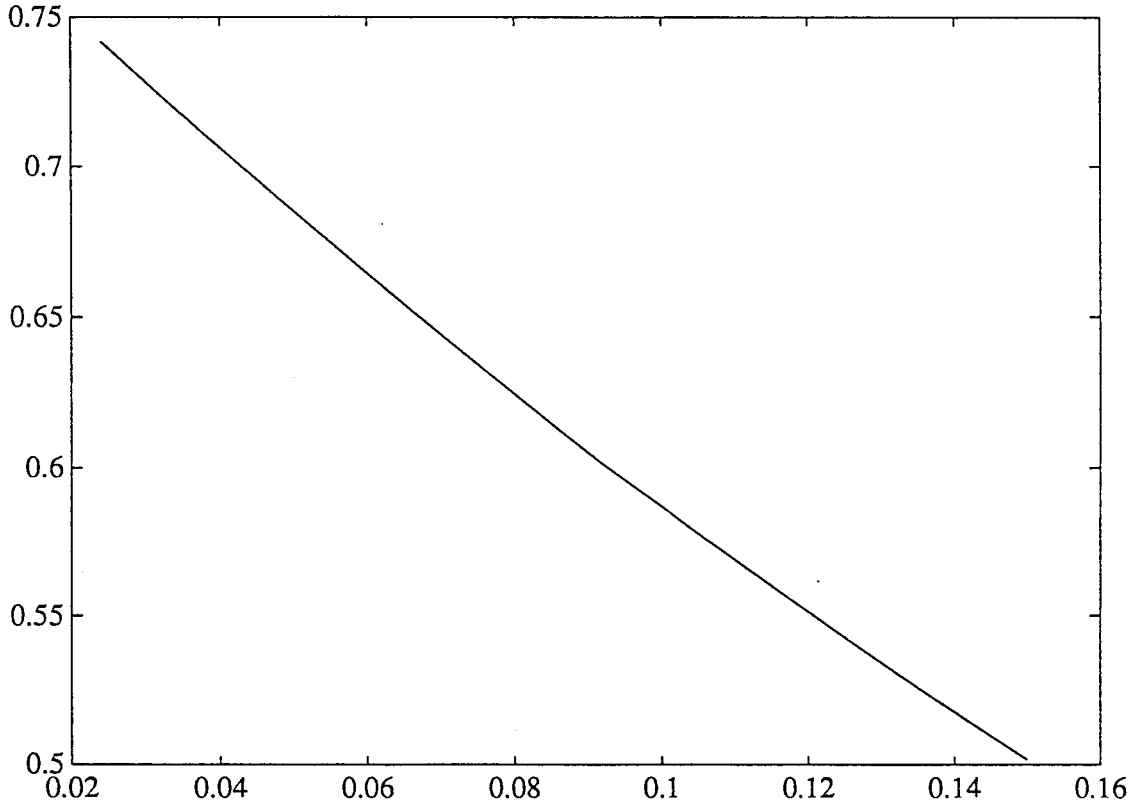

Figure B.2: The dependence of the s-component of the interior equilibrium on ϵ with $D_2 = 0.2555$ and $K = 2.5$.

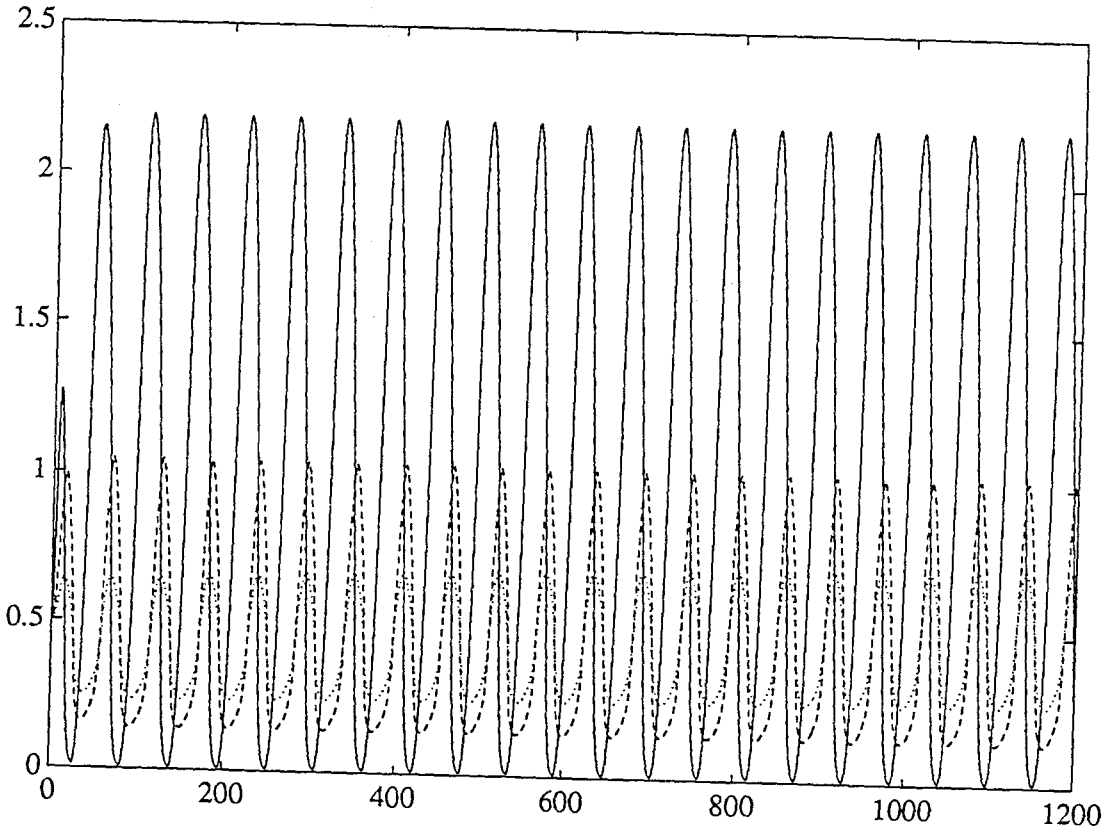

Figure B.3: The $t - s, x_1, x_2$ graphs for the stable interior periodic orbit with $\epsilon = 0$, $D_2 = 0.235$ and the initial value $(0.5, 0.5, 0.5)$.

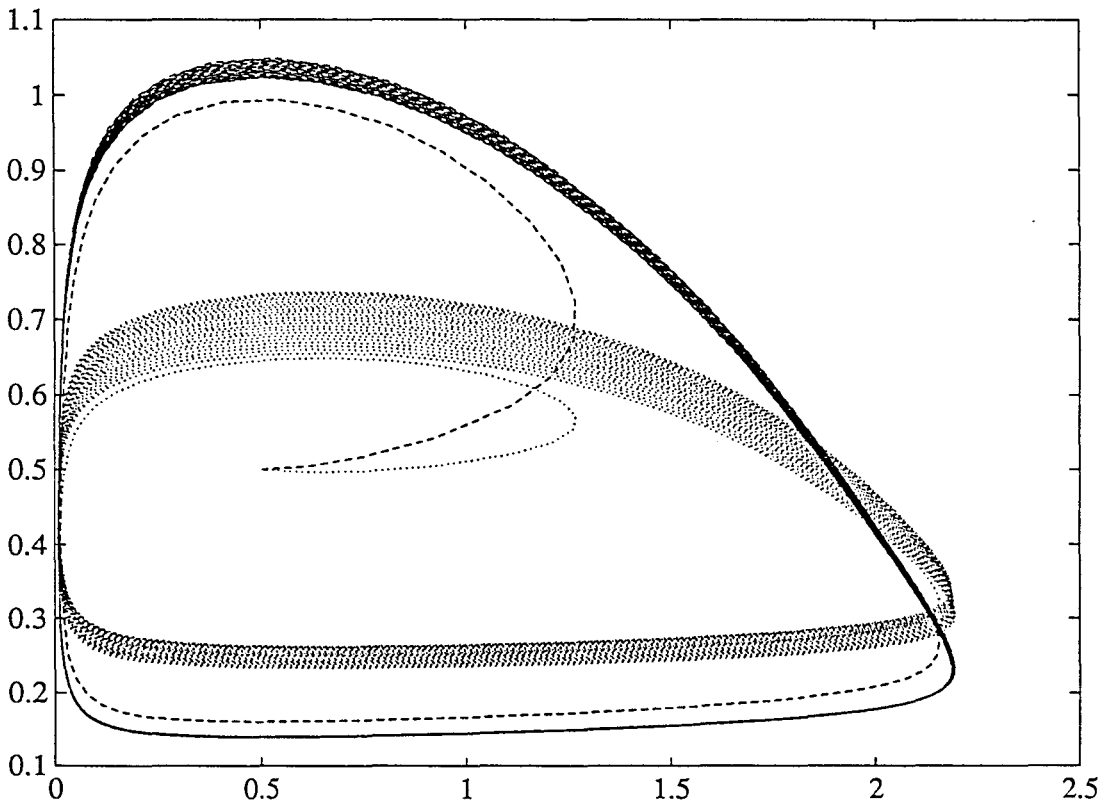

Figure B.4: The $s - x_1, x_2$ graphs under the same conditions as in Figure B.3.

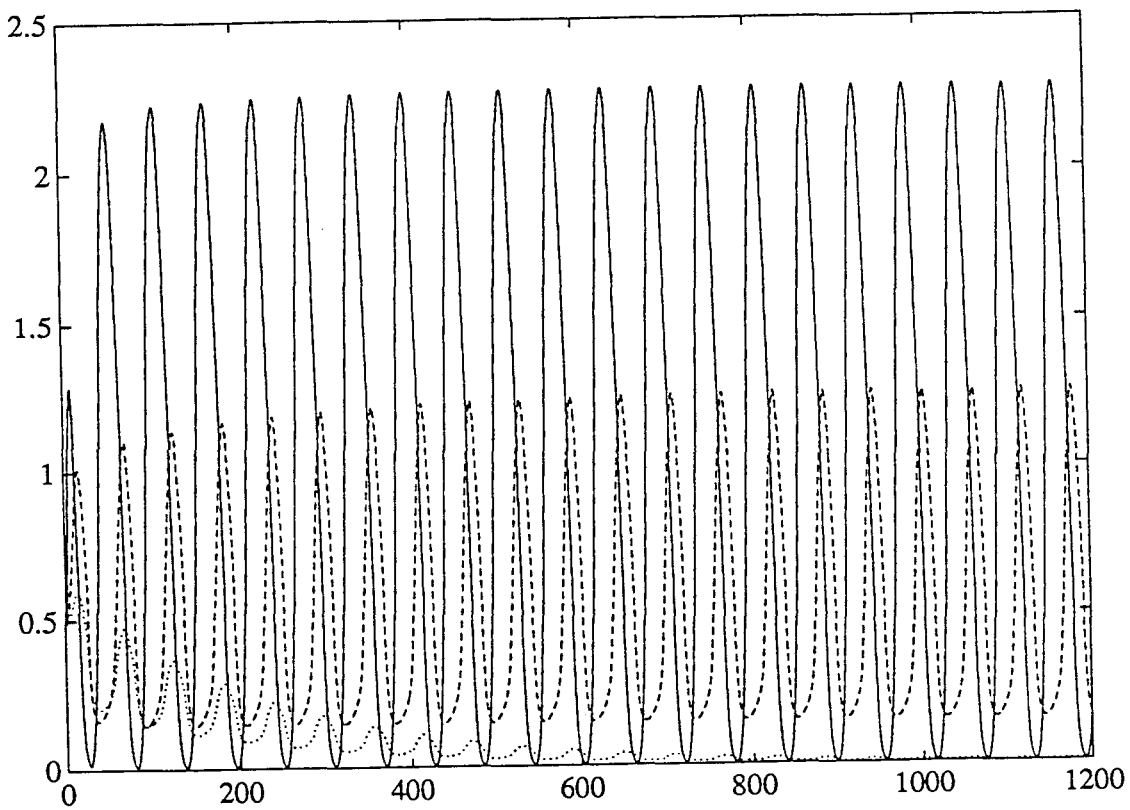

Figure B.5: The $t-s, x_1, x_2$ graphs of the extinction of x_2 with $\epsilon = 0$, $D_2 = 0.2555$ and initial value $(0.5, 0.5, 0.5)$.

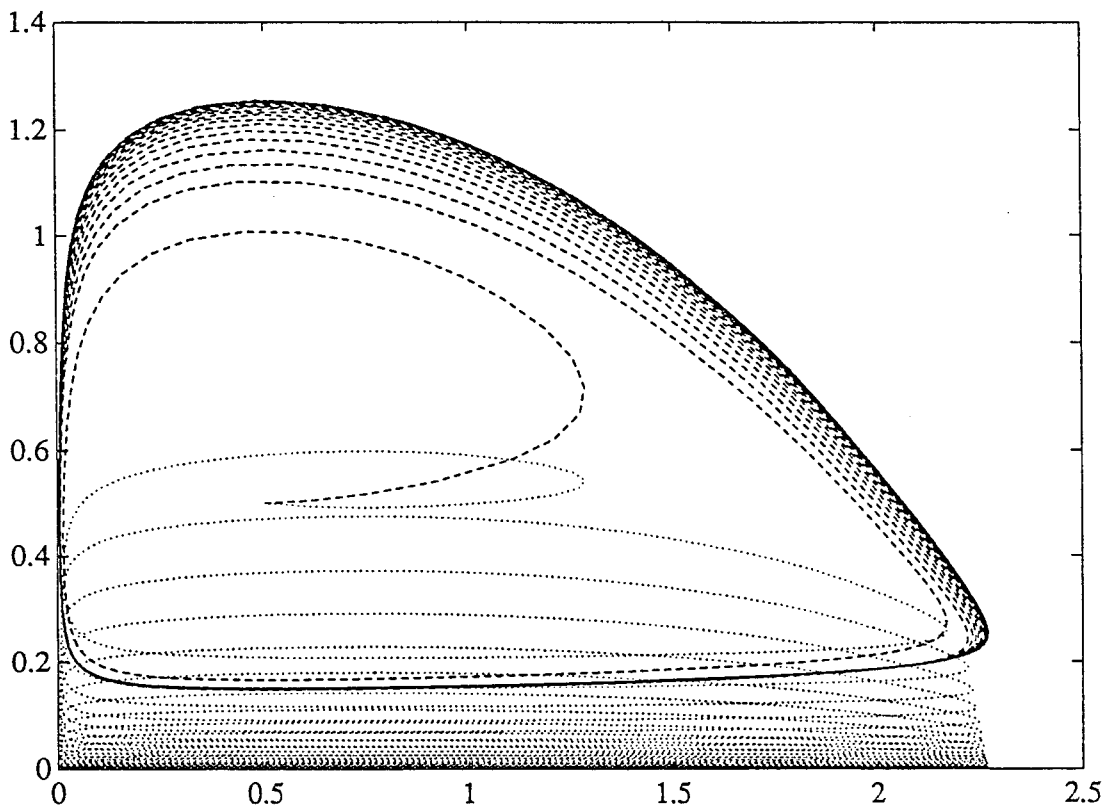

Figure B.6: The $s - x_1, x_2$ graphs under the same conditions as in Figure B.5.

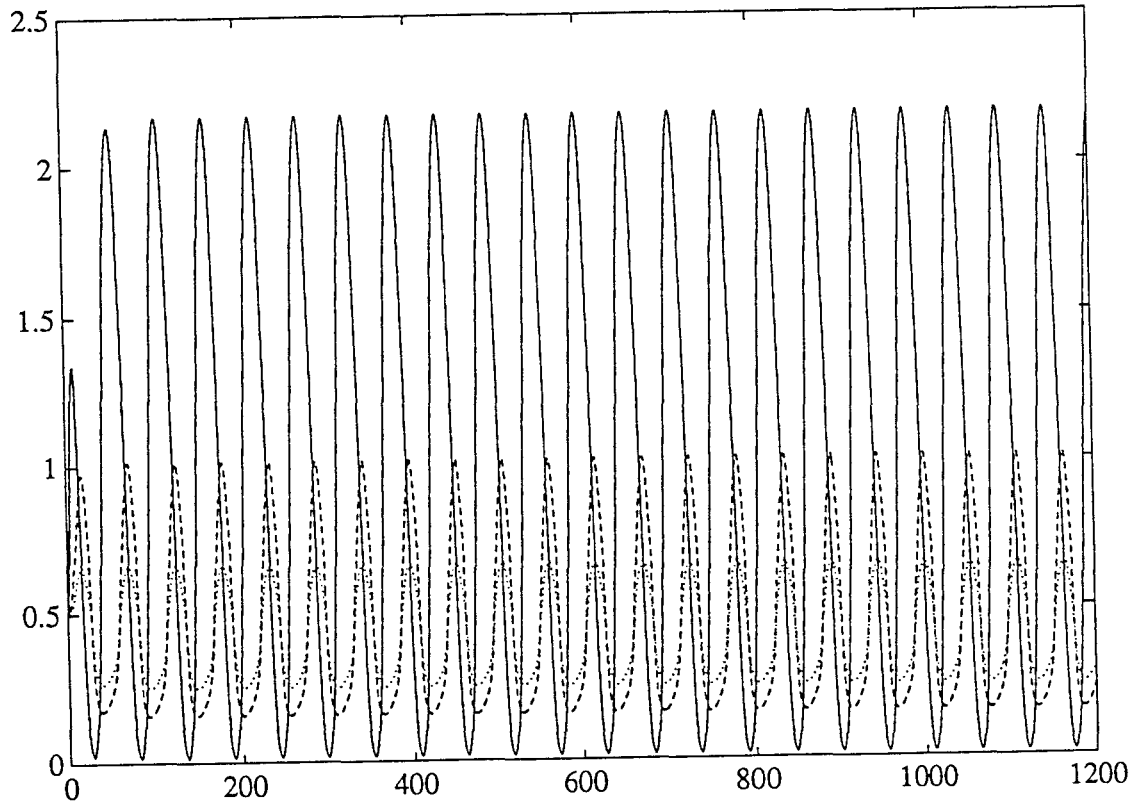

Figure B.7: The $t-s, x_1, x_2$ graphs of the stable interior periodic orbit with $\epsilon = 0.06$, $D_2 = 0.2555$ and the initial value $(0.5, 0.5, 0.5)$.

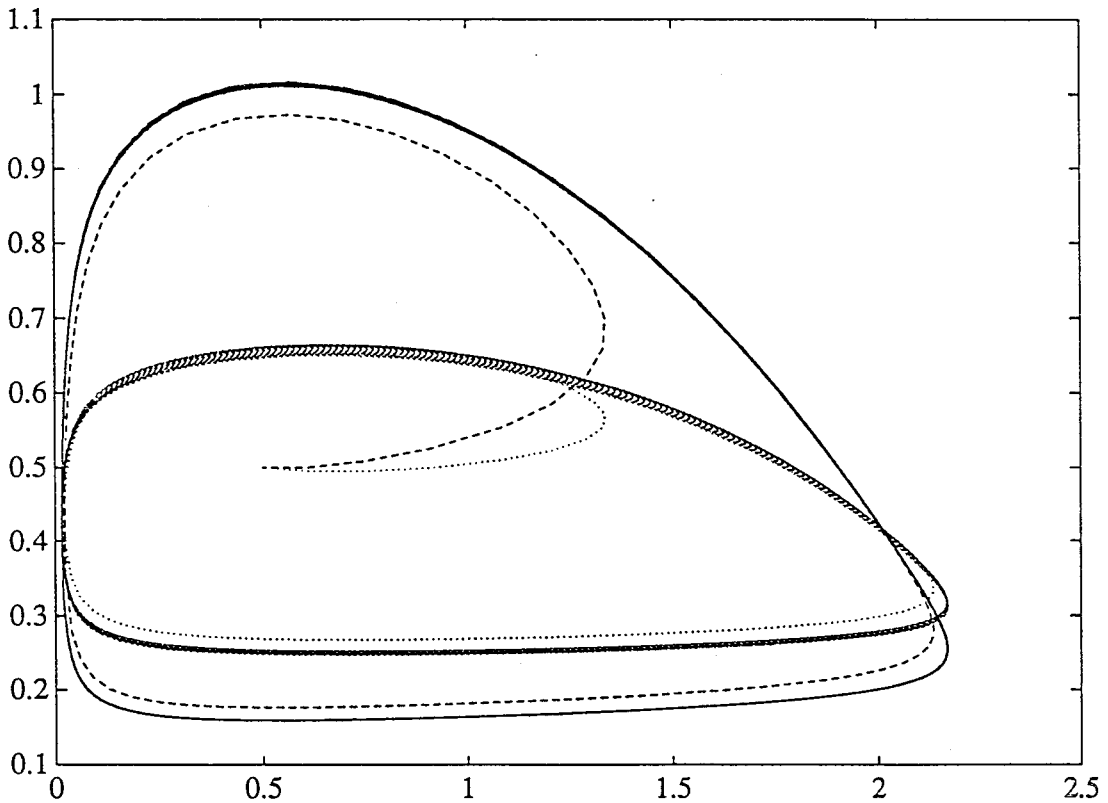

Figure B.8: The $s - x_1, x_2$ graphs under the same conditions as in Figure B.7.

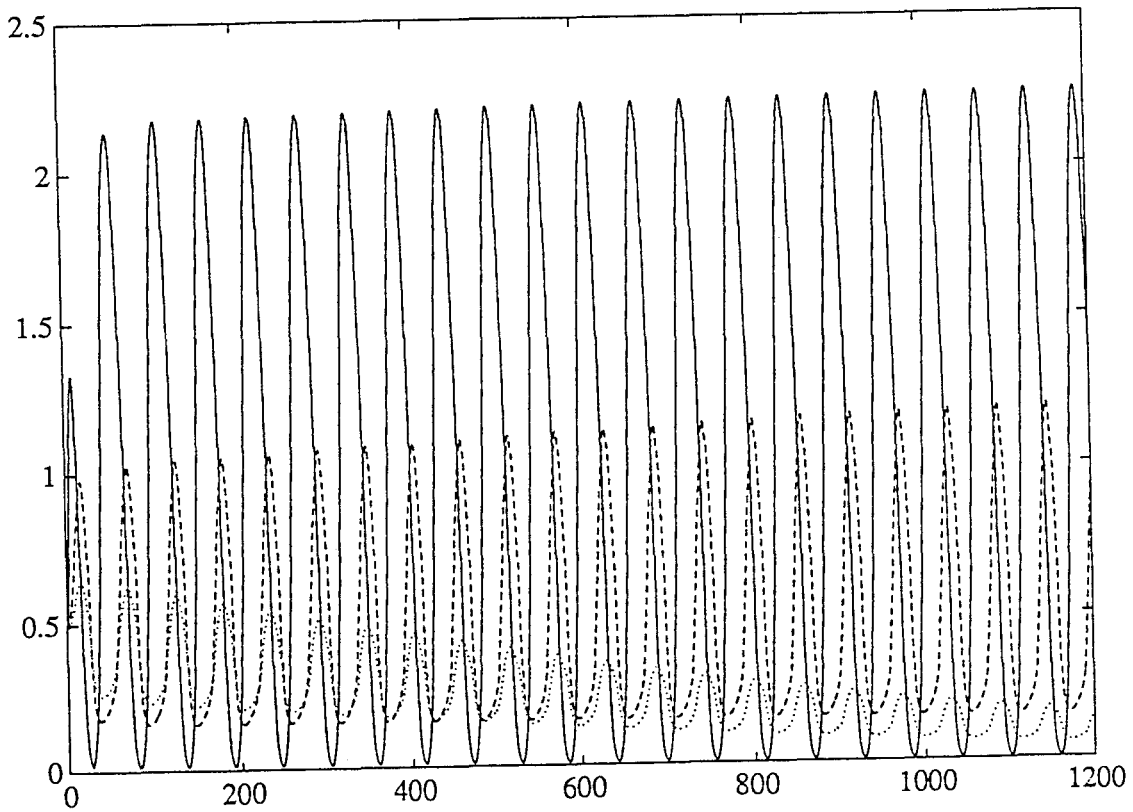

Figure B.9: The $t-s, x_1, x_2$ graphs before the bifurcation at $\bar{\Gamma}_1$ occurs with $\epsilon = 0.05$, $D_2 = 0.2555$ and the initial value $(0.5, 0.5, 0.5)$.

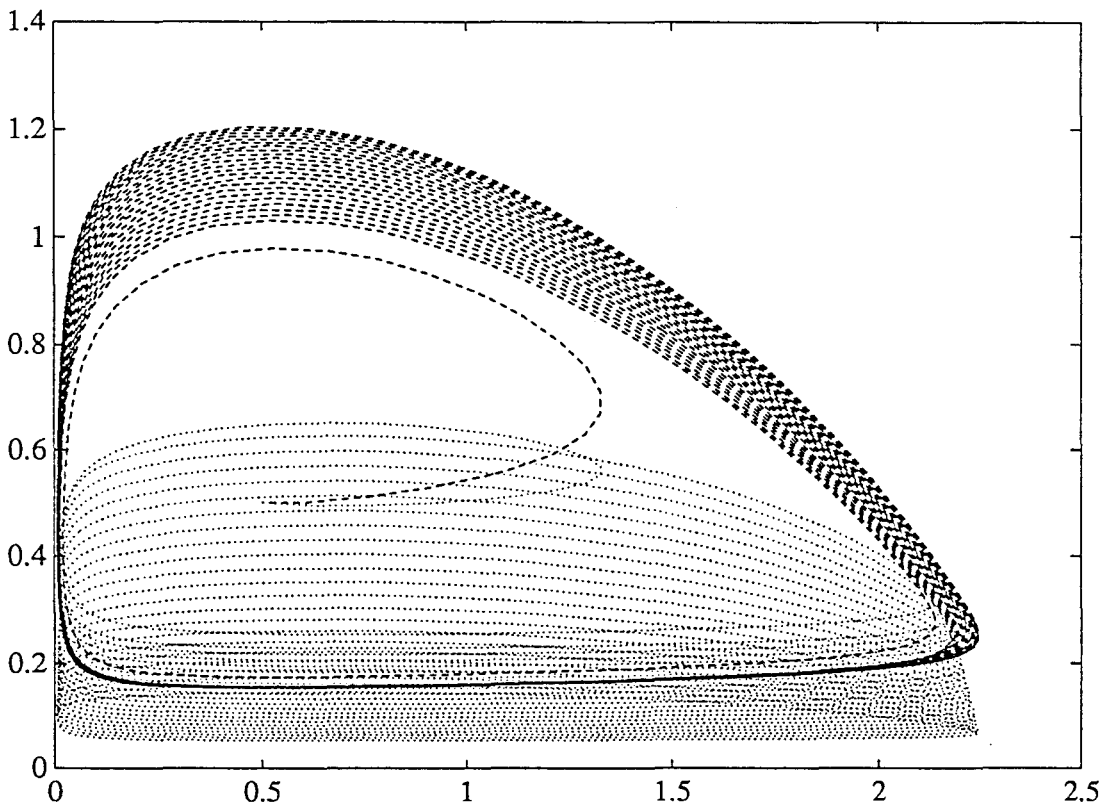

Figure B.10: The $s - x_1, x_2$ graphs under the same conditions as in Figure B.9.

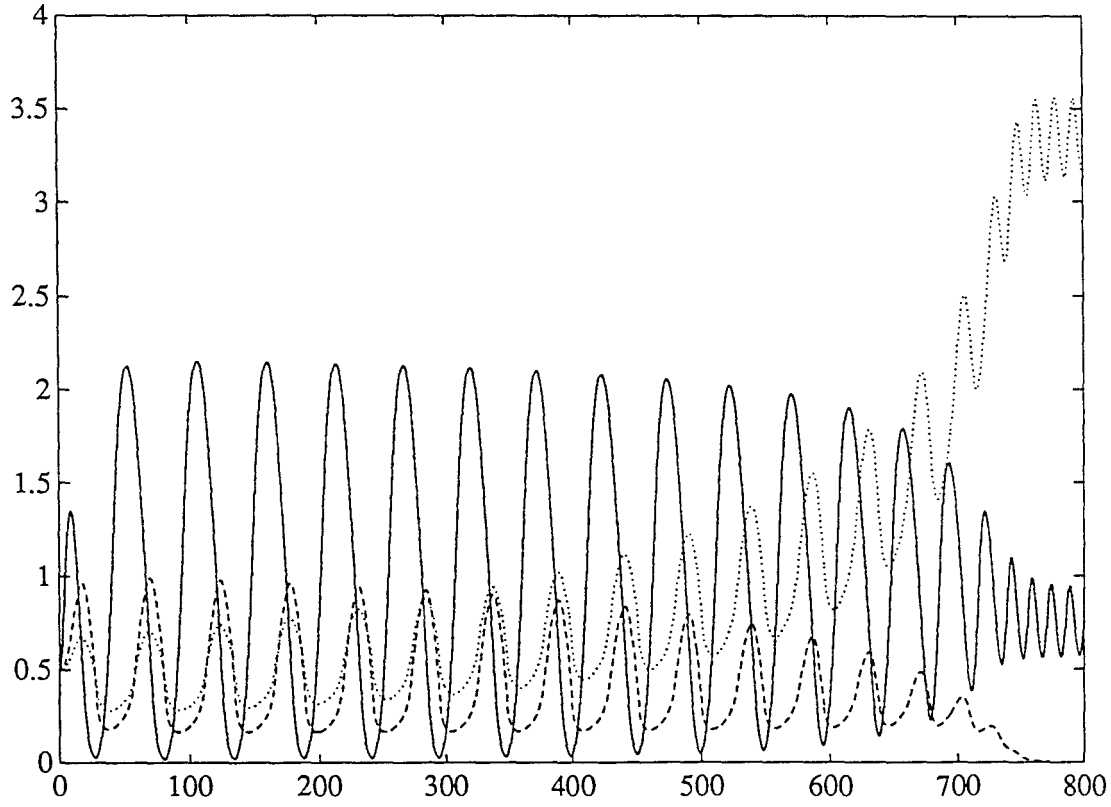

Figure B.11: The $t-s, x_1, x_2$ graphs after the bifurcation at $\bar{\Gamma}_2$ occurs with $\epsilon = 0.07$, $D_2 = 0.2555$ and the initial value $(0.5, 0.5, 0.5)$.

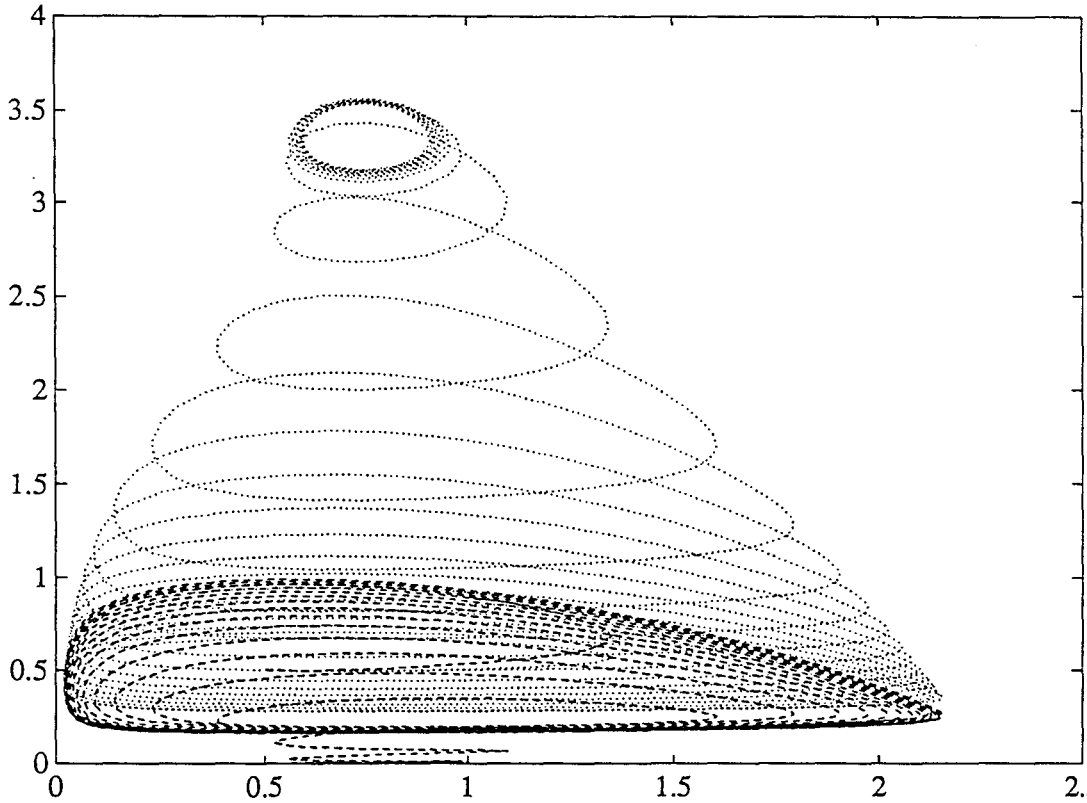

Figure B.12: The $s - x_1, x_2$ graphs under the same conditions as in Figure B.11.

Appendix C

The graphs of the Hopf bifurcation and its unstable periodic orbit in the interior of the positive octant

Illustration

In the $t - s, x_1, x_2$ graphs,

——— represents the $t - s$ curves;

$- \; - \; -$ represents the $t - x_1$ curves;

$\cdots\cdots$ represents the $t - x_2$ curves.

In the $s - x_1, x_2$ graphs,

$- \; - \; -$ represents the $s - x_1$ curves;

$\cdots\cdots$ represents the $s - x_2$ curves.

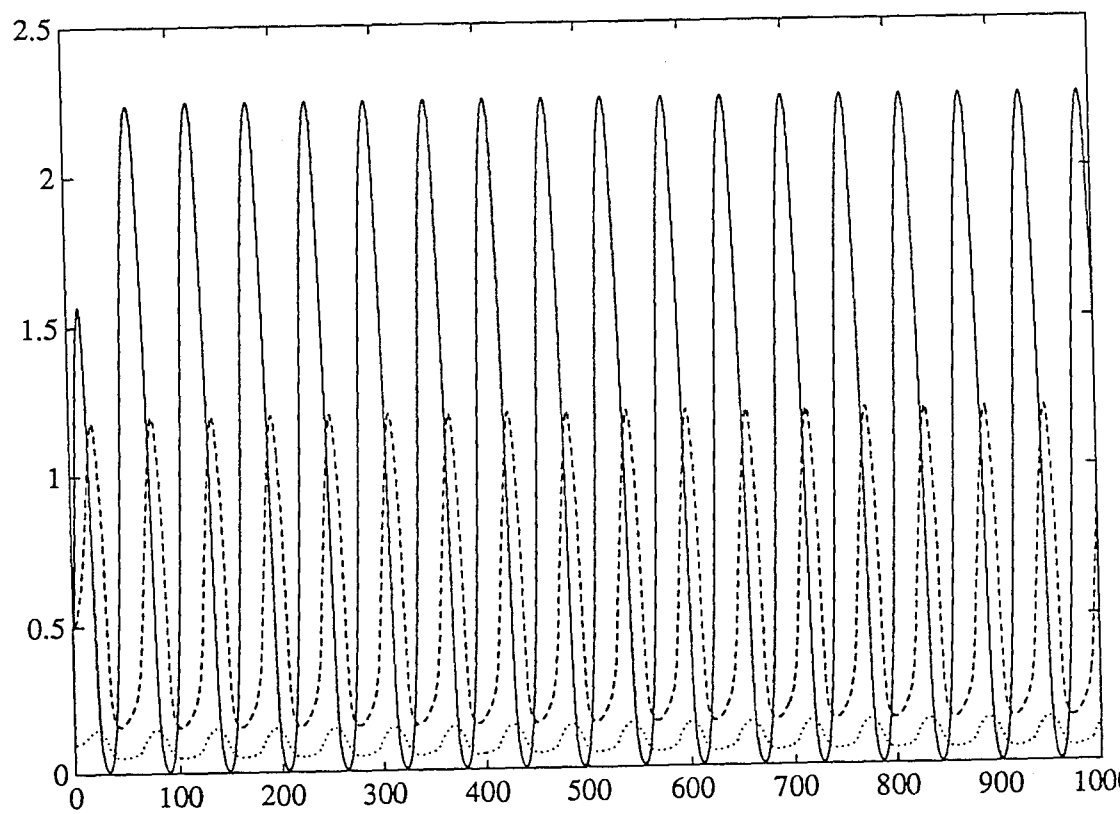

Figure C.1: The $t-s, x_1, x_2$ graphs of the unstable interior periodic orbit from the Hopf bifurcation with $\epsilon = 0.08$, $D_2 = 0.2555$ and the initial value $(0.5, 0.5, 0.1)$.

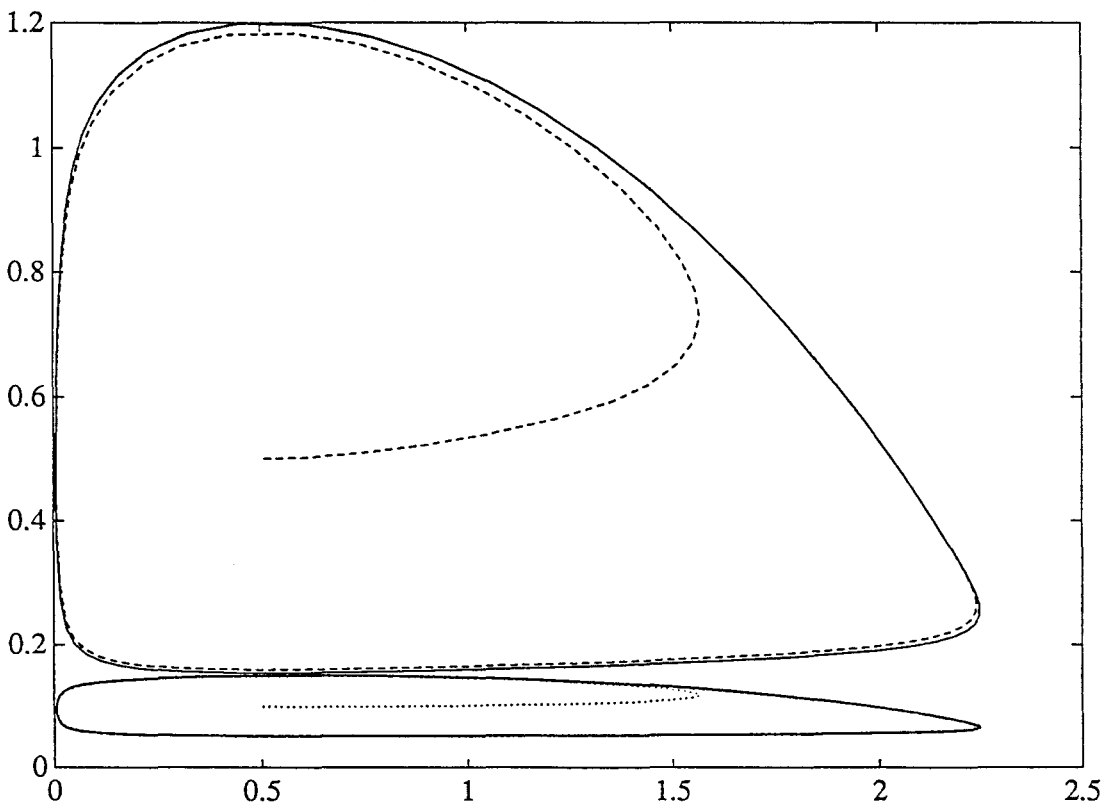

Figure C.2: The $s - x_1, x_2$ graphs under the same conditions as in Figure C.1.

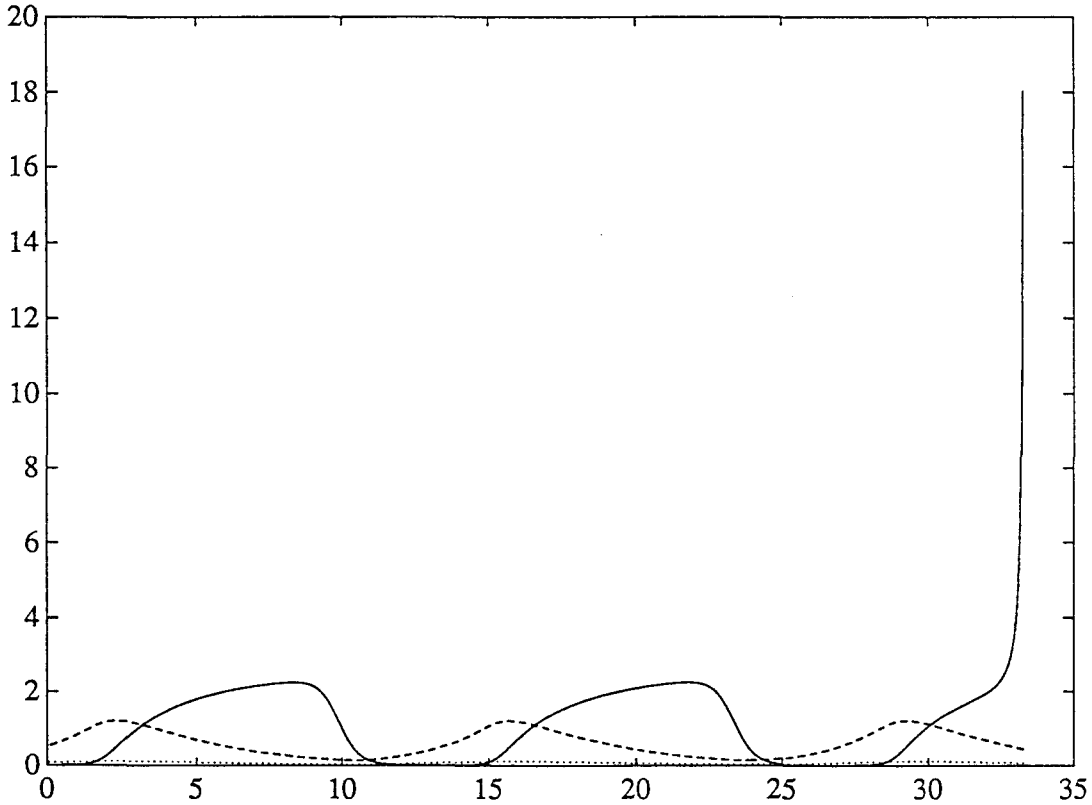

Figure C.3: The backward time $t-s, x_1, x_2$ graphs near the unstable interior periodic orbit from the Hopf bifurcation diverging to infinity with $\epsilon = 0.08$, $D_2 = 0.2555$ and the initial value $(0.0065, 0.5239, 0.08129130603)$.

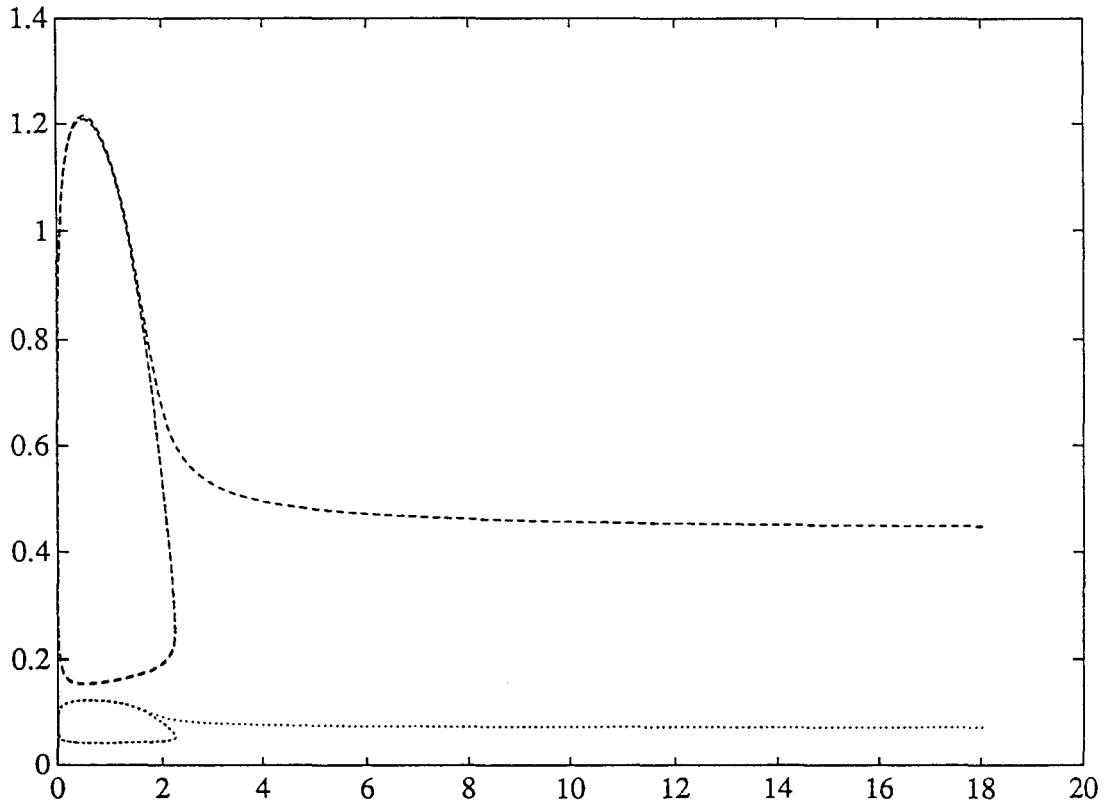

Figure C.4: The $s - x_1, x_2$ graphs under the same conditions as in Figure C.3.

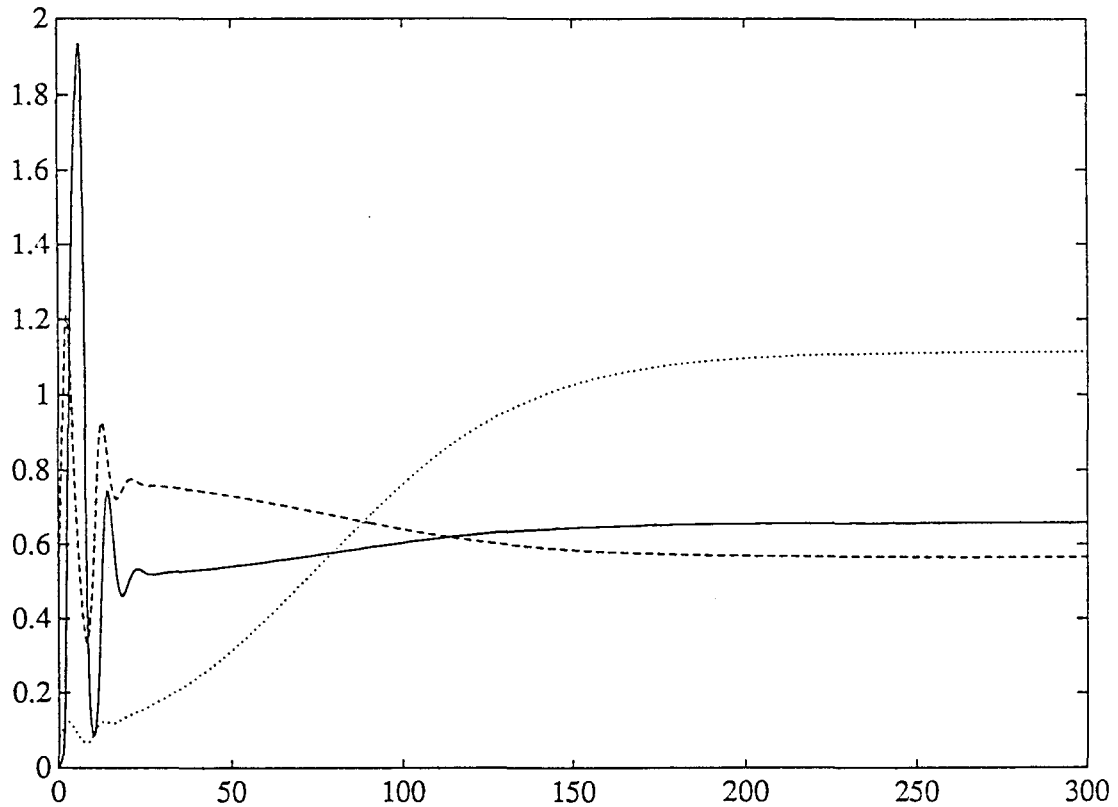

Figure.C.5: The backward time $t-s, x_1, x_2$ graphs near the unstable interior periodic orbit from the Hopf bifurcation converging to the interior equilibrium with $\epsilon = 0.08$, $D_2 = 0.2555$ and the initial value $(0.0065, 0.5239, 0.081291306)$.

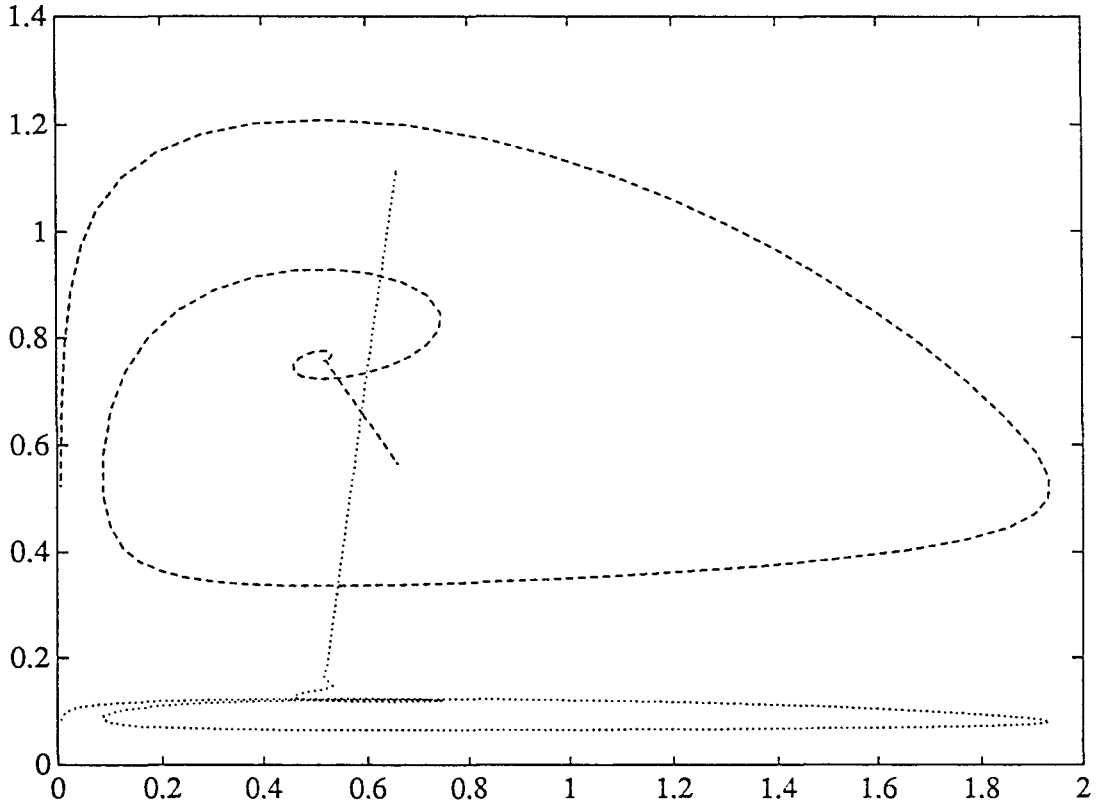

Figure C.6: The $s - x_1, x_2$ graphs under the same conditions as in Figure C.5.

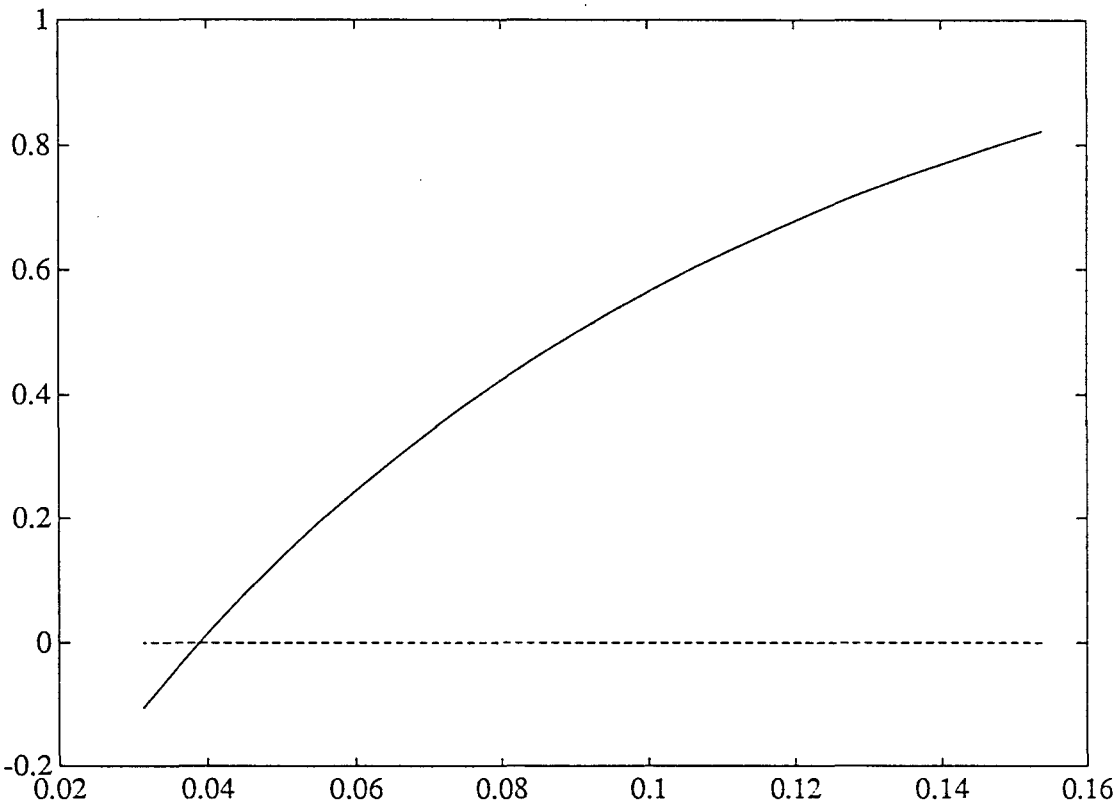

Figure C.7: The dependence of the real part of the complex eigenvalue at the interior equilibrium on ϵ with $K = 2$ and $D_2 = 0.2555$.

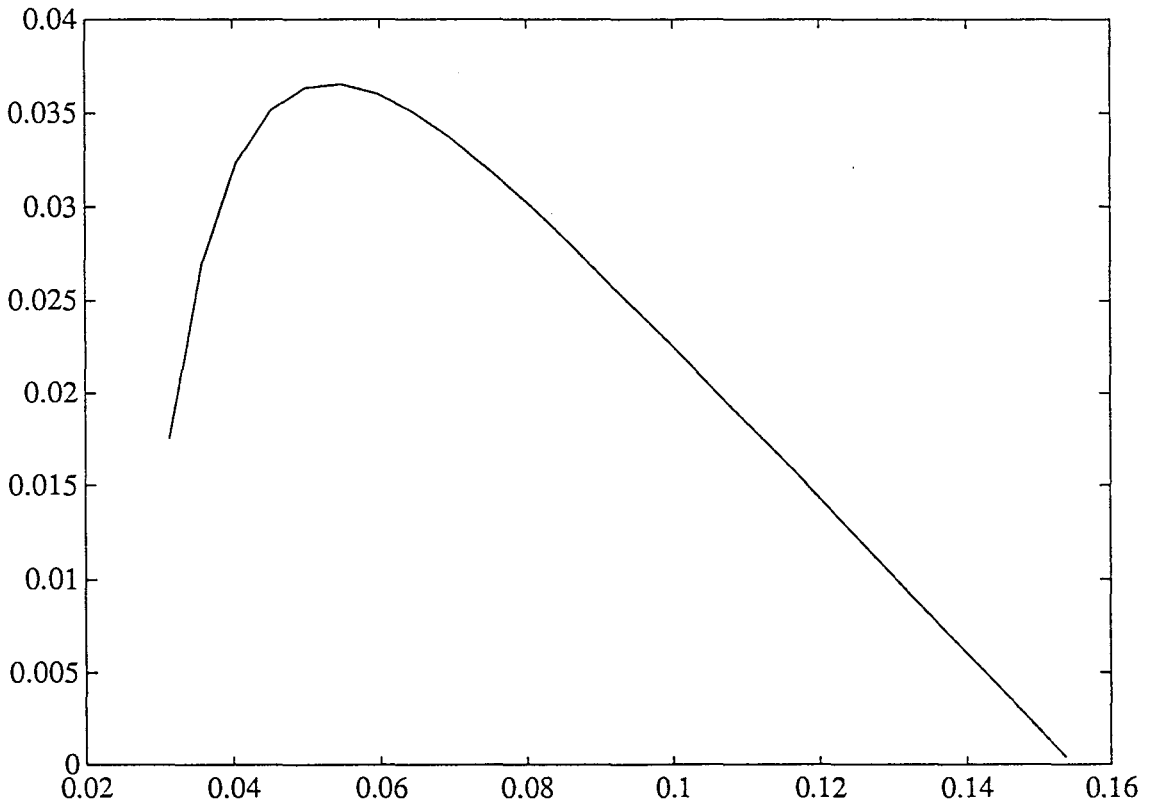

Figure C.8: The dependence of the real eigenvalue at the interior equilibrium on ϵ under the same conditions as in Figure C.7.

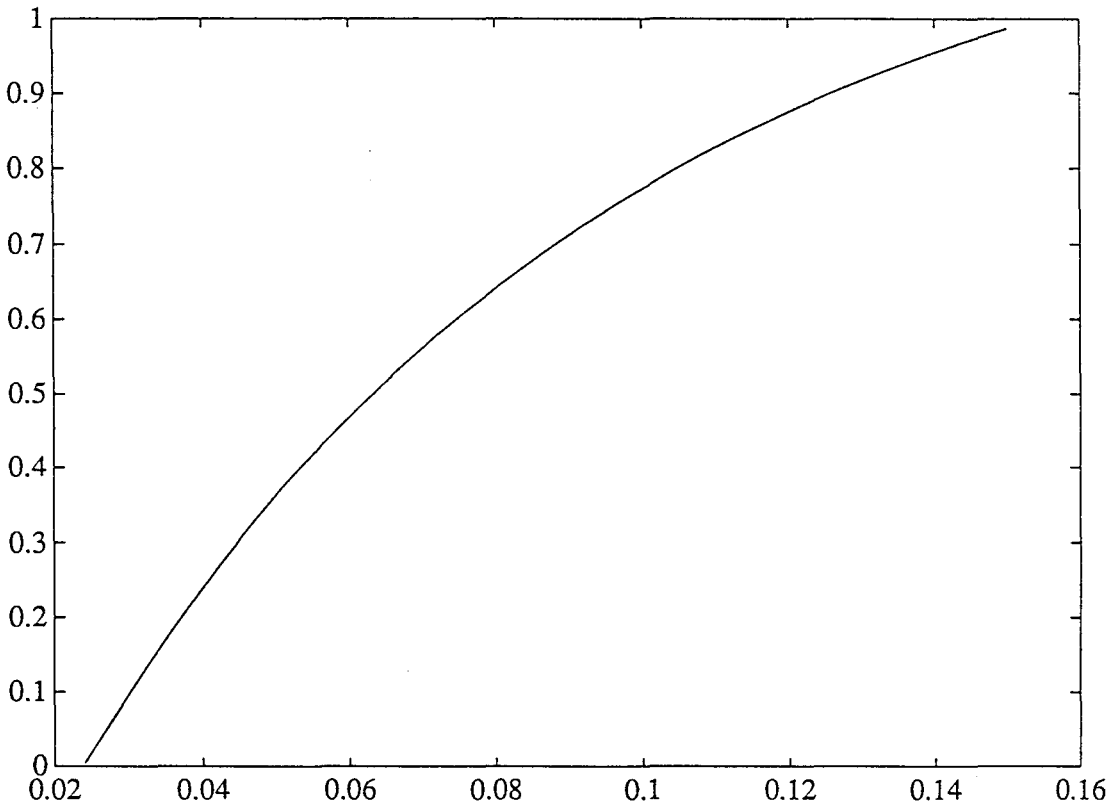

Figure C.9: The dependence of the real part of the complex eigenvalue at the interior equilibrium on ϵ with $K = 2.5$ and $D_2 = 0.2555$.

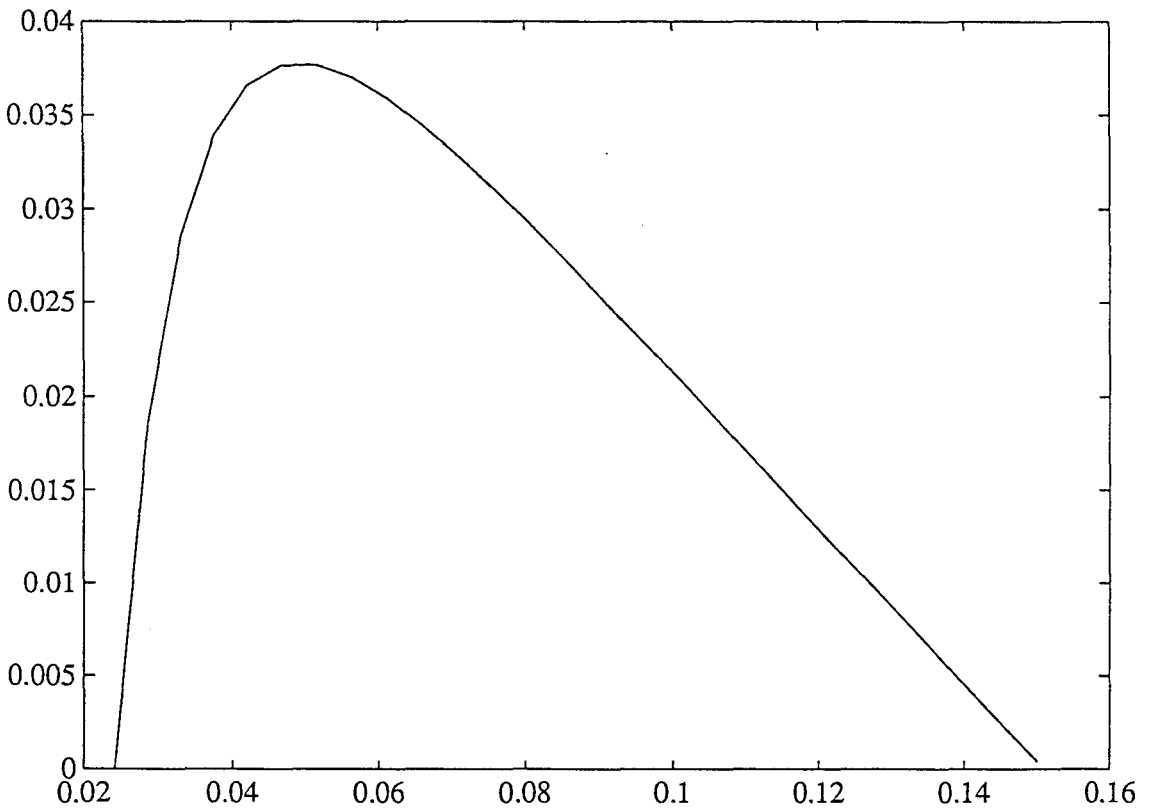

Figure C.10: The dependence of the real eigenvalue at the interior equilibrium on ϵ under the same conditions as in Figure C.9.

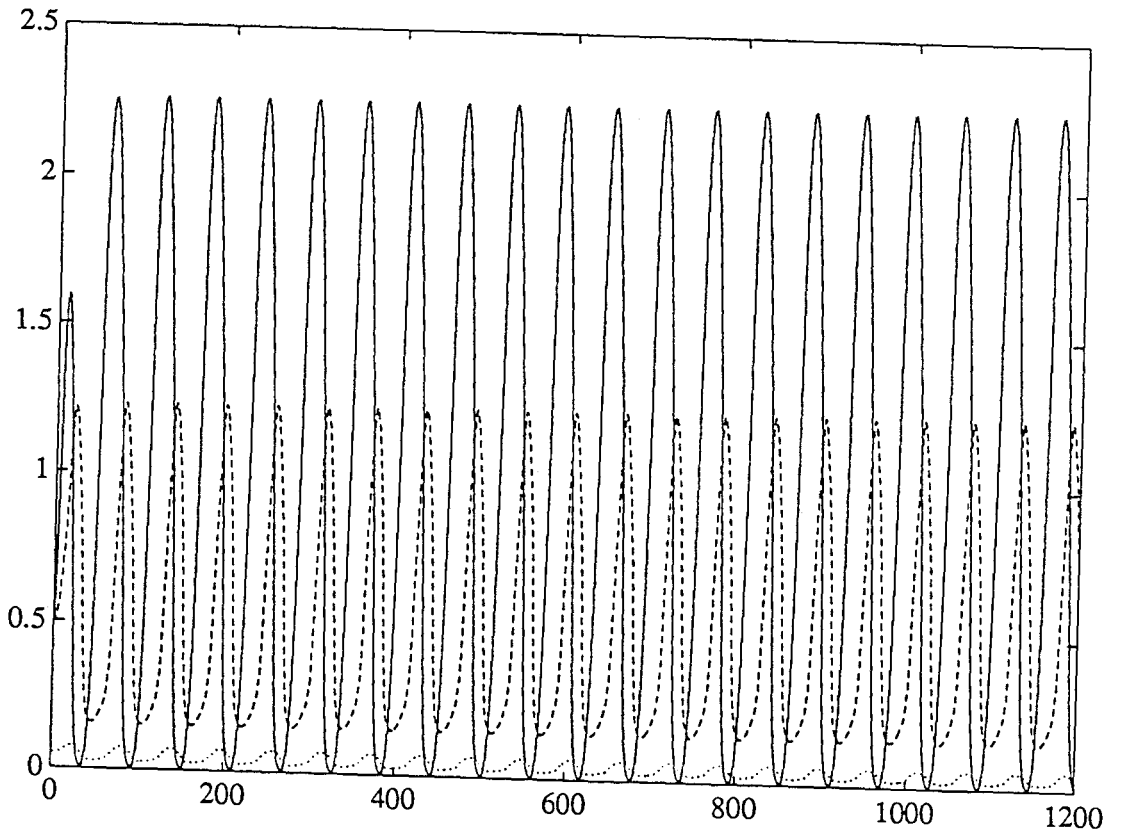

Figure C.11: The $t-s, x_1, x_2$ graphs for the threshold at the interior equilibrium with $K = 2.5, D_2 = 0.2555$, $\epsilon = 0.08$ and initial value (0.5,0.5,0.05).

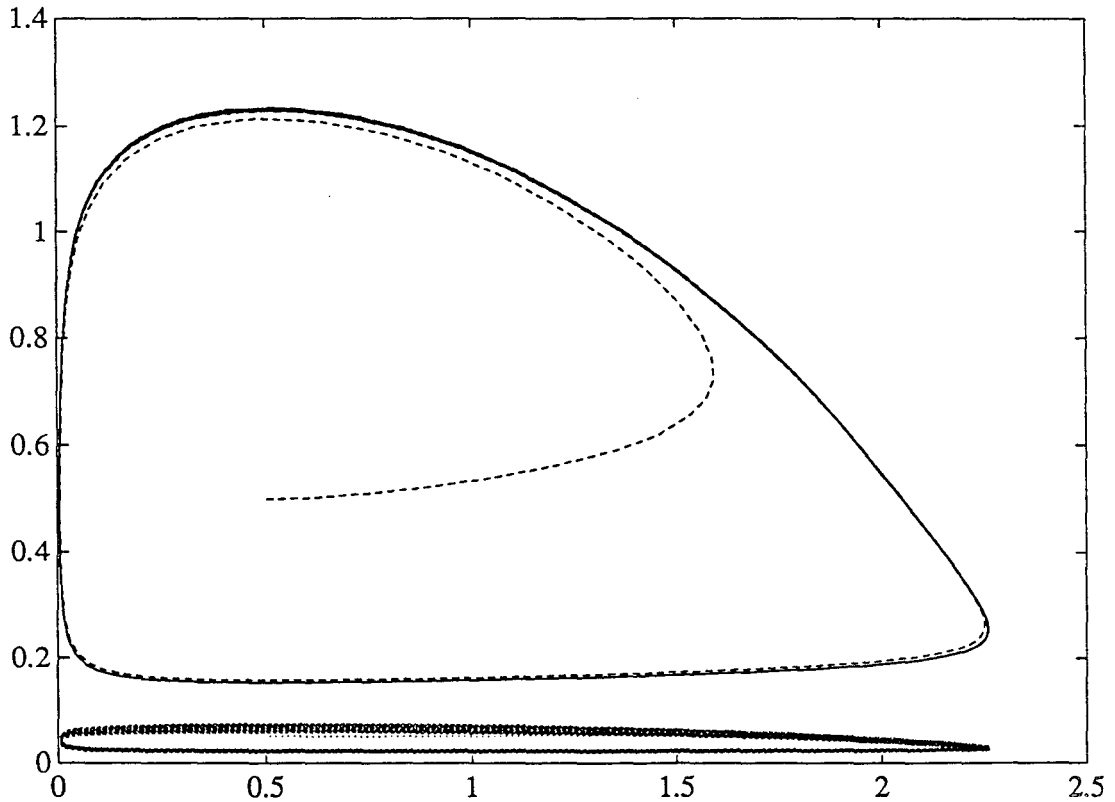

Figure C.12: The $s - x_1, x_2$ graphs for the threshold at the interior equilibrium under the same conditions as in Figure C.11.

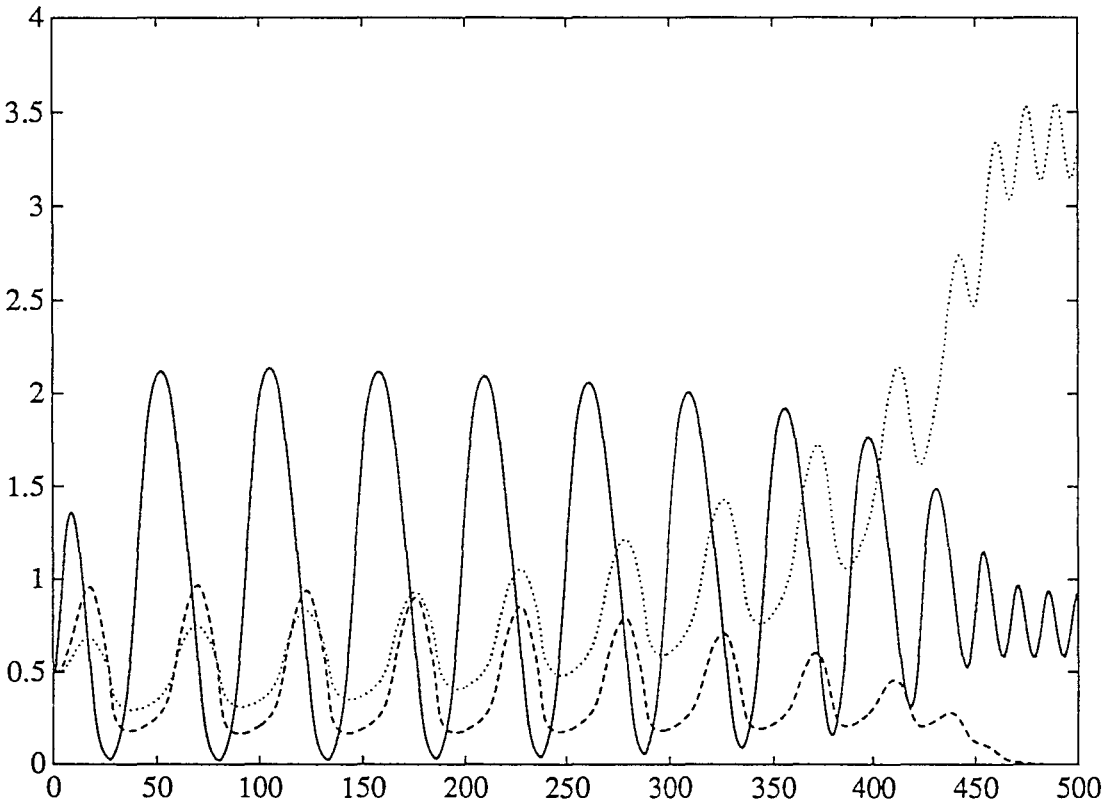

Figure C.13: The $t-s, x_1, x_2$ graphs for the threshold at the interior equilibrium with $K = 2.5, D_2 = 0.2555$, $\epsilon = 0.08$ and initial value (0.5,0.5,0.5).

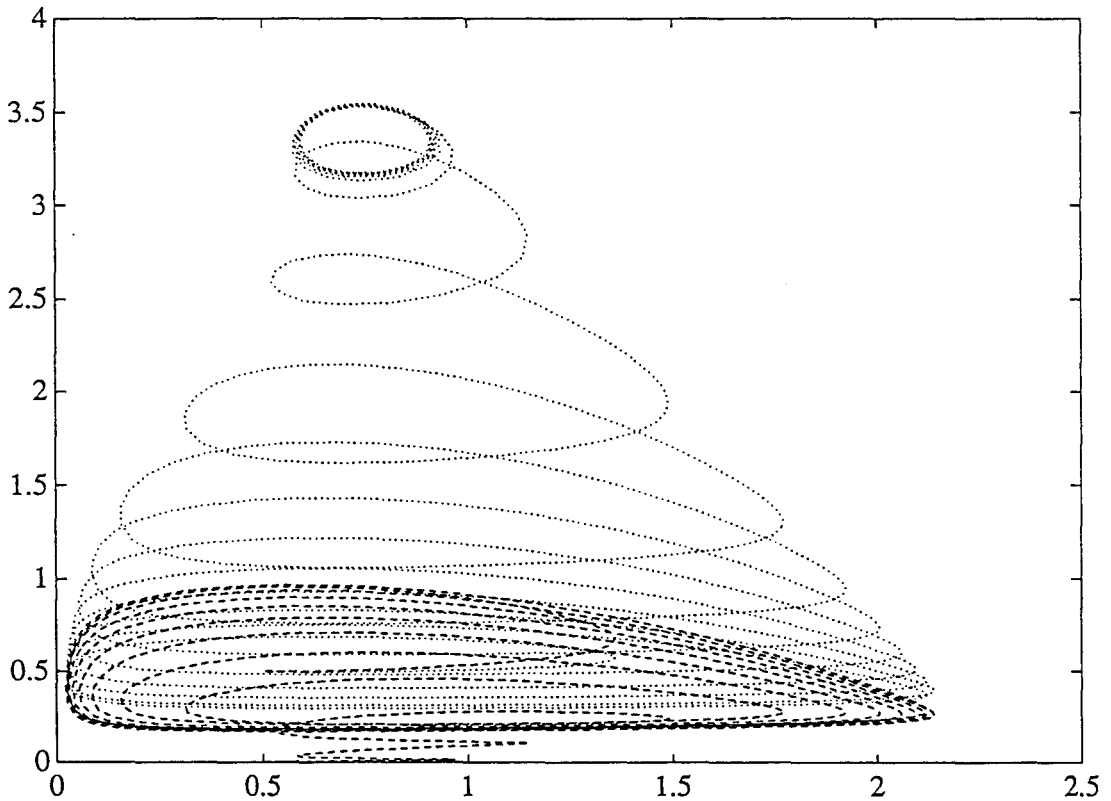

Figure C.14: The $s - x_1, x_2$ graphs for the threshold at the interior equilibrium under the same conditions as in Figure C.13.

Bibliography

[1] Butler, G.J. "Coexistence in Predator-Prey Systems". In: Modeling and Differential Equations in Biology. T. Burton ed. New York: Marcel Dekker, 1980.

[2] Butler, G.J., Hsu, S.B. & Waltman, P. "Coexistence of Competing Predators in a Chemostat". J. Math. Biol. 17(1983), 133-151.

[3] Butler, G.J. & Waltman, P. "Bifurcation from a Limit Cycle in a Two Predator-One Prey Ecosystem Modeled on a Chemostat". J. Math. Biol. 12(1981), 295-310.

[4] Butler, G.J. & Waltman, P. "Persistence in Dynamical Systems". J. Diff. Equ'ns 63(1986), 255-263.

[5] Butler, G.J. & Wolkowicz, G.S.K. "Predator-Mediated Competition in the Chemostat". J. Math. Biol. 24(1986), 167-191.

[6] Fredrickson, A.G. & Stephanopoulos, G. "Microbial Competition". Science 213(1981), 972-979.

[7] Freedman, H.I. "Stability Analysis of a Predator-Prey System with Mutual Interference and Density-Dependent Death Rates". Bull. Math. Biol. 41(1979), 67-78.

[8] Freedman, H.I. Deterministic Mathematical Models in Population Ecology. New York: Marcel Dekker, 1980.

[9] Freedman, H.I. & Waltman, P. "Mathematical Analysis of Some three-species Food-Chain Models". Math. Bios. 33(1977), 257-276.

[10] Freedman, H.I. & Waltman, P. "Persistence in Models of Three Interacting Predator-Prey Populations". Math. Bios. 68(1984), 213-232.

[11] Freedman, H.I. & Waltman, P. "Persistence in a Model of Three Competing Populations". Math. Bios. 73(1985), 89-101.

[12] Gard, T.C. "Persistence in Foodwebs: Holling Type Food Chains". Math. Bios. 49(1980), 61-68.

[13] Gard, T.C. "Uniform Persistence in Multispecies Population Models". Math. Bios. 85(1987), 93-104.

[14] Gard, T.C. & Hallam, T.G. "Persistence in Foodwebs-II: Lotka-Volterra Food Chains". Bull. Math. Biol. 41(1979), 877-891.

[15] Hale, J.K. & Somolinos, A.S. "Competition for Fluctuating Nutrient". J. Math. Biol. 18(1983), 255-280.

[16] Hansen, S.R. & Hubbell, S.P. "Single-Nutrient Microbial Competition: Qualitative Agreement Between Experimental and Theoretically Forecast Outcomes". Science. 207(1980), 28 March.

[17] Hsu, S.B., Hubbell, S.P. & Waltman, P. "Competing predators". SIAM J. Appl. Math. 35(1978), 617-625.

[18] Jannash, H.W. & Mateles, R.T. "Experimental Bacterial Ecology Studied in Continuous Culture". Adv. Microb. Physiol. 11(1974), 165-212.

[19] Jorné, J. & Carmi, S. "Liapunov Stability of the Diffusive Lotka-Volterra Equations". Math. Bios. 37(1977), 51-61.

[20] Kannan, D. "Volterra-Verhulst Prey-Predator Systems with Time Dependent Coefficients: Diffusion Type Approximation and Periodical Solutions". Bull. Math. Biol. 41(1979), 229-251.

[21] Keener, J.P. "Oscillatory Coexistence in the Chemostat: A Codimension Two Unfolding". SIAM J. Appl. Math. 43(1983), 1005-1018.

[22] Kirlinger, G. "Permanence in Lotka-Volterra Equations: Linked Prey Predator Systems". Math. Bios. 82(1986), 165-191.

[23] Kuang, Y. & Freedman, H.I. "Uniqueness of Limit Cycles in Gause-Type Models of Predator-Prey systems". Math. Bios. 88(1988), 67-84.

[24] Liou, L-P. & Cheng, K-S. "On the Uniqueness of a Limit Cycle for a Predator-Prey System". SIAM J. Math. Anal. 19(1988), 867-878.

[25] Lotka, A.J. Elements of Physical Biology. Baltimore: Williams and Wilkins, 1925.

[26] Marsden, J.E. & McCracken, M. Hopf Bifurcation and its Applications. New York: Springer-Verlag, 1976.

[27] Rudin, W. Principles of Mathematical Analysis. New York: McGraw-Hill, 1964.

[28] Ruelle, D. & Takens, F. "On The Nature of Turbulence". Commun. Math. Phys. 20(1971), 167-192.

[29] Smith, H.L. "The Interaction of Steady State and Hopf Bifurcations in A Two-Predator-One-Prey Competition Model". SIAM J. Appl. Math. 42(1982), 27-43.

[30] Takeuchi, Y. "Diffusion Effect on Stability of Lotka-Volterra Models". Bull. Math. Biol. 48(1986), 585-602.

[31] Veldcamp, H. "Ecological Studies with the Chemostat". Adv. Microb. Ecol. 1(1977), 59-95.

[32] Verhulst, P.F. "Notice sur la Loi que la Population Pursuit dans son Accroissement". Correspond. Math. Phys. 10(1938), 113-121.

[33] Volterra,V. "Variations and Fluctuations of the Number of Individuals in Animal Species Living Together". J. Cons. (Cons. Int. Explor. Mer.) 3(1929), 3-51.

[34] Waltman, P. "Coexistence in Chemostat-like Models". Rocky Mountain J. Math. 20(1990), 777-807.

[35] Waltman, P., Hubbell, S.P. & Hsu, S.-B. "Theoretical and Experimental Investigations of Microbial Competition in Continuous Culture". In: Modeling and Differential Equations in Biology T.Burton ed. New York: Marcel Dekker, 1980.

[36] Wolkowicz, G.S.K. & Lu, Z. "Global Dynamics of a Mathematical Model of Competition in the Chemostat: General Response Functions and Differential Death Rates". Preprint.